I. NUMERICAL SOLUTION OF EXACT PAIR EQUATIONS

II. NUMERICAL SOLUTION OF FIRST-ORDER PAIR EQUATIONS

Thesis by

Nicholas Wilhelm Winter

In Partial Fulfillment of the Requirements

For the Degree of

Doctor of Philosophy

California Institute of Technology

Pasadena, California

1970

(Submitted November 10, 1969)

ACKNOWLEDGMENTS

I would like to thank my research advisor, Dr. Vincent McKoy, for his encouragement during my graduate study. I am also indebted to Dr. William A. Goddard for many discussions and helpful advice. The first three years at Caltech were enriched by my interactions with Dr. Russell M. Pitzer.

Perhaps I learned the most from my contacts with other graduate students. I am particularly grateful to Dr. Thomas H. Dunning for the many projects on which we collaborated. I am also thankful for the many discussions with Donald Truhlar and Luis Kahn.

Finally, the most important contribution to my graduate study has been from my wife, Barbara Jo. Her patience and understanding eased the difficult moments.

ABSTRACT

Part I

Numerical solutions to the S-limit equations for the helium ground state and excited triplet state and the hydride ion ground state are obtained with the second and fourth difference approximations. The results for the ground states are superior to previously reported values. The coupled equations resulting from the partial wave expansion of the exact helium atom wavefunction were solved giving accurate S-, P-, D-, F -, and G-limits. The G-limit is -2.90351 a.u. compared to the exact value of the energy of -2.90372 a.u.

Part II

The pair functions which determine the exact first-order wavefunction for the ground state of the three-electron atom are found with the matrix finite difference method. The second- and third-order energies for the $(1s1s)\,^1S$, $(1s2s)\,^3S$, and $(1s2s)\,^1S$ states of the two-electron atom are presented along with contour and perspective plots of the pair functions. The total energy for the three-electron atom with a nuclear charge Z is found to be

$$E(Z) = -1.125 \cdot Z^2 + 1.022805 \cdot Z - 0.408138 - 0.025515 \cdot (1/Z) + O(1/Z^2) \text{ a.u.}$$

TABLE OF CONTENTS

I. NUMERICAL SOLUTION OF EXACT PAIR EQUATIONS

A. INTRODUCTION

It is a well established approach to the study of electron correlation to analyze the many-electron system as a series of simpler two-electron problems. Sinanoglu[1] has shown how the first-order equation can be reduced to two-electron pair equations for the many-electron atom or molecule. He also discusses the equation for "exact pairs" which describes the pair correlations beyond first-order. Nesbet[2] has been successful in reducing the total wavefunction and energy for first-row atoms into their Hartree-Fock and two-body components. The general topic of electron correlation is reviewed in Refs. 3 and 4.

We are not concerned here with the derivation or validity of the various pair approximations but with how to accurately and efficiently solve the resulting equations. There have been two standard approaches in the past, both of which are variational. The first dates back to the early calculations of Hylleraas[5] who used a trial function containing interelectronic coordinates. The unspecified parameters are determined so as to minimize the two-electron energy. This method is capable of high accuracy if enough terms are included, but leads to difficult integrals to evaluate. Indeed, considerable research effort has gone into the study of these integrals themselves. The most successful approach is to use a configuration interaction (CI) trial function. The popularity of this method is due

in part to its general applicability. When applied to the pair equations, the CI method obtains the pair energies and properties without dealing directly with a two-electron equation. Instead, the total N-electron wavefunction is constructed from a set of Slater determinants so as to describe the correlation between a specific pair of electrons while treating the remaining N-2 electrons in the Hartree-Fock approximation. The energy is found by diagonalizing the total Hamiltonian in this basis. This is equivalent to solving a Schrödinger equation describing the pair of electrons correlating in the Hartree-Fock field of the remaining N-2 electrons. The principal disadvantage of the CI method is the slow convergence relative to the use of interelectronic coordinates. Schwartz[6,7] has pointed out the disadvantages of using orbital expansions to represent correlated wavefunctions with particular attention to the convergence as higher angular configurations are included.

We have chosen an alternative to these approaches by simply solving the equations numerically. Since it is not possible to treat a six-dimensional equation, we first eliminate the angular variables by a partial wave expansion. Then the resulting equations for the functional coefficients are solved numerically. The method is not variational and does not necessarily give an upper bound to the two-electron energy. However, once the basic techniques are established, any set of two-variable equations can be solved with high accuracy.

This allows one to consider a variety of approximations to the pair equations (pseudo-potentials, etc.) without additional complications. The numerical methods are highly computer oriented, since the differential equation is reduced to a set of difference equations which are solved by standard matrix techniques.

In two earlier papers[8,9] we applied the matrix finite difference (MFD) method to the solution of the S-limit Schrödinger equation and the first-order pair equation for the helium atom. The results were accurate; however, in order to apply the method to excited states of two-electron atoms and to the valence electron pairs in first-row atoms, it was necessary to reexamine the numerical techniques. The most obvious problem originates from the diffuse nature of the wavefunction describing these electron pairs. This requires that the point at which the solution is required to vanish must be taken further out and consequently the number of points needed to obtain an accurate solution becomes unreasonable. Another refinement is needed when considering the solution of exact pair equations. The partial wave expansion of the exact pair function leads to a set of coupled equations in contrast to the first-order pairs which give uncoupled equations. The exact pair functions are solutions of eigenvalue equations differing from the two-electron atom Schrödinger equation only in the presence of the potential due to the N-2 "core" electrons and orthogonality constraints. In order to solve these we

have to iterate among the equations determining the functional coefficients of the partial wave expansion. To keep the problem within limits we must be able to obtain accurate solutions with a small number of points.

We have corrected for the possible diffuse nature of the pair functions by transforming to a new set of variables which are just the square roots of the original variables. In order to guarantee greater accuracy with fewer points, fourth differences have been included in the approximation of the derivatives. Combining both of these modifications with an extrapolation procedure, we have found the S-limits for the ground states of helium and the hydride ion. The equations were also solved using both transformed and untransformed coordinates and second differences only. With the three sets of results for each atom, we can compare the effectiveness of the modifications for a tightly bound pair (helium) and a diffuse pair (hydride ion). Finally, we have applied the MFD method to the exact Schrödinger equation for the helium atom using successively higher partial waves up to the G-limit. The results proved superior to any previous CI calculation of the angular limits. The properties predicted by the numerical solution compare well to the exact values.

B. PARTIAL WAVE REDUCTION OF THE TWO-ELECTRON EQUATION

The partial wave expansion of the solution of the two-electron Schrödinger equation has previously been considered by Luke, Meyerott, and Clendenin[10] for the ^3S state of Li^+. For a spherically symmetric pair of electrons the exact wavefunction can be expanded in Legendre polynomials of the cosine of the relative angle between the two electrons,

$$\Psi(r_1 r_2 \theta_{12}) = \sum_{\ell=0}^{\infty} \psi_\ell(r_1 r_2) \frac{\sqrt{2\ell+1}}{4\pi} P_\ell(\cos\theta_{12}). \qquad (1)$$

By substituting this into the equation,

$$(-\tfrac{1}{2}\nabla_1^2 - \tfrac{1}{2}\nabla_2^2 + V(r_1) + V(r_2) + 1/r_{12})\Psi = E\Psi \qquad (2)$$

multiplying both sides by $\frac{\sqrt{2\ell+1}}{4\pi} P_\ell(\cos\theta_{12})$, and integrating over all angular variables, we obtain the ℓ-th member of an infinite set of coupled equations for the functional coefficients

$$\left[-\tfrac{1}{2} \left(1/r_1^2 \;\; \partial/\partial r_1 \left(r_1^2 \;\; \partial/\partial r_1\right) + 1/r_2^2 \;\; \partial/\partial r_2 \left(r_2^2 \;\; \partial/\partial r_2\right)\right)\right.$$

$$\left. + \; \ell\,(\ell+1)/2r_1^2 \; + \; \ell(\ell+1)/2r_2^2 \; + \; V(r_1) \; + \; V(r_2) \; + \; M_{\ell\ell} \right] \psi_\ell(r_1 r_2) \; =$$

$$E \cdot \psi_\ell(r_1 r_2) \; - \sum_{\ell' \neq \ell} M_{\ell\ell'} \; \psi_{\ell\ell'}(r_1 r_2) \qquad (3)$$

where

$$M_{\ell\ell'} \; = \sum_{k = |\ell - \ell'|}^{\ell + \ell'} C^k(\ell o, \ell' o) \, \frac{r_<^k}{r_>^{k+1}}$$

$$r_< \; = \; \min\,(r_1, r_2)$$

$$r_> \; = \; \max\,(r_1, r_2)$$

and

$$C^k(\ell o, \ell' o) \; = \; \frac{\sqrt{(2\ell + 1)(2\ell' + 1)}}{2} \int \Big(P_\ell(\cos\theta_{12}) \; P_k(\cos\theta_{12}) \cdot$$

$$P_{\ell'}(\cos\theta_{12}) \Big) d(\cos\theta_{12}) \; .$$

Up to this point we have not made any approximations, although it is clearly an impossible task to solve an infinite set of coupled equations. The expansion is usually truncated when the energy is determined

to the desired accuracy. When using the MFD method it is convenient, but not necessary, to begin by solving the S-limit ($\ell = 0$ partial wave only) and then use this as an initial guess to determine the P-limit ($\ell = 0, 1$ partial waves only) and so forth. After two partial waves, the addition of further terms to the expansion has a small effect on the known functional coefficients and the iterative method of solving the coupled equations converges extremely rapidly. Therefore, the slow convergence of the partial wave expansion pointed out by Schwartz[7] is not a serious drawback.

It is easy to show that a similar reduction of the Schrödinger equation can be made for pairs that are not spherically symmetric. The main difference appears in the angular integrals which couple the equations together. Also the non-local potentials which occur in the Hartree-Fock pair equations offer little complication since the equations already contain nonhomogeneous terms. The numerical techniques needed to solve these equations are presented in the next section.

C. REVIEW OF THE FINITE DIFFERENCE METHOD

The second derivative can be expanded in terms of differences as follows.

$$(\partial^2 \psi/\partial r^2)_{r=r_0} = 1/h^2 \left(\delta_0^2 - \tfrac{1}{12}\delta_0^4 + \tfrac{1}{90}\delta_0^6 - \ldots\right) \qquad (4)$$

where

$$\delta_0^2 = \psi(r_0 + h) - 2\psi(r_0) + \psi(r_0 - h)$$

$$\delta_0^4 = \psi(r_0 + 2h) - 4\psi(r_0 + h) + 6\psi(r_0) - 4\psi(r_0 - h) + \psi(r_0 - 2h)$$

$$\delta_0^6 = \psi(r_0 + 3h) - 6\psi(r_0 + 2h) + 15\psi(r_0 + h) - 20\psi(r_0) +$$

$$15\psi(r_0 - h) - 6\psi(r_0 - 2h) + \psi(r_0 - 3h) \qquad (5)$$

and h is the grid size.[11] The first approximation to the second derivative is just $\partial^2\psi/\partial r^2 \sim 1/h^2\ \delta^2$. In order to find the difference error we expand the second difference in terms of derivatives

$$1/h^2\ \delta_0^2 = (\partial^2\psi/\partial r^2)_0 + \tfrac{1}{12}\cdot h^2(\partial^4\psi/\partial r^4)_0 + \tfrac{1}{360}\cdot h^4(\partial^6\psi/\partial r^6)_0 + \ldots \qquad (6)$$

and as a consequence of choosing central differences, the error contains only even powers of h. Bolton and Scoins[12] have shown that the energy found with a grid size h can be expressed as a power series of the form

$$E(h) = E(0) + C_2h^2 + C_4h^4 + C_6h^6 + \ldots \qquad (7)$$

where E(0) is the exact energy corresponding to h = 0. For most two-dimensional equations it is not possible to use enough points to compete with the accuracy of variational methods, therefore (7) is

used to extrapolate the energies found at several grid sizes to the exact value.[13]

Fox[14] has argued that a substantial amount of the difference error can be eliminated by including the next term in the difference expansion of the derivative in the MFD equations. The difficulty in using fourth differences is satisfying the boundary conditions. The usual conditions are to require $r \cdot \psi(r)$ to vanish at $r = 0$ and $r = r_{max}$ where r_{max} approximates infinity. The fourth difference of $\psi(r)$ at $r = h$ requires that we know the function at $r = -h$, and therefore introduces uncertainties into the MFD equations. A similar difficulty occurs at the other boundary. One solution of this problem is to extract the asymtotic behavior of $\psi(r)$ at $r = 0$ and $r = \infty$ from the differential equation and use this to relate the unknown values of $\psi(r)$ outside the defined grid to the values within. This is the approach we have taken for the first-order pair equations; however, for the eigenvalue equations, it is simpler to replace the fourth difference approximation at the boundary with the usual second difference approximation. This does not appreciably affect the accuracy when combined with the coordinate transformation to be discussed later.

Unfortunately, the fourth difference approximation does not sufficiently reduce the difference error to be used without extrapolation. The approximation does allow accurate results to be obtained from relatively few grids. These various methods are illustrated

for the S-limit equation in the next section.

D. SOLUTION OF THE S-LIMIT EQUATION

Truncating the partial wave expansion at $\ell = 0$, we then obtain the following equation for the two-electron atom,

$$(-\tfrac{1}{2}\,\partial^2/\partial r_1^2 - \tfrac{1}{2}\,\partial^2/\partial r_2^2 - z/r_1 - z/r_2 + 1/r_>)\, u_0(r_1 r_2) = E \cdot u_0(r_1 r_2) \qquad (8)$$

where $u_0(r_1 r_2) = r_1 r_2 \psi_0(r_1 r_2)$. If the derivatives are replaced by the second difference approximation, (8) is transformed to a set of linear equations of the form,

$$\underset{\sim}{D} \cdot \underset{\sim}{u} = E \cdot \underset{\sim}{u} \qquad (9)$$

where $\underset{\sim}{D}$ is a symmetric banded matrix with non-zero off-diagonal elements in only two super-diagonals and two sub-diagonals. The eigenvectors at $\underset{\sim}{D}$ represent the ground and excited states of the two-electron equation and would be exact if we used an infinite number of grid points and satisfied the correct boundary conditions. Since we are usually satisfied with the lowest state and possibly a few excited states, a finite number of points are employed and a reasonable radial cutoff is chosen to approximate the boundary conditions.

We have solved the S-limit equation for the first two states of the helium atom and for the ground state of the hydride ion using the second difference approximation. The radial cutoff for the ground state of helium was taken at 9 a.u. and for the excited state at 20 a.u. For the hydride ion the solution was required to vanish at 25 a.u. Equation (8) was solved for several grid sizes and the eigenvalues extrapolated using the polynomial representation of the difference error. From (7) we see that two eigenvalues are needed to eliminate the h^2-term, three for the h^2- and h^4-terms, etc. We have done this for the three states and present the results in Tables I-III.

The extrapolation of the S-limit for the helium ground state predicts an energy of -2.879031 a.u. with an uncertainty in the last figure. The previous best limit was found by Davis[15] and by Schwartz[7] to be -2.879028 a.u. Table I shows the extrapolated values found using successively more of the initial energies to be converging from above. Thus the best extrapolant should be an upper bound to the true S-limit. This value falls within the error bounds on Davis' predicted limit.

The results for the ^3S state of helium and the ground state of the hydride ion are less satisfactory. Davis[15,16] places the S-limits of these states at -2.1742652 a.u. and -0.5144940 a.u., respectively. The MFD method is more difficult for these states because of their large radial extent. To achieve the accuracy that

we have, it was necessary to diagonalize a matrix as large as 22,500 by 22,5000 for the ^3S state and about 15,000 by 15,000 for the hydride ion.

In order to avoid this problem, we made the following coordinate transformation,

$$\begin{aligned} r_1 &= x_1^2 \\ r_2 &= x_2^2 \end{aligned} \tag{10}$$

and solved the Schrödinger equation on an evenly spaced grid in x_1 and x_2. The effect of this is to give a dense distribution of points near the nucleus and a sparse distribution in the tail regions, as viewed in the untransformed system. Not only is the radial cutoff less important in the new system, but since this is a more optimum distribution of points for our problem, we can use fewer points without losing accuracy.

Substituting the transformation into (3), the derivatives become,

$$1/r^2 \; \partial/\partial r(r^2 \, \partial/\partial r) = 1/4r \, (\partial^2/\partial x^2 - 1/x \, \partial/\partial x) \tag{11}$$

The first derivative is eliminated by the transformation

$$\psi_0 \, (x_1 x_2) = \frac{u_0(x_1 x_2)}{x_1^{3/2} x_2^{3/2}}$$

which leads to the following equation for $u_0(x_1x_2)$,

$$\left[-\tfrac{1}{2}\left(\frac{1}{4r_1}\left(\partial^2/\partial x_1^2 - \frac{3}{4r_1}\right) + \frac{1}{4r_2}\left(\partial^2/\partial x_2^2 - \frac{3}{4r_2}\right)\right) - z/r_1 - z/r_2 + 1/r_>\right]$$

$$u_0(x_1x_2) \cong E \cdot u_0(x_1x_2) \quad . \tag{12}$$

This equation was solved for the hydride ion with a 25 a.u. radial cutoff (5 a.u. on the square root grid) using grids ranging from 25 to 50 strips. The results extrapolated to E = -0.514497 a.u. and were converging from below. Representation of the difference error using only even powers of h was not as efficient for the new coordinates giving an energy of -0.514557 a.u., also converging from below. Therefore a polynomial containing both even and odd powers, but leading off with h^2, was used. The square root grid reduced the computation time by a factor of 7 for this case.

In an effort to improve the MFD method further, the fourth difference approximation was used to re-solve the equations for helium and the hydride ion on the square root grid. The cutoff for helium was kept at 9 a.u. but the cutoff for the hydride ion was taken at 30 a.u. The energies obtained using both second and fourth difference approximations are given in Table IV. While the fourth difference results are improved, the accuracy is not sufficient to be used without extrapolation. In order to find the appropriate extrapolation method, the energies were fitted to various polynomials in

the grid size using successively finer grids. By studying the trends in the extrapolants and the coefficients of the power series, we can determine the most efficient form to represent the difference error. The results for the polynomial fits of the helium energies are given in Table V.

The best representation of the difference error for the second difference approximation is given by the polynomial containing a cubic term in h. For the fourth difference results the polynomial

$$E(h) = E(0) + C_2h^2 + C_4h^4 + C_5h^5 + C_6h^6 + \ldots \qquad (13)$$

appears to give the best extrapolant, but by eliminating odd powers entirely we obtain accurate results and uniform convergence from above. We should point out that while the error in the fourth difference approximation leads off as h^4, using second differences at the boundary introduces the h^2 term. Table VI gives the equivalent information for the hydride ion. The fourth difference approximation predicts an S-limit energy of -0.514491 ± 0.000001 a.u. which is within the error bounds of Davis' result.

Even though the wavefunctions found by the MFD method are only known at discrete points, there is no problem extracting the same information from them that a variational solution can yield. In fact, the numerical solutions are generally of a higher quality over all regions of space than the variational functions. This is

illustrated by the local energy which agrees with the eigenvalue to six or more decimal places at every grid point. Properties are easily calculated by quadrature methods which amount to nothing more than double summations. These are then extrapolated in the same manner as the energy.

We have calculated several properties from the fourth difference S-limit functions for helium and the hydride ion and compare them to the radial CI and Hartree-Fock values in Table VII. The agreement is very good except for $\langle r_1^2 + r_2^2 \rangle$, which indicates that more diffuse basis functions were needed in the radial CI calculations.

Contour and perspective plots of the two helium states and the hydride ion ground state are given in Fig. 1. We have plotted the square of the function $u_0(r_1 r_2)$ in each case. The contour plots show the regions $r_1, r_2 \leq 4.5$ a.u. for the ^1S state of helium, $r_1, r_2 \leq 10$ a.u. for the ^3S state, and $r_1, r_2 \leq 12.5$ a.u. for the hydride ion. The nucleus is positioned at the lower left corner and the constant contour increment is given in the upper right corner. The lowest contour is labeled. In the 3-D plots the regions shown are $r_1, r_2 \leq 7.5$ a.u. for the helium ^1S state, $r_1, r_2 \leq 13.3$ a.u. for the ^3S state, and $r_1, r_2 \leq 18.7$ a.u. for the hydride ion. Figure 2 gives the viewer's orientation for these plots. The functional axis has the same scale in each case so that the heights of the surfaces can be compared. The contour plot for the hydride ion shows the minimum in the solution along

the line $r_1 = r_2$. The helium atom shows a similar feature for large radial distances but only slightly. This minimum is not present for the Hartree-Fock wavefunction which does not predict a stable ground state for the ion.

While including radial correlation relative to the Hartree-Fock model leads to a stable ion, the S-limit functions gives unreasonable values for some properties. The exact value of $\langle r_1^2 + r_2^2 \rangle$ is 23.827 a.u.,[17] which is about two-thirds of the S-limit value. If we include the higher partial waves in our expansion of the exact solution, the S-wave contracts and the expectation values approach the exact results. This is illustrated for the helium atom in the next section.

E. SOLUTION OF THE COUPLED PARTIAL WAVE EQUATIONS FOR THE HELIUM ATOM

The MFD method was applied to the sets of coupled equations that result when (1) is truncated at $\ell = 1, 2, 3$, and 4. We decided to use the second difference approximation on the linear grid with a 9 a.u. cutoff since this proved to be very accurate for the S-limit. For a more diffuse state the square root grid would have been used.

The extrapolation tables for the angular limits are given in Table VIII. The results converge from above so that the best extrapolants should be upper bounds to the true limit. These are compared to various CI calculations in Table IX. We note that the

numerical G-limit is superior to each of the other calculations. Tycko, Thomas, and King[18] were only able to obtain an energy of -2.90344 a.u. using 15 partial waves. This illustrates the difficulty in representing the functional coefficients with orbital products for the higher partial waves. As pointed out by Schwartz,[7] this led to the erroneous conclusion that the majority of the error was in the S-limit and that the contribution from the higher waves could be neglected. The CI calculations generally do worse for the higher angular limits, because to keep the calculations from becoming intractable, fewer configurations are used to represent the functional coefficients. The MFD method actually becomes easier for these equations since the coefficients have less and less amplitude and are concentrated nearer the line $r_1 = r_2$.

The energy can be expressed in the form,

$$E = \sum_{\ell} E_{\ell} \tag{14}$$

where

$$E_{\ell} = \langle \ell \left| -\tfrac{1}{2}\nabla_1^2 - \tfrac{1}{2}\nabla_2^2 - z/r_1 - z/r_2 \right| \ell \rangle + \sum_{\ell'} \sum_{k} \langle \ell \left| r_<^k / r_>^{k+1} \right| \ell' \rangle \, C^k(\ell o, \ell' o)$$

$$= T_{\ell} + V_{\ell} \tag{15}$$

Using the G-limit solution, we have calculated the different terms in this expression. The electron repulsion matrix elements $\sum_k \langle \ell \mid r_<^k / r_>^{k+1} \mid \ell' \rangle \; C^k(\ell o, \ell' o)$ are presented in Table X and the energy analysis in Table XI. These results illustrate the small but important effects the higher partial waves have on the energy. Several properties were studied in the same manner and compared to the exact values in Table XII. The accuracy is very good, being about four decimal places in every case except for $\langle r_1^2 + r_2^2 \rangle$. The value is still too large and would improve if more partial waves were used.

The contour plots of each functional coefficient for the G-limit are given in Fig. 3. Again the squares of the functions $u_\ell(r_1 r_2)$ are plotted over the region $r_1, r_2 \leq 4.5$ a.u. The peakedness of the higher partial waves about the line $r_1 = r_2$ is quite evident. Since the amplitude of the functions for $\ell > 0$ is negative, their effect is to reduce the electron density in this region. Figure 4 gives the perspective plots of the S- and P-waves using the same scale along the functional axis. By integrating over the radial variables, we found the volume under the P-wave surface to be 0.4% of that under the S-wave. The remaining waves were too small to be shown with this scale, but the same integration showed the D-wave to be 5% of the P-wave and the F-wave about 17% of the D-wave.

F. DISCUSSION

The results presented here demonstrate that the numerical solution of partial differential equations can give accuracy competitive with variational methods. The values found for the S-limits of helium and the hydride ion are superior to any previous calculation and agree well with the predicted limits given by Davis. More importantly the same accuracy was found when the coupled equations were solved for helium. The equations describing the pair correlations in atoms offer virtually no new considerations once they are derived. The same program which was used for the helium atom has been used to calculate the valence pair correlation energy for beryllium and the MFD method has been applied to the first-order hydrogenic pair equations for lithium. The results were consistently accurate in all cases.

The calculations reported here were carried out on the CDC 6600 and IBM 360-75 computers. The IBM 360-75 results were found using double precision arithmetic to avoid round-off errors.

REFERENCES

*This work is based on a thesis submitted by N. W. Winter in partial fulfillment of the requirements for the degree of Doctor of Philosophy in Chemistry, California Institute of Technology.

†Present address: Battelle Memorial Laboratory, Columbus, Ohio.

‡Present address: Chemistry Department, Rhode Island College, Providence, Rhode Island.

§Contribution No. .

[1]O. Sinanoglu, J. Chem. Phys. 36, 3198 (1962).

[2]R. K. Nesbet, Phys. Rev. 175, 2 (1968).

[3]O. Sinanoglu, Advan. Chem. Phys. 6, 315 (1964).

[4]R. K. Nesbet, ibid. 9, 321 (1965).

[5]E. A. Hylleraas, Z. Phyzik 54, 347 (1929).

[6]C. Schwartz, Methods in Comp. Phys. 2, 241 (1963).

[7]C. Schwartz, Phys. Rev. 126, 1015 (1962).

[8]N. W. Winter, D. Diestler, and V. McKoy, J. Chem. Phys. 48, 1879 (1968).

[9]V. McKoy and N. W. Winter, ibid. 48, 5514 (1968).

[10]P. Luke, R. Meyerott, and W. Clendenin, Phys. Rev. 85, 401 (1952).

[11]The grid size is given by $h = r_n/n-1$ where r_n is the last grid point and n-1 is the number of strips in the grid.

[12]H. C. Bolton and H. I. Scoins, Proc. Cambridge Phil. Soc. 53, 150 (1956).

[13]This is sometimes called Richardson extrapolation. L. Richardson and J. Gaunt, Trans. Roy. Soc. (London) A226, 299 (1927).

[14]L. Fox, "Numerical Solution of Two-Point Boundary Problems," (Oxford University Press, London, 1957).

[15]H. L. Davis, J. Chem. Phys. 39, 1827 (1963).

[16]H. L. Davis, ibid. 39, 1183 (1963).

[17]C. L. Pekeris, Phys. Rev. 126, 1470 (1962).

[18]D. H. Tycko, L. H. Thomas, and K. M. King, ibid. 109, 369 (1958).

TABLE I. The S-limit energy of the helium atom ground state.

Grid Size	Initial Energies				
9/20	-2.41777793				
	-2.78269471				
25	-2.54914797	-2.86063837			
	-2.82599674	-2.87602834			
30	-2.63374065	-2.87100304	-2.87862431		
	-2.84804064	-2.87797531	-2.87898631		
35	-2.69059575	-2.87525177	-2.87891480	-2.87902636	
	-2.85994551	-2.87862484	-2.87901995	-2.87902778	
40	-2.73028710	-2.87712569	-2.87899367	-2.87902759	-2.87903050
	-2.86673274	-2.87886089	-2.87902601	-2.87903020	
45	-2.75892384	-2.87801064	-2.87901638	-2.87902975	
	-2.87079279	-2.87895340	-2.87902882		
50	-2.78923840	-2.87845474	-2.87902459		
	-2.87332566	-2.87899295			
55	-2.79634490	-2.87869021			
	-2.87496483				
60	-2.80890225				

TABLE II. The S-limit energy of the helium atom triplet excited state.

Grid Size	Initial Energies			
20/50	-1.92155742			
	-2.14582478			
75	-2.04615040	-2.17185406		
	-2.16534674	-2.17411134		
100	-2.09829880	-2.17375017	-2.17425468	
	-2.17072494	-2.17423875		
125	-2.12437221	-2.17411661		
	-2.17260920			
150	-2.13911129			

TABLE III. The S-limit energy of the hydride ion on the linear grid.

Grid Size	Initial Energies			
25/50	-0.48265239			
		-0.51258653		
75	-0.49928247		-0.51438770	
		-0.51393741		-0.51447016
100	-0.50569401		-0.51445695	
		-0.51426992		
125	-0.50878134			

TABLE IV. S-limit energies for the helium atom and the hydride ion on the square-root grid.

Grid Size	2nd Differences	4th Differences
	Helium	
3/20	-2.94612243	-2.91652455
25	-2.92313414	-2.90253697
30	-2.91042377	-2.89514153
35	-2.90260678	-2.89076150
40	-2.89743538	-2.88795443
45	-2.89382642	-2.88604778
50	-2.89120257	-2.88469360
55	-2.88923204	-2.88369718
60	-2.88771261	-2.88294265
	Hydride	
$\sqrt{30}/25$	—	-0.52200314
30	-0.52387559	-0.51960370
35	-0.52151323	-0.51819644
40	-0.51996146	-0.51730055
45	-0.51888329	-0.51669499
50	-0.51810167	-0.51626649
55	-0.51751582	-0.51595212
60	-0.51706469	-0.51571463

TABLE V. Polynomial fits for the helium atom S-limit.[a]

Grids Used in the Polynomial Fit	$h^2\ h^4\ h^6\ldots$	$h^2\ h^3\ h^4\ldots$	$h^2\ h^4\ h^5\ldots$
		Second Differences	
(20-25)	-2.88226607	-2.88226607	-2.88226607
(20-30)	-2.88095296	-2.88066116	-2.88095296
(20-35)	-2.88007081	-2.87954872	-2.87997000
(20-40)	-2.87968114	-2.87930272	-2.87955936
(20-45)	-2.87946967	-2.87918352	-2.87935227
(20-50)	-2.87934222	-2,87912250	-2.87923738
(20-55)	-2.87926080	-2.87909307	-2.87917124
(20-60)	-2.87920098	-2.87903506	-2.87911356
		Fourth Differences	
(20-25)	-2.87767016	-2.87767016	-2.87767016
(20-30)	-2.87886455	-2.87912997	-2.87886455
(20-35)	-2.87898118	-2.87905020	-2.87899451
(20-40)	-2.87901272	-2.87904011	-2.87902257
(20-45)	-2.87902253	-2.87903181	-2.87902766
(20-50)	-2.87902500	-2.87902523	-2.87902645
(20-55)	-2.87902682	-2.87903194	-2.87902896
(20-60)	-2.87902886	-2.87903698	-2.87903236

[a]Square root grid with a 9 a.u. cutoff.

TABLE VI. Polynomial fits for the hydride ion S-limit.[a]

Grids Used in the Polynomial Fit	$h^2\ h^4\ h^6 \ldots$	$h^2\ h^3\ h^4 \ldots$	$h^2\ h^4\ h^5 \ldots$
		Second Differences	
(30-35)	-0.51459713	-0.51459713	-0.51459713
(30-40)	-0.51479082	-0.51474569	-0.51479082
(30-45)	-0.51466352	-0.51457709	-0.51464655
(30-50)	-0.51460482	-0.51453888	-0.51458322
(30-55)	-0.51457261	-0.51452280	-0.51455157
(30-60)	-0.51454715	-0.51448762	-0.51452128
		Fourth Differences	
(25-30)	-0.51415043	-0.51415043	-0.51415043
(25-35)	-0.51445461	-0.51452703	-0.51445461
(25-40)	-0.51447961	-0.51449563	-0.51448274
(25-45)	-0.51448779	-0.51449584	-0.51449060
(25-50)	-0.51448998	-0.51449172	-0.51449120
(25-55)	-0.51449188	-0.51449635	-0.51449370
(25-60)	-0.51449172	-0.51448720	-0.51449081

[a]Square root grid with a 30 a.u. cutoff.

TABLE VII. Comparison of the properties predicted by the S-limit wavefunctions to the radial configuration interaction and Hartree-Fock results for He and H^-.

	Helium (^1S)			Hydride Ion		
Property	FD	RCI[a]	HF	FD	RCI[b]	HF[c]
E	-2.87903	-2.87900	-2.86168	-0.51449	-0.51446	-0.4880
V	-5.7581	-5.7580	-5.7238	-1.0290	-1.0289	–
V/E	2.0000	2.0000	2.0000	2.0001	2.0000	–
$\langle 1/r_{12} \rangle$	0.9867	0.9867	1.0258	0.2983	(0.2973)	–
$\langle 1/r_1 + 1/r_2 \rangle$	3.3724	3.3724	3.3748	1.3273	–	1.3714
$\langle r_1 + r_2 \rangle$	1.8690	1.8688	1.8546	6.2079	6.207	5.0078
$\langle r_1^2 + r_2^2 \rangle$	2.4221	2.4206	2.3696	34.518	34.44	18.821

[a]The basis set for the RCI calculation consisted of 1s, 2s, and 3s Slater orbitals with $\zeta = 3.7530$ and 1s′ and 2s′ orbitals with $\zeta = 1.5427$.

[b]W. A. Goddard, J. Chem. Phys. 48, 1008 (1968); the value in parenthesis is from a G_1 calculation.

[c]K. E. Baynard, J. Chem. Phys. 48, 2121 (1968).

TABLE VIII. Extrapolation tables for the angular limits of the helium atom.

P-Limit

Grid Size				
9/20	-2.44961031			
		-2.80393359		
25	-2.57716669		-2.88179394	
		-2.84718934		-2.89746339
30	-2.65967361		-2.89234683	
		-2.86930729		-2.89945145
35	-2.71529071		-2.89667621	
		-2.88128120		-2.90011032
40	-2.75419473		-2.89858405	
		-2.88811689		-2.90034786
45	-2.78230185		-2.89948359	
		-2.89220890		
50	-2.80318419			

D-Limit

9/20	-2.45315095			
		-2.80642476		
25	-2.58032952		-2.88406803	
		-2.84955991		-2.89970953
30	-2.66259436		-2.89460210	
		-2.87162139		-2.90169399
35	-2.71805051		-2.89892372	
		-2.88356616		-2.90235339
40	-2.75684324		-2.90082909	
		-2.89038608		-2.90259251
45	-2.78487075		-2.90172844	
		-2.89446933		
50	-2.80569448			

TABLE VIII. cont'd.

F-Limit

Grid Size				
9/20	-2.45423836			
	-2.80714175			
25	-2.58128358	-2.88465952		
	-2.85020718	-2.90026697		
30	-2.66345468	-2.88517066	-2.90290473	
	-2.87223011	-2.90224529	-2.90326875	
35	-2.71884408	-2.89948176	-2.90319684	-2.90331188
	-2.88415271	-2.90290315	-2.90330498	
40	-2.75758829	-2.90138254	-2.90327795	
	-2.89095955	-2.90314302		
45	-2.78557979	-2.90228038		
	-2.89503505			
50	-2.80637629			

G-Limit

9/20	-2.45471902			
	-2.80744677			
25	-2.58170101	-2.88489007		
	-2.85047082	-2.90047129		
30	-2.66382512	-2.89538354	-2.90310098	
	-2.87246889	-2.90244355	-2.90346346	
35	-2.71917959	-2.89968574	-2.90339186	-2.90350556
	-2.88437626	-2.90309917	-2.90349882	
40	-2.75789756	-2.90158209	-2.90347208	
	-2.89117363	-2.90333783		
45	-2.78586908	-2.90247752		
	-2.89524303			
50	-2.80665013			

TABLE IX. Comparison of the angular limits for the helium atom.

Limit	Numerical		Weiss[b]		Nesbet[c]		Tycko[d]	
S	-2.87903		-2.87896		-2.87887		-2.87892	
		-0.02148		-0.02143		-0.02142		-0.02152
P	-2.90051		-2.90039		-2.90029		-2.90044	
		-0.00225		-0.00219		-0.00209		-0.00225
D	-2.90276		-2.90258		-2.90238		-2.90269	
		-0.00055		-0.00049		-0.00038		-0.00054
F	-2.90331		-2.90307		-2.90276		-2.90323	
		-0.00020		-0.00013		—		-0.00014
G	-2.90351		-2.90320		—		-2.90337	
Exact[a]	-2.90372							

[a]C. L. Pekeris, Phys. Rev. 115, 1216 (1959).

[b]A. W. Weiss, Phys. Rev. 122, 1826 (1961).

[c]R. K. Nesbet and R. E. Watson, Phys. Rev. 110, 1073 (1958).

[d]D. H. Tycko, L. H. Thomas, and K. M. King, Phys. Rev. 109, 369 (1958).

TABLE X. Electron repulsion matrix.

ℓ	$\langle \ell \vert 1/r_{12} \vert 0 \rangle$	$\langle \ell \vert 1/r_{12} \vert 1 \rangle$	$\langle \ell \vert 1/r_{12} \vert 2 \rangle$	$\langle \ell \vert 1/r_{12} \vert 3 \rangle$	$\langle \ell \vert 1/r_{12} \vert 4 \rangle$
0	0.988972	-0.020919	-0.002646	-0.000695	-0.000255
1	-0.020919	0.004461	0.000428	0.000107	0.000038
2	-0.002646	0.000428	0.000225	0.000041	0.000014
3	-0.000695	0.000107	0.000041	0.000033	0.000008
4	-0.000255	0.000038	0.000014	0.000008	0.000007_8
$\sum_{\ell}$	0.964457	-0.015885	-0.001938	-0.000506	-0.000187

TABLE XI. Partial wave analysis of the energy for helium.

ℓ	T_ℓ	$V_{\ell\ \mathrm{nuc}}$	V_ℓ	E_ℓ
0	2.877088	-6.732944	-5.768487	-2.891399
1	0.022998	-0.018653	-0.034538	-0.011490
2	0.002222	-0.000810	-0.002748	-0.000527
3	0.000542	-0.000110	-0.000615	-0.000073
4	0.000194	-0.000024	-0.000211	-0.000017
$\sum_\ell$	2.903044	-6.752541	-5.806599	-2.903506

TABLE XII. Partial wave analysis of expectation values for helium.

ℓ	$\langle r_1 + r_2 \rangle_\ell$	$\langle r_1^2 + r_2^2 \rangle_\ell$	$\langle 1/r_1 + 1/r_2 \rangle_\ell$	$\sum_{\ell'} \langle 1/r_{12} \rangle_{\ell\ell'}$
0	1.85014	2.37618	3.36647	0.96446
1	0.00837	0.01064	0.00933	0.01589
2	0.00039	0.00050	0.00041	0.00194
3	0.00006	0.00007	0.00006	0.00051
4	0.00001_3	0.00001_6	0.00001_2	0.00019
$\sum_\ell$	1.85897	2.38741	3.37627	0.94594
Exact[a]	1.85894	2.38697	3.37663	0.94582

[a]C. L. Pekeris, Phys. Rev. 115, 1216 (1959).

Figure 1. Contour and perspective plots of the S-limit for the $(1s^2)\ ^1S$ and $(1s2s)\ ^3S$ states of helium and the $(1s^2)\ ^1S$ state of the hydride ion.

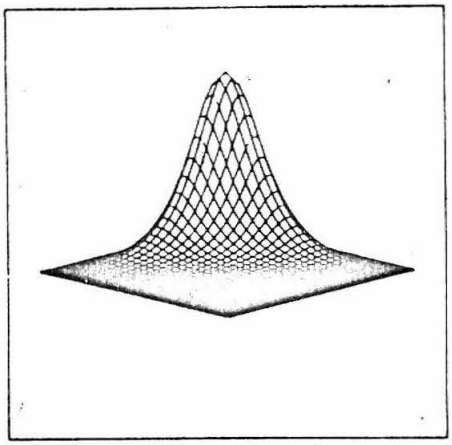

HELIUM GROUND STATE S-LIMIT FUNCTION

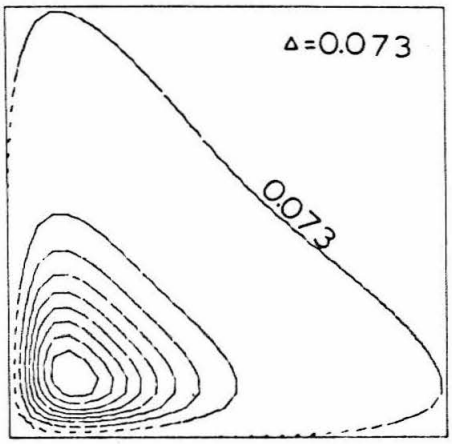

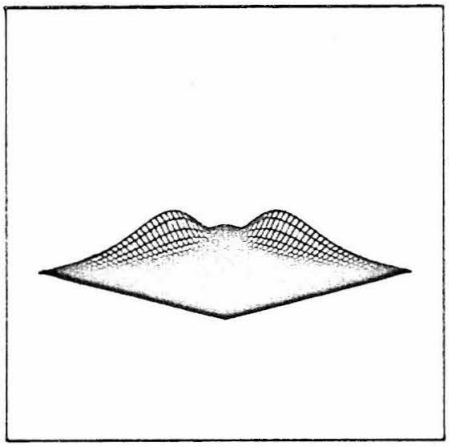

HELIUM TRIPLET STATE S-LIMIT FUNCTION

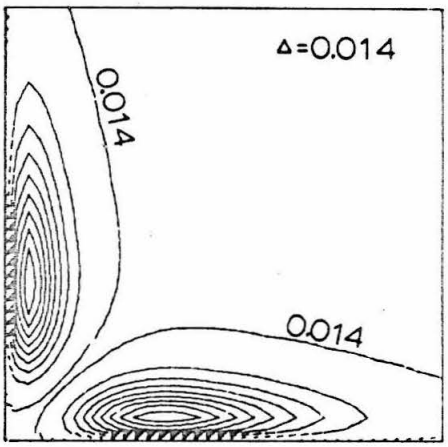

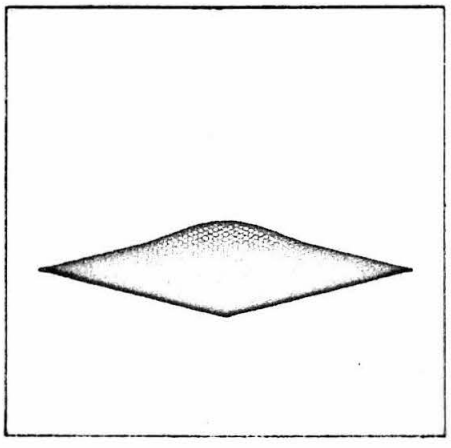

HYDRIDE ION S-LIMIT FUNCTION

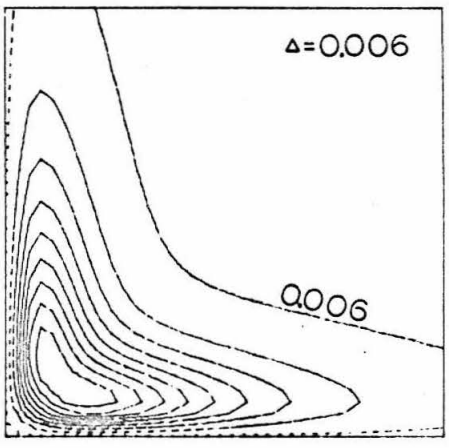

Figure 1

Figure 2. The viewer's orientation for the perspective plots.

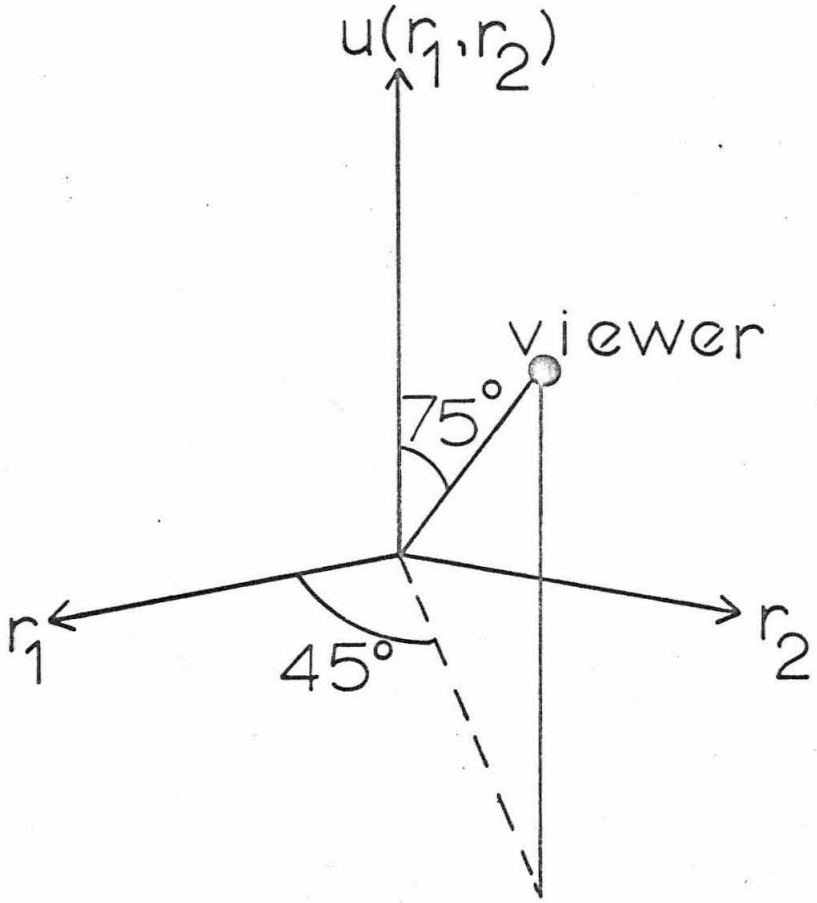

Figure 2

Figure 3. Contour plots of the functional coefficients for the helium G-limit wavefunction.

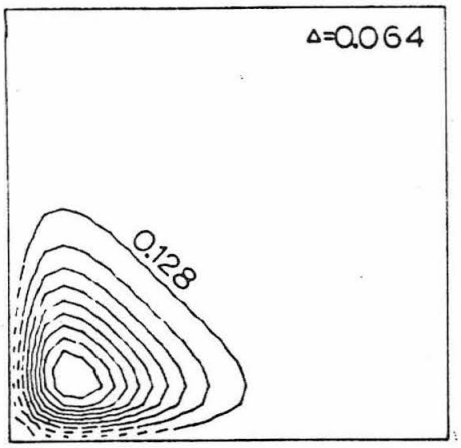

S-PARTIAL WAVE FOR THE HELIUM ATOM

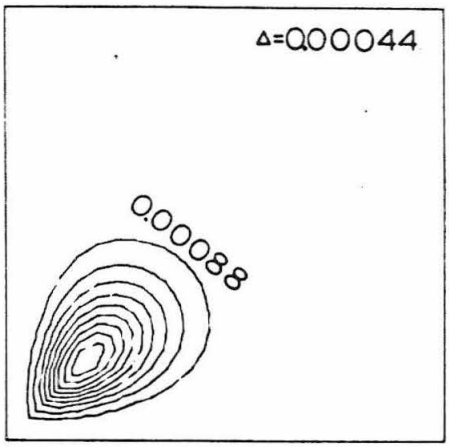

P-PARTIAL WAVE FOR THE HELIUM ATOM

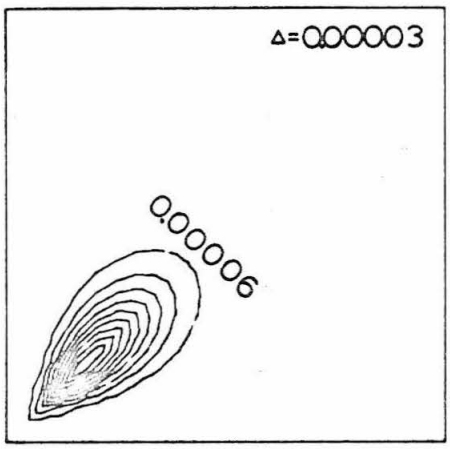

D-PARTIAL WAVE FOR THE HELIUM ATOM

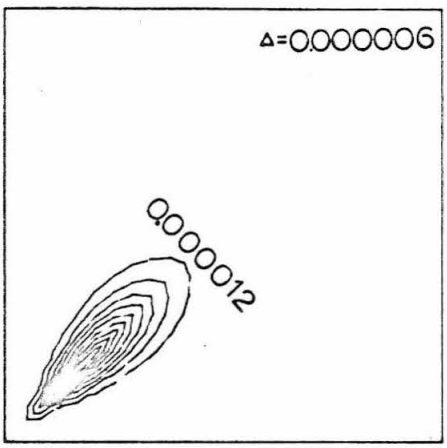

F-PARTIAL WAVE FOR THE HELIUM ATOM

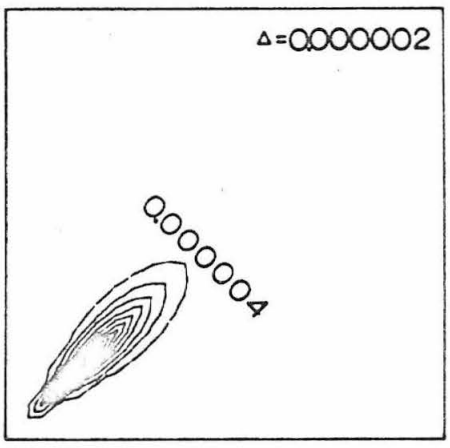

G-PARTIAL WAVE FOR THE HELIUM ATOM

Figure 3

Figure 4. Perspective plots of the S- and P-wave functional coefficients for the helium atom.

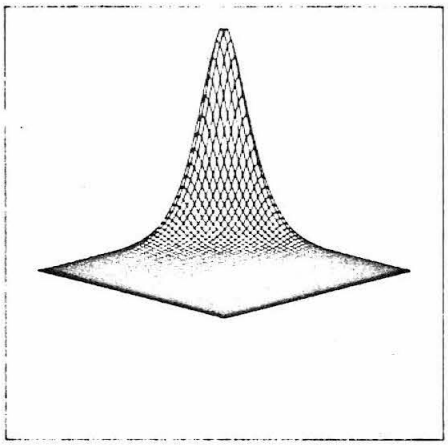

S-PARTIAL WAVE FOR THE HELIUM ATOM

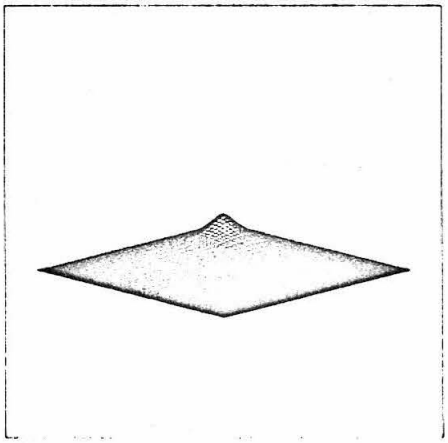

P-PARTIAL WAVE FOR THE HELIUM ATOM

Figure 4

II. NUMERICAL SOLUTION OF FIRST-ORDER PAIR EQUATIONS

A. INTRODUCTION

It was previously shown that the functional coefficients of the partial wave expansion for the first-order pair functions could be obtained with the matrix finite difference (MFD) method.[1] Taking the full electron interaction as the perturbation, the method has been extended to the three pair equations that determine the first-order wavefunction for the lithium isoelectronic series. The pair functions are independent of the nuclear charge and can be used to construct the first-order wavefunctions for other atoms when the remaining hydrogenic pair functions are determined.[2] The method is not variational and therefore can be applied without orthogonality constraints to the excited pair functions that are not the lowest of their symmetry. In addition, the calculation of the total second- and third-order energy involves none of the difficult integrals that occur for the complicated variational functions containing interelectronic coordinates.

The first-order equation is reduced to its pair components in the first section, using the theory developed by Sinanoglu.[3] The pair functions are then expanded in a partial wave series and the coefficients are determined with the MFD method. The results found using both the second difference and fourth difference approximations are presented for the ground and excited states of the two-electron atom. Finally, the total second- and third-order energies are calculated for the lithium series.

B. REDUCTION OF THE FIRST-ORDER EQUATION

With the entire electron interaction as the perturbation, the dependence on the nuclear charge can be removed from the perturbation equations. By scaling the radial distance to the nuclear charge Z and measuring the energy in units of Z^2, the zero-order Hamiltonian can be written,

$$H_0 = \sum_i \left(-\tfrac{1}{2}\nabla_i^2 - 1/r_i\right) = \sum_i h_i \qquad (1)$$

and the perturbation becomes,

$$H_1 = 1/Z \sum_{i<j} 1/r_{ij} \quad . \qquad (2)$$

In these coordinates the expansion parameter is seen to be 1/Z and accordingly the total energy and wavefunction can be expressed as follows,

$$\begin{aligned} E &= E_0 + 1/Z \cdot E_1 + 1/Z^2 \cdot E_2 + 1/Z^3 \cdot E_3 + \cdots \\ \Psi &= \Psi_0 + 1/Z \cdot \Psi_1 + 1/Z^2 \cdot \Psi_2 + 1/Z^3 \cdot \Psi_3 + \cdots \end{aligned} \qquad (3)$$

where knowledge of Ψ_1 is sufficient to determine the energy through third-order. The zero-order solution and energy are

$$\Psi_0 = \mathcal{A}\,(\phi_1(1)\ \phi_2(2)\ \phi_3(3)\cdots\phi_N(N))$$
$$E_0 = \sum_i \epsilon_i \tag{4}$$

where $\mathcal{A} = \frac{1}{\sqrt{N!}}\sum_P (-1)^P P$ is the antisymmetrizer and ϕ_i are hydrogenic spin-orbitals which satisfy $h_i\phi_i = \epsilon_i\phi_i$. For some states Ψ_0 will be a linear combination of determinants. The first-order equation is

$$\sum_i (h_i - \epsilon_i)\ \Psi_1 = (E_1 - \sum_{i<j} 1/r_{ij})\ \Psi_0 \tag{5}$$

with

$$E_1 = \langle\Psi_0|\sum_{i<j} 1/r_{ij}|\Psi_0\rangle \tag{6}$$
$$= \sum_{i<j} J_{ij} - K_{ij}$$

and

$$J_{ij} = \langle\phi_i(1)\ \phi_j(2)\,|\,1/r_{12}\,|\,\phi_i(1)\ \phi_j(2)\rangle$$
$$K_{ij} = \langle\phi_i(1)\ \phi_j(2)\,|\,1/r_{12}\,|\,\phi_i(2)\ \phi_j(1)\rangle$$

The right-hand side of (5) can be rewritten as,

$$(E_1 - \sum_{i<j} 1/r_{ij})\,\Psi_0 = a\sum_{i<j} \Phi_{ij}\,(J_{ij} - K_{ij} - 1/r_{ij})^{\frac{1}{2}}(1 - P_{ij})\phi_i(i)\phi_j(j) \tag{7}$$

where Φ_{ij} is the orbital product without $\phi_i(i)$ and $\phi_j(j)$. The permutation P_{ij} operates only on the particle labels. Equation (7) suggests the following form for Ψ_1,

$$\Psi_1 = a\sum_{i<j} \Phi_{ij}\,\tfrac{1}{2}(1 - P_{ij})\,w_{ij}(i,j) \quad . \tag{8}$$

Substituting into the first-order equation and making use of the orbital equations, we obtain

$$a\sum_{i<j} \Phi_{ij}(h_i + h_j - \epsilon_i - \epsilon_j)\,\tfrac{1}{2}(1 - P_{ij})\,w_{ij}(ij) =$$

$$a\sum_{i<j} \Phi_{ij}\,(J_{ij} - K_{ij} - 1/r_{ij})^{\frac{1}{2}}\,(1 - P_{ij})\,\phi_i(i)\,\phi_j(j) \tag{9}$$

A sufficient condition that Ψ_1 satisfies (9) is

$$(h_1 + h_2 - \epsilon_i - \epsilon_j)\,(1 - P_{12})\,w_{ij}(1,2) =$$

$$(J_{ij} - K_{ij} - 1/r_{12})\,(1 - P_{12})\,\phi_i(1)\,\phi_j(2) \quad . \tag{10}$$

The necessary condition that a solution to this pair equation exists is[4]

$$\langle \phi_k(1)\, \phi_\ell(2) \,|\, J_{ij} - K_{ij} - 1/r_{12} \,|\, (1 - P_{12})\, \phi_i(1)\, \phi_j(2) \rangle \;=\; 0 \qquad (11a)$$

where $\phi_k(1)\, \phi_\ell(2)$ is any solution to

$$(h_1 + h_2 - \epsilon_i - \epsilon_j)\, \phi_k(1)\, \phi_\ell(2) \;=\; 0\,. \qquad (11b)$$

For the ground state of the three-electron atom the following three-pair equations must be solved,

$$(h_1 + h_2 - 2\epsilon_{1s})\, G(1,2)\, (\alpha\beta - \beta\alpha) \;=$$

$$(J_{1s1s} - 1/r_{12})\, 1s(1)\, 1s(2)\, (\alpha\beta - \beta\alpha) \qquad (12a)$$

$$(h_1 + h_2 - \epsilon_{1s} - \epsilon_{2s})\, T(1,2)\, \alpha\alpha \;=$$

$$(J_{1s2s} - K_{1s2s} - 1/r_{12})\, (1s(1)2s(2) - 1s(2)2s(1))/\sqrt{2}\, \alpha\alpha \qquad (12b)$$

$$(h_1 + h_2 - \epsilon_{1s} - \epsilon_{2s})\, (1 - P_{12})\, F(1,2)\beta\alpha \;=$$

$$(J_{1s2s} - 1/r_{12})\, (1s(1)\beta\; 2s(2)\alpha \;-\; 1s(2)\beta\; 2s(1)\alpha) \qquad (12c)$$

Both (12a) and (12b) satisfy the existence condition; however, (12c) does not, since the function $(1 - P_{12})\, 1s(1)\alpha\, 2s(2)\beta$ is a solution to (11b) and $\langle 1s(1)\alpha\, 2s(2)\beta \,|\, J_{1s2s} - 1/r_{12} \,|\, (1 - P_{12})\, 1s(1)\beta\; 2s(2)\alpha \rangle \neq 0$. Sinanoglu[5] has shown that by expanding both sides of (12c) in sym-

metry states of the two-electron atom,

$$(1 - P_{12})\ 1s(1)\beta\ 2s(2)\alpha = \tfrac{1}{2}[\,(1s(1)2s(2) - 1s(2)2s(1))\,(\alpha\beta + \beta\alpha) - (1s(1)2s(2) + 1s(2)2s(1))\,(\alpha\beta - \beta\alpha)] \tag{13}$$

$$(1 - P_{12})\ F(1,2)\beta\alpha = T(1,2)(\alpha\beta + \beta\alpha)/\sqrt{2} - S(1,2)(\alpha\beta - \beta\alpha)/\sqrt{2}$$

an equation for T(1, 2) is obtained which is identical to (12b) except for the spin function, and the following equation is obtained for S(1, 2),

$$(h_1 + h_2 - \epsilon_{1s} - \epsilon_{2s})\,S(1,2)\,(\alpha\beta - \beta\alpha) = (J_{1s2s} + K_{1s2s} - 1/r_{12})\,(1s(1)\,2s(2) + 1s(2)\,2s(1))/\sqrt{2}\ (\alpha\beta - \beta\alpha) \tag{14}$$

The total first-order function can be expressed in terms of the solutions to (12a), (12b), and (14) as follows,

$$\Psi_1 = 1/\sqrt{2}\,\mathcal{A}\Big|G(1,2)\,(\alpha\beta - \beta\alpha)/\sqrt{2}\quad 2s(3)\,\alpha + [\,T(1,2)\,(\alpha\beta + \beta\alpha)/\,2 - S(1,2)\,(\alpha\beta - \beta\alpha)/\,2]\,1s(3)\alpha - T(1,2)\,\alpha\alpha\ 1s(3)\beta\Big| \tag{15}$$

where (11a) is satisfied in each case. The pair functions G(1, 2), T(1, 2), and S(1, 2) are identically the first-order wavefunctions for the $(1s1s)^1S$, $(1s2s)^3S$, and $(1s2s)^1S$ states of the helium series.

C. SOLUTION OF THE FIRST-ORDER PAIR EQUATION

Because the pair functions G, T, and S are spherically symmetric, the partial wave expansion for each is simply

$$U(r_1 r_2 \theta_{12}) = \sum_{\ell} u_{\ell}(r_1 r_2) \; P_{\ell}(\cos \theta_{12}) \tag{16}$$

By substituting this into the pair equation, multiplying both sides by $P_{\ell}(\cos \theta_{12})$, and integrating over the angular variables, the following partial differential equation for $u_{\ell}(r_1 r_2)$ is obtained,

$$\begin{aligned} &\left(-\tfrac{1}{2}\left(1/r_1^2 \; \partial/\partial r_1 \left(r_1^2 \; \partial/\partial r_1\right) + 1/r_2^2 \; \partial/\partial r_2 \left(r_2^2 \; \partial/\partial r_2\right)\right) - 1/r_1 - 1/r_2\right. \\ &\quad \left. + \ell(\ell+1)/2r_1^2 + \ell(\ell+1)/2r_2^2 - \epsilon_i - \epsilon_j\right) \cdot u_{\ell}(r_1 r_2) \\ &= \left(E_1(\text{pair})\, \delta_{\ell 0} - \frac{r_<^{\ell}}{r_>^{\ell+1}}\right) R(r_1 r_2) \end{aligned} \tag{17}$$

where $E_1 = 5/8$ for the (1s1s) pair, $E_1 = 137/729$ for the $(1s2s)\,^3S$ pair, and $E_1 = 169/729$ for the $(1s2s)\,^1S$ pair. The function R is the radial part of the zero-order function for each state. The boundary conditions on $u_{\ell}(r_1 r_2)$ require that it is finite for r_1 or $r_2 = 0$ and that it vanish for r_1 or $r_2 = \infty$. The set of equations for the functional coefficients are not coupled and are solved independently for each partial wave using the MFD method.

The details of the numerical analysis have already been discussed;[1, 6, 7] however, two important modifications have been

introduced which allow the diffuse excited states to be handled efficiently. First, the radial cutoff (the point at which $u_\ell(r_1 r_2)$ is required to vanish) for these states must be taken farther out than for the (1s1s) pair previously treated. Therefore, even with extrapolation, a very large number of points are needed to achieve comparable accuracy. To avoid this difficulty, the following coordinate transformation was introduced into the pair equation,

$$\begin{aligned} r_1 &= x_1^2 \\ r_2 &= x_2^2 \end{aligned} \tag{18}$$

The grid points in the transformed system are closely spaced near the nucleus and farther apart in the tail regions, as viewed in the untransformed system. This means that by using a large radial cutoff and relatively few points, the regions important to the accurate solution of (17) are not neglected.

The second modification in the MFD method was to improve the difference approximation of the derivatives. Instead of truncating the difference expansion at the second difference approximation, the fourth difference is included giving the following improved approximation for the second derivative,

$$\begin{aligned} \left(\partial^2/\partial x^2\ u(x)\right)_{x=x_0} &= 1/h^2\left(-\tfrac{1}{12}\cdot u(x_0 + 2h) + \tfrac{4}{3}\cdot u(x_0 + h)\right. \\ &\left. - \tfrac{15}{6}\cdot u(x_0) + \tfrac{4}{3}\cdot u(x_0 - h) - \tfrac{1}{12}\cdot u(x_0 - 2h)\right) + O(h^4) \end{aligned} \tag{19}$$

where h is the grid size. The only difficulty occurs at the boundary points, where (19) requires values of the function outside the defined grid. This was resolved with the following approximations: at the point $x = x_{max} - h$, where x_{max} is the radial cutoff, $u(x + 2h)$ was set to zero, and at $x = h$ the value $u(x - 2h)$ was set equal to $u(x)$. The latter assumption was arrived at by investigating the power series form of $u(x)$ for small x and can be shown to introduce an error of the order of the difference truncation error, if the coordinate transformation (18) is used. An alternative would be to use the usual second difference approximation at the boundaries and the fourth difference approximation elsewhere. Actually both approaches were used, depending on which method was used to solve the difference equations.

When substituted into (17), both the second difference and the fourth difference approximations lead to a set of simultaneous equations of the form

$$D \cdot \underset{\sim}{u} = \underset{\sim}{b} \qquad (20)$$

where D is a banded matrix. The second difference approximation produces a symmetric matrix, as does the fourth difference approximation with the modified boundary conditions. However, the mixed difference method leads to an unsymmetric matrix. The difference equations were solved with Gaussian elimination for the $\ell = 0$ partial wave and with the Gauss-Seidel method for $\ell > 0$. It was found that

for the higher partial wave equations the Gauss-Seidel method converged extremely fast, while for the S-wave the method diverged. Because the Gaussian elimination method is more efficient for symmetric matrices, the mixed difference approximation was not used for the S-wave, but was used for each of the higher waves.

D. CALCULATION OF THE SECOND- AND THIRD-ORDER ENERGIES FOR THE TWO-ELECTRON STATES

The partial-wave equations for each pair function were solved using both the usual second difference approximation and the improved difference formula given by (19). The second-order energy for each pair was found from

$$E_2(\text{pair}) = \sum_{\ell} \frac{1}{2\ell+1} \int u_\ell(r_1 r_2) \left(\frac{r_<^\ell}{r_>^{\ell+1}} - E_1(\text{pair}) \right) \cdot R(r_1 r_2)\, r_1^2 r_2^2\, dr_1 dr_2 \qquad (21)$$

The radial integral was calculated by the trapezoidal rule. The calculations were carried out at several grid sizes and the results extrapolated with Richardson's[8] method. Therefore, the difference and quadrature errors were eliminated in one step.

The extrapolation tables for the partial wave contributions to E_2 for the (1s1s) pair are given in Table I. The results were found using the second difference approximation and the untrans-

formed (linear) grid with a 12 a.u. cutoff. The first column of each table lists the number of strips used in each direction. The second column gives the initial results and the remaining columns contain the extrapolants. The latter were obtained using different sets of results from the first column. By displaying the results in this manner, it is possible to determine if the extrapolants are converging from above or below the true value. The partial wave contributions from all but the S-wave are converging from below and have converged to at least six decimal places. The results for the S-wave appear to oscillate, but the sub-table produced by the 45, 60, and 75 strip calculations is converging smoothly from below. The extrapolation tables for the ^3S and ^1S excited states are given in Tables II and III. These results illustrate the need for the modifications that were discussed in section C. The 120 strip S-wave calculation required the solution of nearly 14,000 linear equations which took about one hour on the IBM 360-75. The S-wave cutoff was taken at 24 a.u., which was still not far enough from the nucleus. Clearly it was not practical to re-solve the equations with a larger cutoff. The functions for $\ell > 0$ were much less diffuse and could be obtained easily in only a few minutes. For the ^3S state these waves were nearly converged without extrapolation. The S-wave for both states converged from above.

The three-pair equations were re-solved using the fourth difference approximation and the transformed (square root) grid.

The initial results and the final extrapolants for the first 10 partial wave contributions to E_2 are given for the three states in Tables IV, V, and VI. In addition, the third-order and total energies are also given for Z = 2. The radial cutoff was taken at 32 a.u. for all three calculations. The first important result that should be noted is the relatively few points that were needed to obtain better accuracy than the linear grid calculations. All of the numbers were found at one time with the same program, and the total time was about one hour. This could have been reduced to about 20 minutes, if fewer grids were used. For example, the results from the 20, 25, and 30 strip calculations gave the following extrapolants for the (1s1s) pair,

$$E_2(0) = -0.12532 \text{ a.u.}$$
$$E_2(1) = -0.02648 \text{ a.u.}$$
$$E_2(2) = -0.00387 \text{ a.u.}$$

which agree well with the best results.

The third-order energy for each pair was calculated from,

$$E_3(\text{pair}) = \sum_{\ell,\ell',k} \Omega^k(\ell o, \ell' o) \int u_\ell(r_1 r_2) \frac{r_<^k}{r_>^{k+1}} u_{\ell'}(r_1 r_2)\, r_1^2 r_2^2 dr_1 dr_2$$

$$- E_1(\text{pair}) \sum_\ell \frac{1}{2\ell+1} \int u_\ell(r_1 r_2)\, u_\ell(r_1 r_2)\, r_1^2 r_2^2 dr_1 dr_2$$

$$-2E_2(\text{pair}) \int u_0(r_1 r_2)\, R(r_1 r_2)\, r_1^2 r_2^2 dr_1 dr_2 \qquad (22)$$

where

$$\Omega^k(\ell o, \ell' o) = \int P_\ell(\cos\theta_{12})\, P_k(\cos\theta_{12})\, P_{\ell'}(\cos\theta_{12})\, d(\cos\theta_{12})$$

The total energies were found for the helium atom and compare well to the following values given by Knight and Scherr,[9]

$$E(1s1s, {}^1S) = -2.90331692 \text{ a.u.}$$
$$E(1s2s, {}^3S) = -2.17398777 \text{ a.u.}$$
$$E(1s2s, {}^1S) = -2.14611980 \text{ a.u.}$$

The partial wave contributions to the second-order energy have been calculated variationally by Byron and Joachain.[10] The contributions found by the two numerical approximations are compared to variational results in Tables VII, VIII, and IX. For the (1s1s) pair the first three columns agree closely for each partial wave. The values of $E_2(1)$ and $E_2(2)$ predicted by Knight and Scherr[9] are less accurate, but their total second-order energy was not found by a partial wave expansion and represents the most accurate value. The third-order energy shows somewhat worse agreement which is due in part to the finite number of partial waves used in the calculation. Comparison of the results for the ^3S and ^1S excited states illustrates the importance of the accurate difference formula and the increased cutoff. The agreement with Knight and Scherr[9] is generally better than for the ground state. In fact, Knight[11] has recently re-evaluated the ^1S second-order energy and found the improved value

to be -0.1145094 a.u. This indicates that the fourth difference value is the most accurate of those given in Table IX. The variational calculation of the partial wave contributions by Byron and Joachain[10] compares unfavorably for this pair. Since this is not the lowest state of its symmetry, it is expected that the variational method would have more difficulty. The convergence of the partial wave expansion is quite reasonable for both excited states.

Schwartz[12] has given an asymptotic formula for $E_2(\ell)$, which Byron and Joachain[10] have used to estimate the contributions from partial waves with $\ell > 20$ for the ground state and with $\ell > 6$ for the excited states. They obtain $E_2(\ell > 10) = -0.000042$ a.u., $E_2(\ell > 6, {}^3S) = -0.000001$ a.u., and $E_2(\ell > 6, {}^1S) = -0.000041$ a.u. If the contribution for the ground state is added to the second difference result, we obtain -0.157661 a.u., which agrees well with the correct value of -0.157666 a.u. The fourth difference results predict that $E_2(\ell > 6, {}^3S) \simeq -0.000016$ a.u. and $E_2(\ell > 6, {}^1S) \simeq -0.000069$ a.u. using the accurate values of the second-order energy given by Knight[11] for comparison. Because the functional coefficients $u_\ell(r_1 r_2)$ are found as arrays of numbers, it is not possible to communicate them in a compact form. Each coefficient could be polynomial fitted, but these results would still require a large amount of space to display. However, qualitative information can be given in the form of contour plots of each pair function. The discussion of the plots of the functional coefficients for the three pairs is given in the next section.

E. CONTOUR AND PERSPECTIVE PLOTS OF THE PAIR FUNCTIONS

The numerical functions found on the linear grid were plotted over a square region with the boundaries set at one-half the radial cutoff. In each contour plot the nucleus is located at the lower left corner, with the r_1 and r_2 axes running horizontally and vertically from this point. The positive contours are given by solid lines and the negative contours by dashed lines. Due to an artifact of the Calcomp plotter, some of the solid lines tend to break up in regions of small r_1 or r_2. These should not be mistaken for negative contours, which are dashed lines in all regions. Each functional coefficient was multiplied by $r_1 r_2$ and plotted with a constant contour interval. The values of the contour interval and of the largest positive and negative contours for the three states are given in Table X. Ideally, these values should have been found for several grids and extrapolated to obtain quantitative results. Instead, the values are given for the particular function plotted and represent the exact results to no more than two or three significant figures.

Figure 1 gives the plots for the first six partial waves of the first-order function for the (1s1s) pair. For $\ell = 0$, the effect on the zero-order function is to subtract amplitude in the region close to the nucleus and along the line $r_1 = r_2$. The functional coefficients for $\ell > 0$ are negative in all regions, becoming more peaked along $r_1 = r_2$ as ℓ is increased. These waves have a simpler form,

since the orthogonality to the zero-order function is insured by the angular factor. In Fig. 2 the perspective plots of the first two partial waves are given along with the zero-order, first-order, and total functions. The viewer's orientation for these plots is shown in Fig. 3. Each perspective plot was drawn to the same scale and can be directly compared. The contour plots of ψ_0, ψ_1, and ψ for all three pairs are given in Fig. 4. The total first-order function was found by taking $\theta_{12} = 0$ and summing the partial wave components as follows,

$$\psi_1 = \sum_{\ell} u_{\ell}(r_1 r_2) \tag{23}$$

then the total function was approximated by,

$$\psi = \psi_0 + \psi_1 \tag{24}$$

The first-order function shows a deep minimum near the nucleus and two well-separated maxima farther out. When this is added to the zero-order function, the total function is found to have two separated maxima with a minimum along $r_1 = r_2$. This is qualitatively what the exact solution should look like.

The partial wave contributions to the first-order function for the ^3S state are shown in Fig. 5. The trends are approximately the same as for the ground state except that the effects contributed by higher partial waves are smaller. This is expected because of the exact node at $r_1 = r_2$. From the perspective plots of ψ_0 and ψ given

in Fig. 6, the total first-order function serves to reduce the amplitude near the nucleus and increase it farther out (for the positive region). The contour plots of the functional coefficients for the ^1S excited state are shown in Fig. 7. They exhibit the intricate nodal structure expected for a state which is not the lowest of its symmetry. In each case the functions subtract amplitude from the nuclear region and build amplitude in the region $r_1, r_2 \simeq 4$ a.u., when added to ψ_0. In Figs. 4 and 8 the zero-order function is shown to have a maximum at $r_1, r_2 \simeq 1$ a.u. and separated minima at $r_1, r_2 \simeq 1,6$ a.u. and $r_1, r_2 \simeq 6,1$ a.u. Adding the first-order function for $\theta_{12} = 0$, the total function has two maxima occurring at $r_1, r_2 \simeq 1, 1.75$ a.u. and $r_1, r_2 \simeq 1.75, 1$ a.u. The minima are moved out from 6 a.u. to 8 a.u. For both of the excited states the perspective plots are drawn to the same scale as the ground state, so that amplitudes for the three states can be directly compared.

Up to this point the discussion has been concerned with electron correlation in the two-electron states. In the next section the pair functions are used to construct the total first-order function and calculate the total second- and third-order energies.

F. CALCULATION OF E_2 AND E_3 FOR THE THREE-ELECTRON ATOM

In order to calculate the second-order energy, Ψ_1 given by (15) is substituted into

$$E_2 = \langle \Psi_1 \left| \sum_{i<j} 1/r_{ij} \right| \Psi_1 \rangle \tag{25}$$

which expressed in terms of the pair functions is,

$$E_2 = E_2(1s1s, {}^1S) + \tfrac{3}{2} E_2(1s2s, {}^3S) + \tfrac{1}{2} E_2(1s2s, {}^1S)$$

$$+ 4w_1 - 2w_2 - w_3 - \sqrt{2}\, w_4 + 1/\sqrt{2}\, w_5 + 3/\sqrt{2}\, w_6 \tag{26}$$

The first three terms are the additive contributions from the pairs. Using the best numerical results, we obtain $E_2(\text{add}) = -0.286013$ a.u. This includes the correction for partial wave contributions from $\ell > 10$ for the (1s1s) pair. The second-order energies found by Knight and Scherr[9] and by Knight[11] predict the additive contribution to be -0.286035 a.u. The next six terms in (26) are defined as follows,

$$\begin{aligned}
w_1 &= \langle G(12)\ 2s(3) \left| 1/r_{13} \right| 1s(1)\ 1s(2)\ 2s(3) \rangle \\
w_2 &= \langle G(12)\ 2s(3) \left| 1/r_{13} \right| 1s(1)\ 1s(3)\ 2s(2) \rangle \\
w_3 &= \langle G(12)\ 2s(3) \left| 1/r_{13} \right| 1s(3)\ 1s(2)\ 2s(1) \rangle \\
w_4 &= \langle S(12)\ 1s(3) \left| 1/r_{13} \right| 1s(1)\ 1s(2)\ 2s(3) \rangle \\
w_5 &= \langle S(12)\ 1s(3) \left| 1/r_{13} \right| 1s(1)\ 1s(3)\ 2s(2) \rangle \\
w_6 &= \langle T(12)\ 1s(3) \left| 1/r_{13} \right| 1s(1)\ 1s(3)\ 2s(2) \rangle
\end{aligned} \tag{27}$$

Both the second and fourth difference solutions were used to calculate

these integrals. The extrapolated results are compared to those found by Chisholm and Dalgarno[13] in Table XI. The fourth difference results give the best agreement, which is better than six decimal places for the (1s1s) terms. The excited pairs are not quite as accurate and the total non-additive contribution is off by 0.000006 a.u. This is considerably better than the variational calculation of Seung and Wilson,[14] which is below the true value. Chisholm and Dalgarno did not obtain their results by solving for the pair functions, but these represent the most accurate values. Combining the additive and non-additive contributions, the numerical results predict the total second-order energy to be -0.408138 a.u. compared to the accurate value -0.408165 a.u. found by Knight.[11]

While the variational calculation gives an accurate result if enough terms are included, it is not easy to calculate the third-order energy due to the large number of difficult integrals. For the numerical function, E_3 is nearly as easy to calculate as E_2. The first-order solution is substituted into the equation

$$E_3 = \langle \Psi_1 | \sum_{i<j} 1/r_{ij} | \Psi_1 \rangle - E_1 \langle \Psi_1 | \Psi_1 \rangle \qquad (28)$$

which leads to the following expression in terms of the pair functions,

$$
\begin{aligned}
E_3 = \Big(& \langle G(12)\,2s(3) \,|\, H_1 \,|\, G(12)\,2s(3)\rangle - \langle G(12)\,2s(3) \,|\, H_1 \,|\, G(32)\,2s(1)\rangle \\
& + \tfrac{3}{2}\langle T(12)\,1s(3) \,|\, H_1 \,|\, T(12)\,1s(3)\rangle + \tfrac{3}{2}\langle T(12)\,1s(3) \,|\, H_1 \,|\, T(32)\,1s(1)\rangle \\
& + \tfrac{1}{2}\langle S(12)\,1s(3) \,|\, H_1 \,|\, S(12)\,1s(3)\rangle - \tfrac{1}{2}\langle S(12)\,1s(3) \,|\, H_1 \,|\, S(32)\,1s(1)\rangle \\
& - \sqrt{2}\,\langle G(12)\,2s(3) \,|\, H_1 \,|\, S(12)\,1s(3)\rangle + \sqrt{2}\,\langle G(12)\,2s(3) \,|\, H_1 \,|\, S(32)\,1s(1)\rangle \\
& - 3\sqrt{2}\cdot\langle G(12)\,2s(3) \,|\, H_1 \,|\, T(32)\,1s(1)\rangle + 3.\,\langle S(12)\,1s(3) \,|\, H_1 \,|\, T(32)\,1s(1)\rangle \Big) \\
- E_1 \cdot \Big(& \langle G(12) \,|\, G(12)\rangle - \langle G(12)\,2s(3) \,|\, G(32)\,2s(1)\rangle \\
& + \tfrac{3}{2}\langle T(12) \,|\, T(12)\rangle + \tfrac{3}{2}\langle T(12)\,1s(3) \,|\, T(32)\,1s(1)\rangle \\
& + \tfrac{1}{2}\langle S(12) \,|\, S(12)\rangle - \tfrac{1}{2}\langle S(12)\,1s(3) \,|\, S(32)\,1s(1)\rangle \\
& + \sqrt{2}\,\langle G(12)\,2s(3) \,|\, S(32)\,1s(1)\rangle \\
& - 3\sqrt{2}\cdot\langle G(12)\,2s(3) \,|\, T(32)\,1s(1)\rangle + 3.\,\langle S(12)\,1s(3) \,|\, H_1 \,|\, T(32)\,1s(1)\rangle \Big)
\end{aligned}
\tag{29}
$$

The integrals were calculated by the trapezoidal rule and the extrapolated results were used to find E_3. The pair contributions and the total third-order energy are compared to the calculations of Seung and Wilson[14] and Knight and Scherr[9] in Table XII. The total E_3 is estimated to be in error by less than ± 0.0002 a.u.

Substituting the second- and third-order energies into (3) and multiplying by Z^2, the total energy for the three-electron atom of nuclear charge Z is,

$$E(Z) = -1.125\cdot Z^2 + 1.022805\cdot Z - 0.408138 - 0.025515\,(1/Z) \tag{30}$$

with an error $O(1/Z^2)$. For Z = 3, 4, and 5, the energies given by

(30) and by the configuration interaction calculations of Weiss[15] compare as follows,

	MFD	Weiss	Exact[15]
E(Li)	-7.47332	-7.47710	-7.47807
$E(Be^{+})$	-14.32339	-14.32350	-14.32479
$E(B^{++})$	-23.42432	-23.42312	-23.42471

where the results are in atomic units. The MFD energies are superior to those of Weiss for $Z \geq 5$. Using variational pair functions, Seung and Wilson[14] calculated the following energies for these atoms, E(Li) = -7.47262 a.u., $E(Be^{+})$ = -14.32289 a.u., and $E(B^{++})$ = -23.42393 a.u.

G. DISCUSSION

The MFD method has been shown to be capable of solving the first-order pair equations for a many-electron atom with accuracy comparable to the best variational solutions. The numerical pair functions allow the calculation of the total second- and third-order energies with simple quadrature methods. Because of the unsophisticated techniques used to solve the equations and perform the numerical integration, the entire calculation can be easily programed and carried out in one step. It is also easily applied to excited states using the same programs. The method has been applied to the solution of the exact pair equations and to the first-order Hartree-Fock pair equations with consistent accuracy in each case.

REFERENCES

*This work is based on a thesis submitted by N. W. Winter in partial fulfillment of the requirements for the degree of Doctor of Philosophy in Chemistry, California Institute of Technology.

†Present Address: Battelle Memorial Laboratory, Columbus, Ohio.

‡Contribution No.

[1]V. McKoy and N. W. Winter, J. Chem. Phys. 48, 5514 (1968).

[2]The first-order solutions for the (1s2p),(2s2p) pairs have already been obtained and will be communicated separately.

[3]O. Sinanoglu, Advan. Chem. Phys. 6, 315 (1964).

[4]Bernard Friedman, Principles and Techniques of Applied Mathematics (John Wiley and Sons, Inc., New York, 1956), p. 45.

[5]O. Sinanoglu, Phys. Rev. 122, 493 (1961).

[6]N. W. Winter, D. Diestler, and V. McKoy, J. Chem. Phys. 48, 1879 (1968).

[7]N. W. Winter, A. Laferrière, and V. McKoy, Numerical Solution of the Two-Electron Schrödinger Equation, Phys. Rev. (submitted for publication).

[8]L. Richardson and J. Gaunt, Trans. Roy. Soc. (London) A226, 299 (1927); cf. H. C. Bolton and H. I. Scoins, Proc. Cambridge Phil. Soc. 53, 150 (1956).

[9]R. E. Knight and C. W. Scherr, Rev. Mod. Phys. 35, 436 (1963).

[10]F. W. Byron and C. J. Joachain, Phys. Rev. 157, 1 (1967).

[11]R. E. Knight, Phys. Rev. 183, 45 (1969).

[12]C. Schwartz, Phys. Rev. 126, 1015 (1962).

[13]C. D. Chisholm and A. Dalgarno, Proc. Roy Soc. (London) A292, 264 (1964).

[14]S. Seung and E. B. Wilson, J. Chem. Phys. 47, 5343 (1967).

[15]A. W. Weiss, Phys. Rev. 110, 1826 (1961).

TABLE I. Extrapolation of the partial wave contributions to E_2 for the $(1s1s)\,^1S$ pair.[a]

S-Wave

30	-0.12679967		
		-0.12593307	
45	-0.12631823		-0.12525667
		-0.12542577	-0.12535412
60	-0.12592778		-0.12533853
		-0.12536994	
75	-0.12572696		

P-Wave

30	-0.03038709		
		-0.02623053	
45	-0.02807789		-0.02649339
		-0.02642767	-0.02649522
60	-0.02735592		-0.02649493
		-0.02647072	
75	-0.02703725		

D-Wave

30	-0.00498619		
		-0.00385649	
45	-0.00435858		-0.00389785
		-0.00388751	-0.00390419
60	-0.00415249		-0.00390318
		-0.00389754	
75	-0.00406071		

F-Wave

30	-0.00160636		
		-0.00106341	
45	-0.00130472		-0.00107088
		-0.00106902	-0.00107572
60	-0.00120160		-0.00107495
		-0.00107282	
75	-0.00115524		

G-Wave

30	-0.00071573		
		-0.00040480	
45	-0.00054299		-0.00040141
		-0.00040226	-0.00040431
60	-0.00048142		-0.00040385
		-0.00040328	
75	-0.00045329		

I-Wave

30	-0.00038466		
		-0.00018910	
45	-0.00027602		-0.00018205
		-0.00018381	-0.00018352
60	-0.00023568		-0.00018329
		-0.00018348	
75	-0.00021689		

[a]The results were obtained on a linear grid with a 12 a.u. cutoff using second differences only.

TABLE II. Extrapolation of the partial wave contributions to E_2 for the (1s2s) ^3S pair.[a]

S-Wave

30	-0.02663438		
		-0.04134552	
60	-0.03766774		-0.04477454
		-0.04439354	-0.04525766
90	-0.04140430		-0.04522747
		-0.04501899	
120	-0.04298573		

P-Wave

25	-0.00204199		
		-0.00190603	
50	-0.00194002		-0.00191020
		-0.00190974	-0.00190983
75	-0.00192320		-0.00190985
		-0.00190982	
100	-0.00191735		

D-Wave

25	-0.00014864		
		-0.00014641	
50	-0.00014696		-0.00014558
		-0.00014567	-0.00014558
75	-0.00014625		-0.00014558
		-0.00014561	
100	-0.00014596		

F-Wave

25	-0.00002376		
		-0.00002418	
50	-0.00002407		-0.00002386
		-0.00002389	-0.00002385
75	-0.00002398		-0.00002385
		-0.00002386	
100	-0.00002392		

G-Wave

25	-0.00000560		
		-0.00000602	
50	-0.00000592		-0.00000589
		-0.00000590	-0.00000588
75	-0.00000591		-0.00000588
		-0.00000589	
100	-0.00000589		

I-Wave

25	-0.00000167		
		-0.00000196	
50	-0.00000189		-0.00000188
		-0.00000189	-0.00000186
75	-0.00000189		-0.00000186
		-0.00000186	
100	-0.00000188		

[a]The results for the S-wave were obtained on a linear grid with a 24 a.u. cutoff. The remaining waves were obtained with a 20 a.u. cutoff. Both calculations used second differences only.

TABLE III. Extrapolation of the partial wave contributions to E_2 for the (1s2s) ^1S pair.[a]

S-Wave

30	-0.05441913		
		-0.10033859	
60	-0.08885873		-0.10541639
		-0.10485129	-0.10647934
90	-0.09774399		-0.10641291
		-0.10602273	
120	-0.10136594		

P-Wave

25	-0.01025575		
		-0.00622971	
50	-0.00723623		-0.00646183
		-0.00643604	-0.00650048
75	-0.00679167		-0.00649806
		-0.00648256	
100	-0.00665644		

D-Wave

25	-0.00181852		
		-0.00089550	
50	-0.00112626		-0.00092240
		-0.00091942	-0.00092806
75	-0.00101135		-0.00092770
		-0.00092563	
100	-0.00097384		

F-Wave

25	-0.00061922		
		-0.00025769	
50	-0.00034808		-0.00025114
		-0.00025187	-0.00025269
75	-0.00029463		-0.00025259
		-0.00025241	
100	-0.00027616		

G-Wave

25	-0.00028376		
		-0.00010462	
50	-0.00014941		-0.00009472
		-0.00009582	-0.00009450
75	-0.00011963		-0.00009451
		-0.00009484	
100	-0.00010879		

I-Wave

25	-0.00015385		
		-0.00005221	
50	-0.00007761		-0.00004379
		-0.00004473	-0.00004286
75	-0.00005934		-0.00004292
		-0.00004337	
100	-0.00005236		

[a]The results for the S-wave were obtained on a linear grid with a 24 a.u. cutoff. The remaining waves were obtained with a 20 a.u. cutoff. Both calculations used second differences only.

TABLE IV. Extrapolated results for the (1s1s) pair on the square root grid.

N	20	25	30	35	40	Extrapolant
$E_2(0)$	-0.13120097	-0.12865971	-0.12747945	-0.12683508	-0.12644447	-0.12532722
$E_2(1)$	-0.03153428	-0.02957117	-0.02857186	-0.02799378	-0.02762863	-0.02649491
$E_2(2)$	-0.00581606	-0.00507296	-0.00468910	-0.00446720	-0.00432790	-0.00390532
$E_2(3)$	-0.00207665	-0.00169997	-0.00149740	-0.00137821	-0.00130291	-0.00107561
$E_2(4)$	-0.00100259	-0.00078835	-0.00066755	-0.00059441	-0.00054746	-0.00040268
$E_2(5)$	-0.00056940	-0.00043870	-0.00036170	-0.00031361	-0.00028208	-0.00018091
$E_2(6)$	-0.00035692	-0.00027284	-0.00022147	-0.00018844	-0.00016630	-0.00009172
$E_2(7)$	-0.00023910	-0.00018257	-0.00014704	-0.00012361	-0.00010757	-0.00005080
$E_2(8)$	-0.00016810	-0.00012862	-0.00010329	-0.00008623	-0.00007433	-0.00003023
$E_2(9)$	-0.00012265	-0.00009417	-0.00007562	-0.00006291	-0.00005390	-0.00001915
$\sum_{\ell} E_2$	-0.17308672	-0.16690907	-0.16381450	-0.16204339	-0.16093555	-0.15757856
E_3	0.01051900	0.00786948	0.00660995	0.00591483	0.00549180	0.00428606
E	-2.91256772	-2.90903959	-2.90720455	-2.90612856	-2.90544375	-2.90329249

TABLE V. Extrapolated results for the (1s2s) ^{3}S pair on the square root grid.

N	20	25	30	35	40	Extrapolant
$E_2(0)$	-0.05595414	-0.05129746	-0.04919849	-0.04805544	-0.04735900	-0.04531808
$E_2(1)$	-0.00191119	-0.00191069	-0.00191038	-0.00191020	-0.00191011	-0.00190994
$E_2(2)$	-0.00014381	-0.00014492	-0.00014529	-0.00014544	-0.00014551	-0.00014559
$E_2(3)$	-0.00002271	-0.00002340	-0.00002364	-0.00002375	-0.00002380	-0.00002386
$E_2(4)$	-0.00000520	-0.00000558	-0.00000573	-0.00000580	-0.00000583	-0.00000587
$E_2(5)$	-0.00000148	-0.00000168	-0.00000177	-0.00000182	-0.00000184	-0.00000187
$E_2(6)$	-0.00000048	-0.00000059	-0.00000065	-0.00000068	-0.00000069	-0.00000071
$E_2(7)$	-0.00000017	-0.00000023	-0.00000026	-0.00000028	-0.00000029	-0.00000031
$E_2(8)$	-0.00000007	-0.00000010	-0.00000012	-0.00000013	-0.00000014	-0.00000015
$E_2(9)$	-0.0000000_{26}	-0.0000000_{43}	-0.0000000_{55}	-0.0000000_{63}	-0.0000000_{68}	-0.00000008
$\sum_\ell E_2$	-0.05803928	-0.05338468	-0.05128639	-0.05014359	-0.04944727	-0.04740647
E_3	-0.00665006	-0.00458120	-0.00376779	-0.00335343	-0.00311029	-0.00243836
E	-2.18883199	-2.18210855	-2.17919685	-2.17763968	-2.17670023	-2.17398749

TABLE VI. Extrapolated results for the (1s2s) ^{1}S pair on the square root grid.

N	20	25	30	35	40	Extrapolant
$E_2(0)$	-0.13942467	-0.12510529	-0.11863254	-0.11510183	-0.11294819	-0.10662165
$E_2(1)$	-0.00734360	-0.00700853	-0.00684048	-0.00674412	-0.00668365	-0.00649785
$E_2(2)$	-0.00125644	-0.00112858	-0.00106279	-0.00102485	-0.00100108	-0.00092929
$E_2(3)$	-0.00042550	-0.00036086	-0.00032610	-0.00030563	-0.00029269	-0.00025355
$E_2(4)$	-0.00019794	-0.00016110	-0.00014039	-0.00012784	-0.00011977	-0.00009473
$E_2(5)$	-0.00010976	-0.00008706	-0.00007381	-0.00006556	-0.00006015	-0.00004267
$E_2(6)$	-0.00006784	-0.00005301	-0.00004411	-0.00003842	-0.00003462	-0.00002178
$E_2(7)$	-0.00004512	-0.00003498	-0.00002874	-0.00002468	-0.00002192	-0.00001219
$E_2(8)$	-0.00003163	-0.00002442	-0.00001992	-0.00001693	-0.00001487	-0.00000734
$E_2(9)$	-0.00002307	-0.00001779	-0.00001444	-0.00001219	-0.00001062	-0.00000469
$\sum_\ell E_2$	-0.14892558	-0.13398162	-0.12718331	-0.12346206	-0.12118756	-0.11448574
E_3	0.00071579	0.00295108	0.00366729	0.00399378	0.00417363	0.00462579
E	-2.18456096	-2.16738171	-2.15986719	-2.15581944	-2.15336509	-2.14621112

TABLE VII. Comparison of the perturbation energies for the (1s1s) pair.

	2nd differences[a]	4th differences[b]	BJ[c]	KS[d]
$E_2(0)$	-0.125339	-0.125327	-0.125334	-0.125332
$E_2(1)$	-0.026495	-0.026495	-0.026495	-0.026446
$E_2(2)$	-0.003904	-0.003905	-0.003906	-0.003612
$E_2(3)$	-0.001076	-0.001076	-0.001077	–
$E_2(4)$	-0.000404	-0.000403	-0.000405	–
$E_2(5)$	-0.000184	-0.000181	-0.000183	–
$E_2(6)$	-0.000094	-0.000092	-0.000093	–
$E_2(7)$	-0.000054	-0.000051	-0.000053	–
$E_2(8)$	-0.000033	-0.000030	-0.000032	–
$E_2(9)$	-0.000021	-0.000019	-0.000021	–
$E_2(10)$	-0.000015	–	-0.000014	–
$\sum_{\ell} E_2(\ell)$	-0.157619	-0.157579	-0.157614	-0.157666[e]
E_3	0.008478	0.008572	–	0.008699

[a]The second difference results were obtained on a linear grid with a 12 a.u. cutoff.

[b]The fourth difference results were obtained on a square root grid with a 32 a.u. cutoff.

[c]F. W. Byron and C. J. Joachain, Phys. Rev. 157, 1 (1967).

[d]R. E. Knight and C. W. Scherr, Rev. Mod. Phys. 35, 436 (1963).

[e]The total E_2 was not obtained from a partial wave expansion for this calculation.

TABLE VIII. Comparison of the perturbation energies for the $(1s2s)\ ^3S$ pair.

	2nd differences[a]	4th differences[b]	BJ[c]	KS[d]
$E_2(0)$	-0.045258	-0.045318	-0.045316	-0.045318
$E_2(1)$	-0.001909	-0.001910	-0.001898	-0.001902
$E_2(2)$	-0.000146	-0.000146	-0.000137	-0.000135
$E_2(3)$	-0.000024	-0.000024	-0.000020	–
$E_2(4)$	-0.000006	-0.000006	-0.000004	–
$E_2(5)$	-0.000002	-0.000002	-0.000001	–
$E_2(6)$	–	-0.000000_7	–	–
$E_2(7)$	–	-0.000000_3	–	–
$E_2(8)$	–	-0.000000_2	–	–
$E_2(9)$	–	-0.000000_1	–	–
$\sum_\ell E_2(\ell)$	-0.047345	-0.047406	-0.047377	-0.047409[e]
E_3	-0.003732	-0.004876	-0.005000	-0.004872

[a] The second difference results were obtained on a linear grid with a 20 a.u. cutoff except for the S-wave which was calculated with a 24 a.u. cutoff.

[b] The fourth difference results were obtained on a square root grid with a 32 a.u. cutoff.

[c] F. W. Byron and C. J. Joachain, Phys. Rev. 157, 1 (1967).

[d] R. E. Knight and C. W. Scherr, Rev. Mod. Phys. 35, 436 (1963).

[e] The total E_2 was not obtained from a partial wave expansion for this calculation.

TABLE IX. Comparison of the perturbation energies for the $(1s2s)\ ^1S$ pair.

	2nd differences[a]	4th differences[b]	BJ[c]	KS[d]
$E_2(0)$	-0.106479	-0.106622	-0.106335	
$E_2(1)$	-0.006500	-0.006498	-0.006239	
$E_2(2)$	-0.000928	-0.000929	-0.000816	
$E_2(3)$	-0.000253	-0.000254	-0.000199	
$E_2(4)$	-0.000095	-0.000095	-0.000066	
$E_2(5)$	-0.000043	-0.000043	-0.000027	
$E_2(6)$	–	-0.000022	–	
$E_2(7)$	–	-0.000012	–	
$E_2(8)$	–	-0.000007	–	
$E_2(9)$	–	-0.000005	–	
$\sum E_2(\ell)$	-0.114339	-0.114486	-0.113681	-0.114476[e]
E_3	0.012114	0.009251	0.007000	0.009415

[a] The second difference results were obtained on a linear grid with a 20 a.u. cutoff except for the S-wave which was calculated with a 24 a.u. cutoff.

[b] The fourth difference results were obtained on a square root grid with a 32 a.u. cutoff.

[c] F. W. Byron and C. J. Joachain, Phys. Rev. 157, 1 (1967).

[d] R. E. Knight and C. W. Scherr, Rev. Mod. Phys. 35, 436 (1963).

[e] The total E_2 was not obtained from a partial wave expansion for this calculation.

TABLE X. The values of the most positive and negative contours and the contour interval for the plots of the first-order pair functions.

	$(1s1s)\ ^1S$			$(1s2s)\ ^3S$			$(1s2s)\ ^1S$		
ℓ	Interval	Positive	Negative	Interval	Positive	Negative	Interval	Positive	Negative
0	0.02776	0.11686	-0.29953	0.01819	0.13641	-0.13641	0.02936	0.23954	-0.20093
1	0.00936	—	-0.14046	0.00316	0.02373	-0.02373	0.00679	0.05066	-0.05117
2	0.00359	—	-0.05383	0.00090	0.00673	-0.00673	0.00283	0.02219	-0.02029
3	0.00194	—	-0.02917	0.00037	0.00277	-0.00277	0.00160	0.01249	-0.01155
4	0.00125	—	-0.01869	0.00019	0.00139	-0.00139	0.00105	0.00808	-0.00765
5	0.00088	—	-0.01323	0.00011	0.00080	-0.00080	0.00075	0.00568	-0.00551
ψ_0	0.07187	1.07808	—	0.06183	0.46370	-0.46370	0.05965	0.46263	-0.43218
ψ_1	0.03923	0.09699	-0.49143	0.02042	0.15318	-0.15318	0.03894	0.28817	-0.29593
ψ	0.04716	0.70733	—	0.05699	0.42744	-0.42744	0.04799	0.26458	-0.45532

TABLE XI. Comparison of the non-additive contributions to the second-order energy.

Term	2nd Differences[a]	4th Differences[b]	CD[c]	SW[d]
W1	-0.005058	-0.0050576	-0.0050577	–
W2	-0.006245	-0.0062434	-0.0062436	–
W3	-0.023743	-0.0237581	-0.0237590	–
W4	0.007159	0.0071474	0.0071465	–
W5	-0.048875	-0.0489486	-0.0489523	–
W6	-0.043984	-0.0440383	-0.0440409	–
Total	-0.121986	-0.1221247	-0.1221307	-0.1223319

[a]Linear grid.

[b]Square root grid.

[c]C.D.H.Chisholm and A. Dalgarno, Proc. Roy. Soc. (London) A292, 264 (1964).

[d]S. Seung and E. B. Wilson, J. Chem. Phys. 47, 5343 (1967).

TABLE XII. Comparison of the third-order energy contributions.

	2nd Differences[a]	4th differences[b]	SW[c]	KS[d]
$E_3(1s1s, {}^1S)$	0.008478	0.008572	–	0.008699
$E_3(1s2s, {}^3S)$	-0.003732	-0.004876	-0.004906	-0.004872
$E_3(1s2s, {}^1S)$	0.012114	0.009251	0.008217	0.009415
Total E_3	–	-0.025515	-0.023043	–

[a]The (1s1s) pair results were obtained on a linear grid with a 12 a.u. cutoff using 11 partial waves. The (1s2s) pair results were obtained on a linear grid with a 20 a.u. cutoff using only 6 partial waves.

[b]All results were obtained on a square root grid with a 32 a.u. cutoff using 10 partial waves.

[c]S. Seung and E. B. Wilson, J. Chem. Phys. 47, 5343 (1967).

[d]R. E. Knight and C. W. Scherr, Rev. Mod. Phys. 35, 436 (1963).

Figure 1. Contour plots of the functional coefficients for the (1s1s) pair.

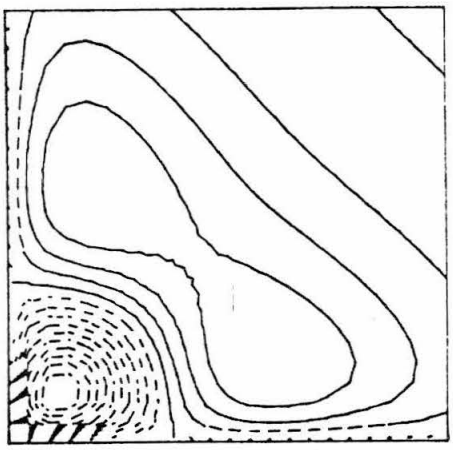

(1S1S) PAIR FUNCTION (L=0)

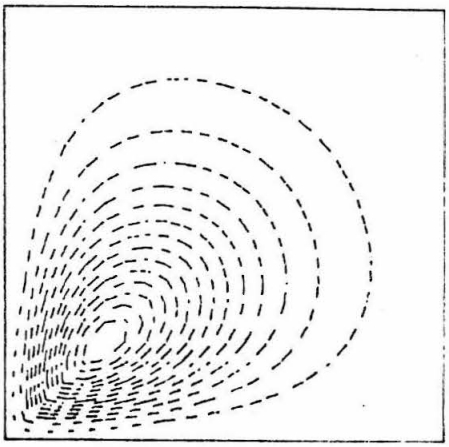

(1S1S) PAIR FUNCTION (L=1)

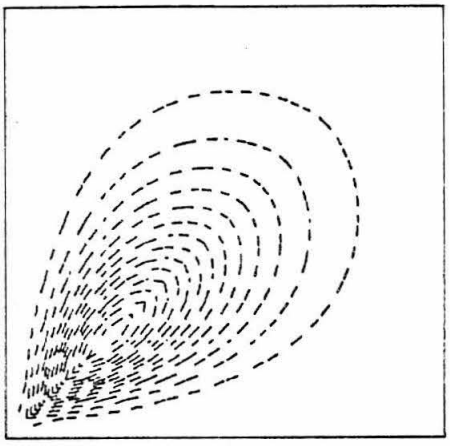

(1S1S) PAIR FUNCTION (L=2)

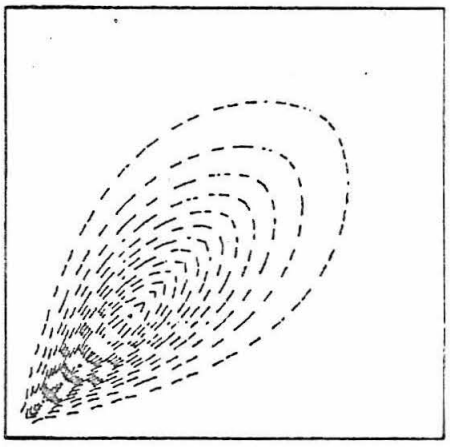

(1S1S) PAIR FUNCTION (L=3)

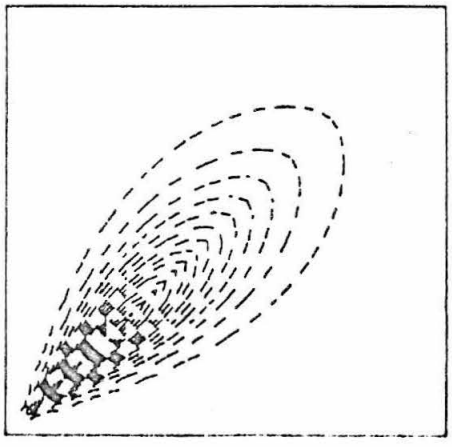

(1S1S) PAIR FUNCTION (L=4)

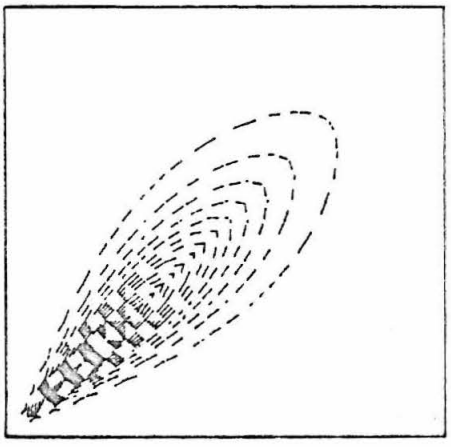

(1S1S) PAIR FUNCTION (L=5)

Figure 1

Figure 2. Perspective plots of the S- and P-waves and of the zero-order, first-order, and total wavefunctions for the (1s1s) pair.

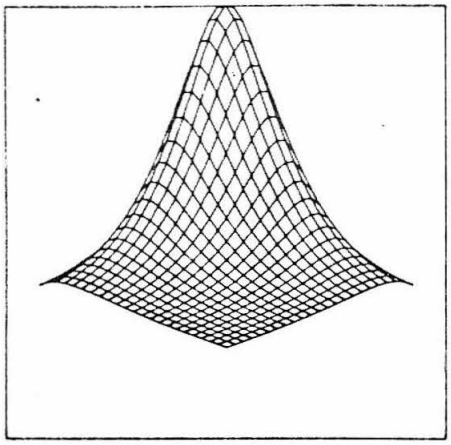

(1S1S) HYDROGENIC ZERO-ORDER FUNCTION

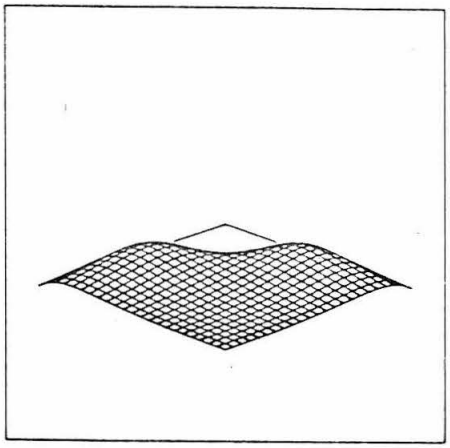

(1S1S) PAIR FUNCTION (L=0)

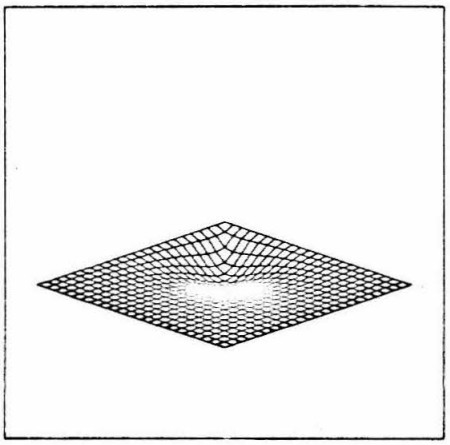

(1S1S) PAIR FUNCTION (L=1)

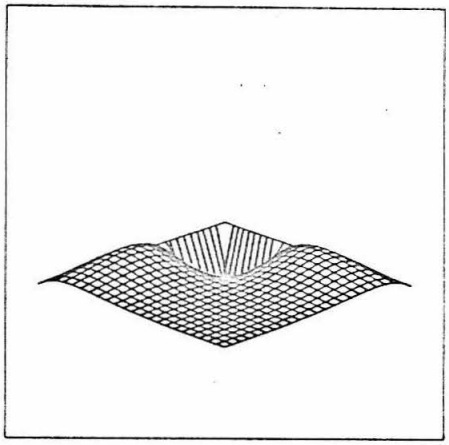

FIRST-ORDER FUNCTION FOR THE (1S1S) PAIR

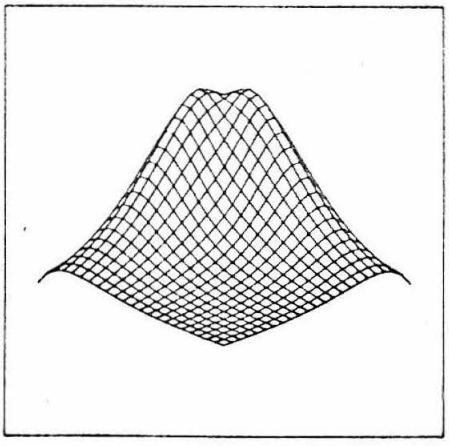

TOTAL FUNCTION FOR THE (1S1S) PAIR

Figure 2

Figure 3. The viewer's orientation for the perspective plots.

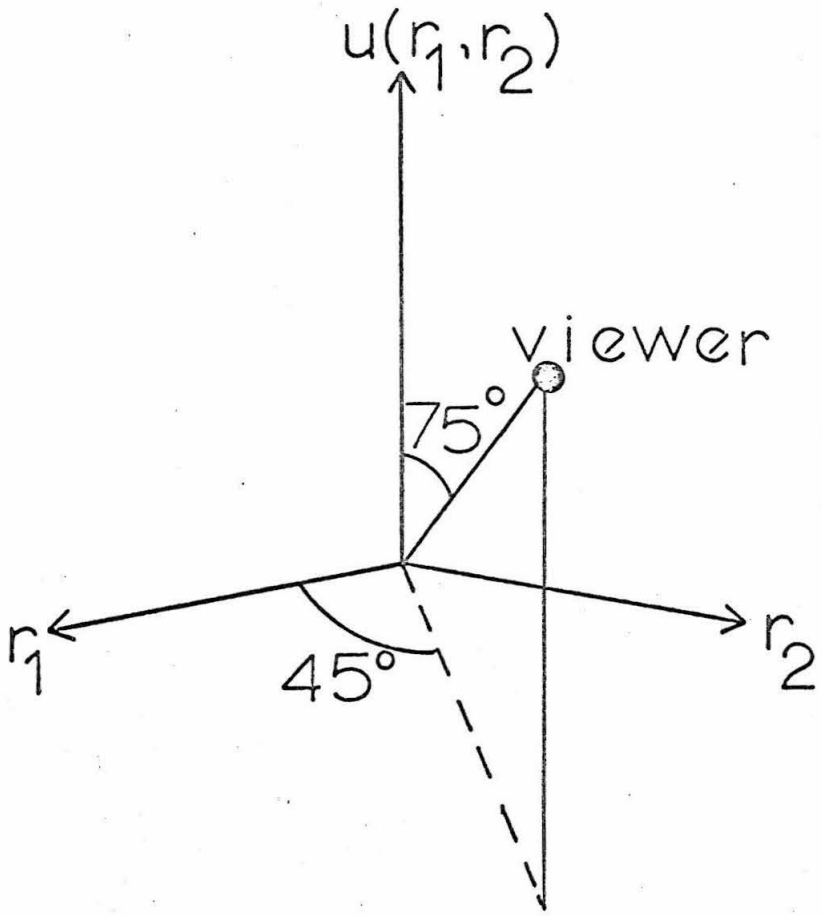

Figure 3

Figure 4. Contour plots of the zero-order, first-order, and total wavefunctions for the $(1s1s)\,^1S$, $(1s2s)\,^3S$, and $(1s2s)\,^1S$ pairs.

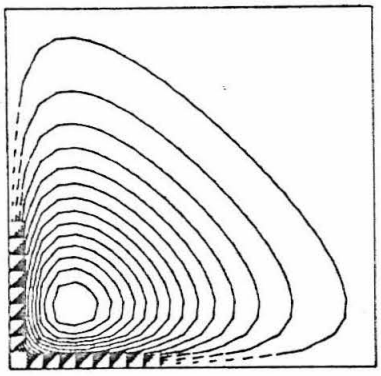

(1S1S) HYDROGENIC ZERO-ORDER FUNCTION

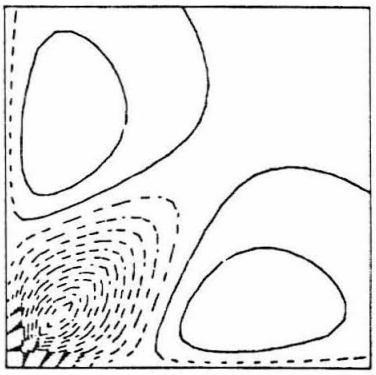

FIRST-ORDER FUNCTION FOR (1S1S) PAIR

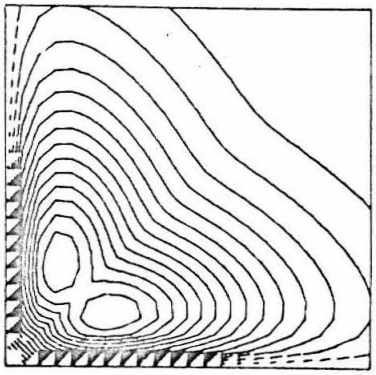

TOTAL FUNCTION FOR THE (1S1S) PAIR

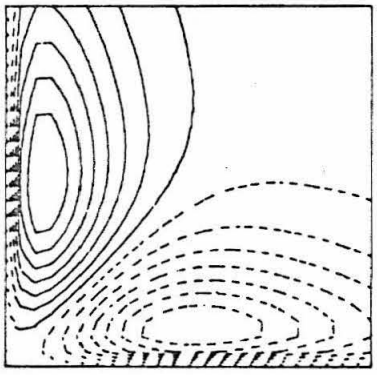

(1S2S) TRIPLET ZERO-ORDER FUNCTION

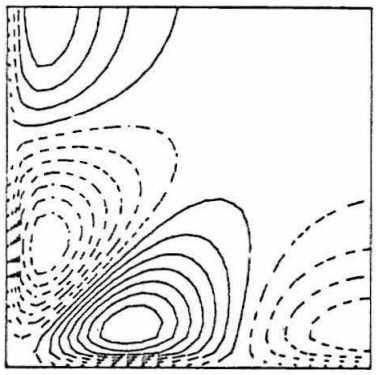

FIRST-ORDER FUNCTION FOR (1S2S) TRIPLET

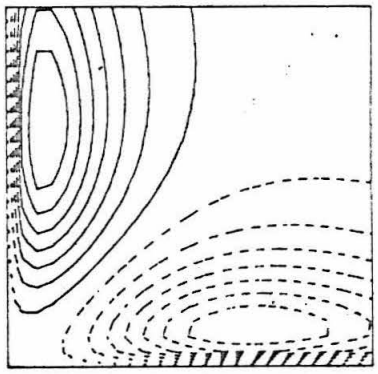

TOTAL FUNCTION FOR (1S2S) TRIPLET PAIR

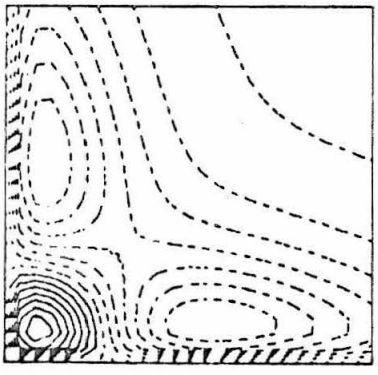

(1S2S) SINGLET ZERO-ORDER FUNCTION

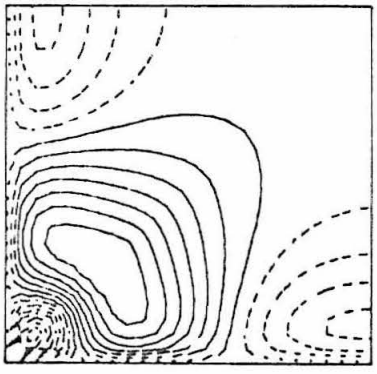

FIRST-ORDER FUNCTION FOR (1S2S) SINGLET

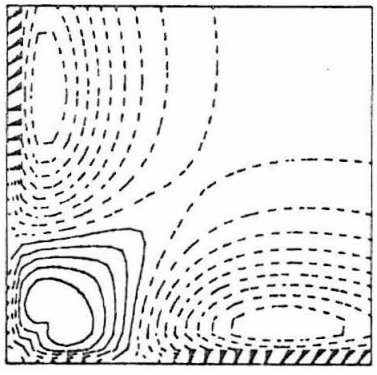

TOTAL FUNCTION FOR (1S2S) SINGLET PAIR

Figure 4

Figure 5. Contour plots of the functional coefficients for the $(1s2s)\,^3S$ pair.

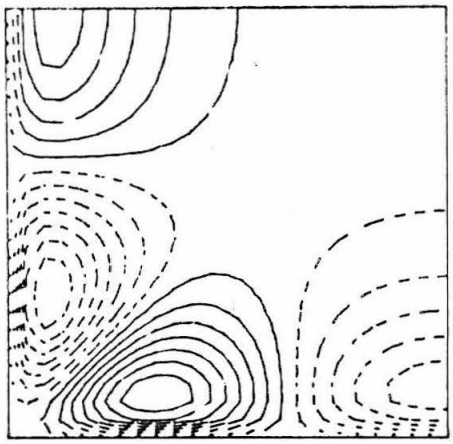

(1S2S) TRIPLET PAIR FUNCTION (L=0)

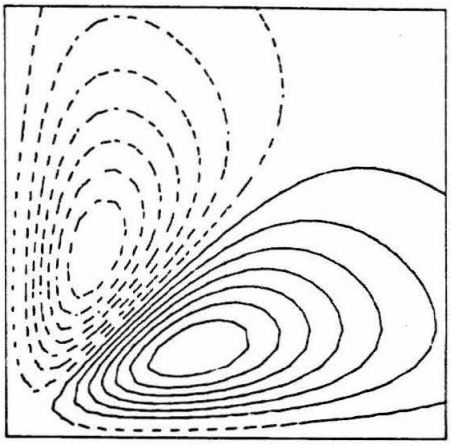

(1S2S) TRIPLET PAIR FUNCTION (L=1)

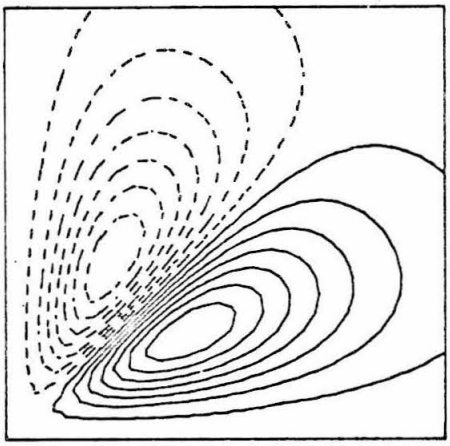

(1S2S) TRIPLET PAIR FUNCTION (L=2)

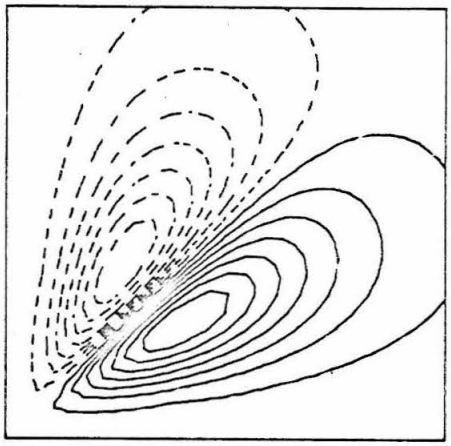

(1S2S) TRIPLET PAIR FUNCTION (L=3)

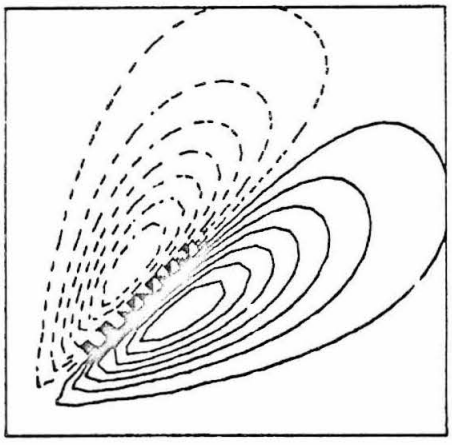

(1S2S) TRIPLET PAIR FUNCTION (L=4)

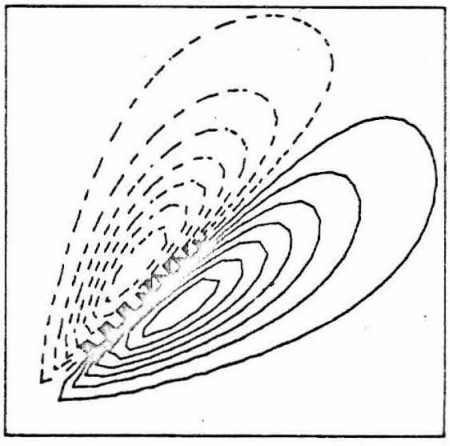

(1S2S) TRIPLET PAIR FUNCTION (L=5)

Figure 5

Figure 6. Perspective plots of the S- and P-waves and of the zero-order, first-order, and total wavefunctions for the $(1s2s)\,^3S$ pair.

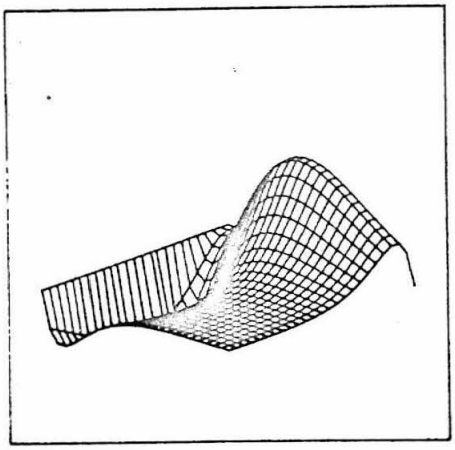

(1S2S) TRIPLET ZERO-ORDER FUNCTION

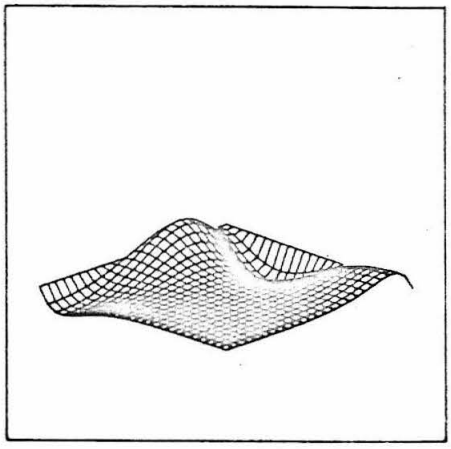

(1S2S) TRIPLET PAIR FUNCTION (L=0)

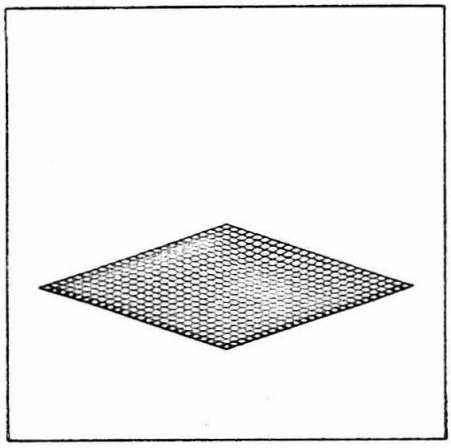

(1S2S) TRIPLET PAIR FUNCTION (L=1)

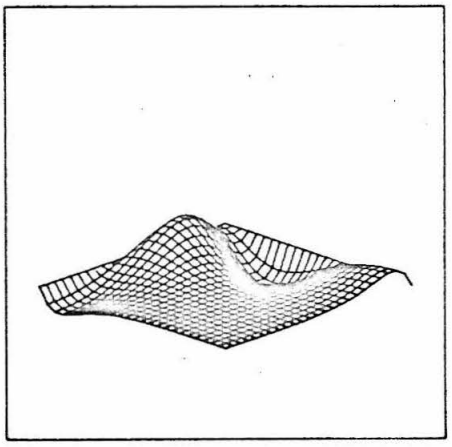

FIRST-ORDER FUNCTION FOR (1S2S) TRIPLET

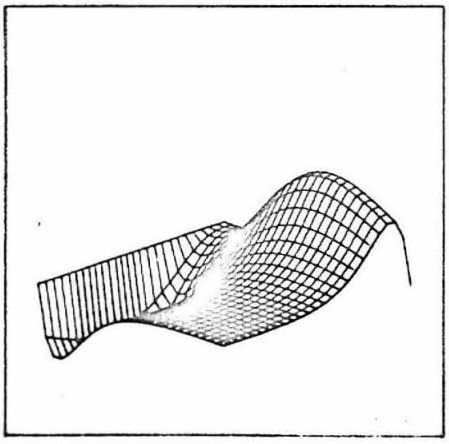

TOTAL FUNCTION FOR (1S2S) TRIPLET PAIR

Figure 6

Figure 7. Contour plots of the functional coefficients for the $(1s2s)\,^1S$ pair.

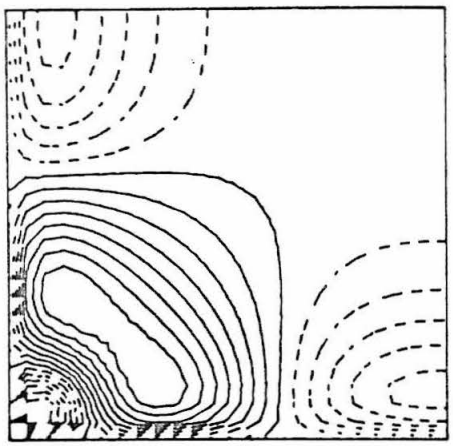

(1S2S) SINGLET PAIR FUNCTION (L=0)

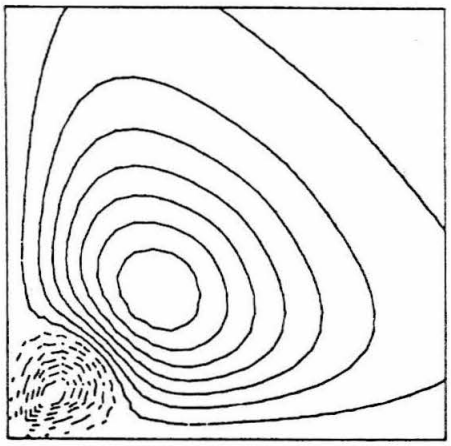

(1S2S) SINGLET PAIR FUNCTION (L=1)

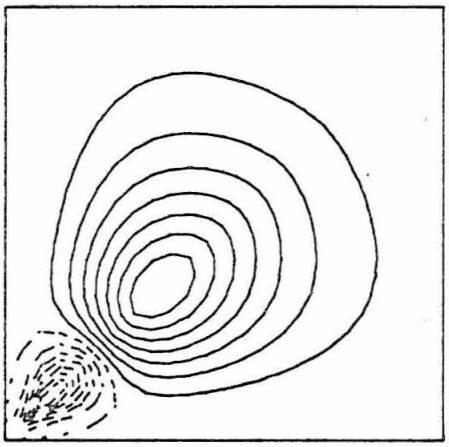

(1S2S) SINGLET PAIR FUNCTION (L=2)

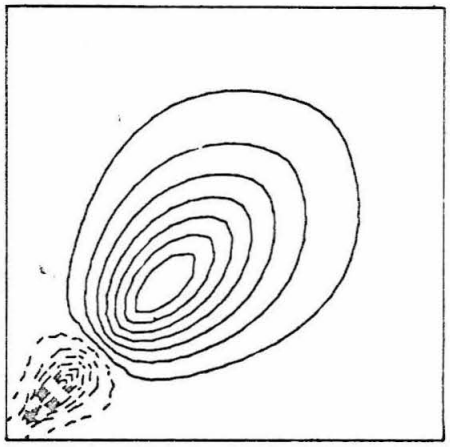

(1S2S) SINGLET PAIR FUNCTION (L=3)

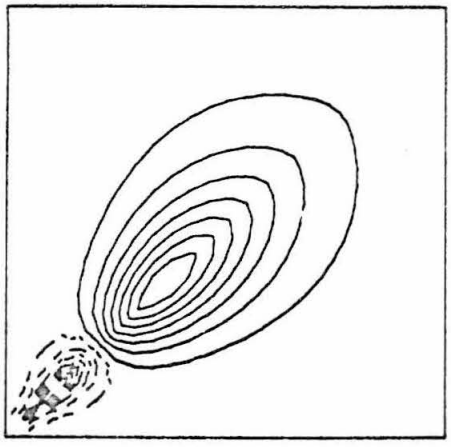

(1S2S) SINGLET PAIR FUNCTION (L=4)

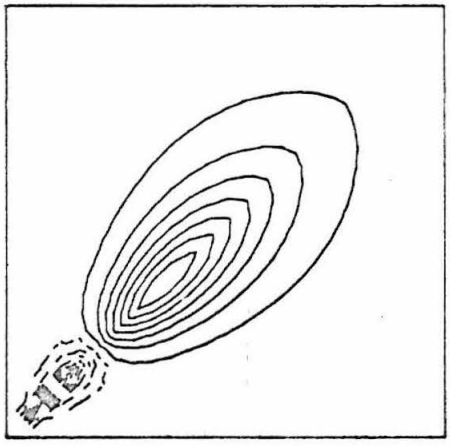

(1S2S) SINGLET PAIR FUNCTION (L=5)

Figure 7

Figure 8. Perspective plots of the S- and P-waves and of the zero-order, first-order, and total wavefunctions for the $(1s2s)\,^1S$ pair.

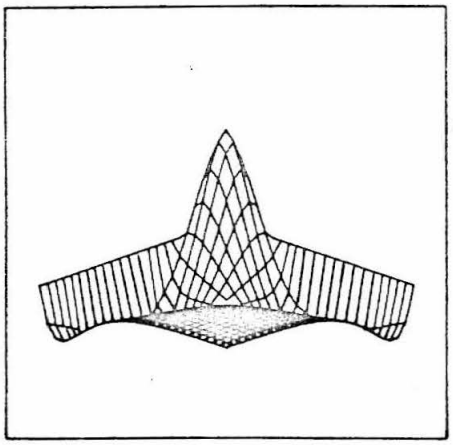

(1S2S) SINGLET ZERO-ORDER FUNCTION

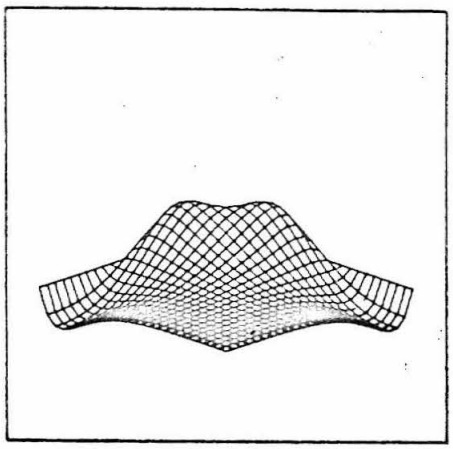

(1S2S) SINGLET PAIR FUNCTION (L=0)

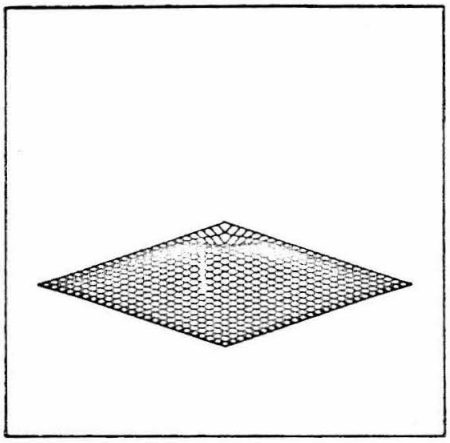

(1S2S) SINGLET PAIR FUNCTION (L=1)

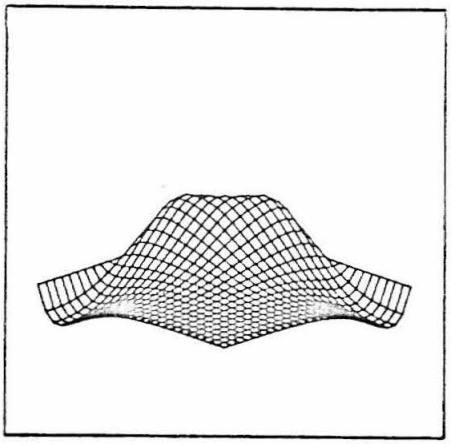

FIRST-ORDER FUNCTION FOR (1S2S) SINGLET

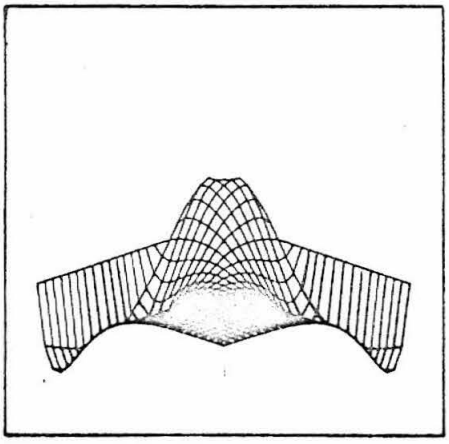

TOTAL FUNCTION FOR (1S2S) SINGLET PAIR

Figure 8

III. PUBLICATIONS

Reprinted from THE JOURNAL OF CHEMICAL PHYSICS, Vol. 49, No. 4, 1871–1877, 15 August 1968
Printed in U. S. A.

Formaldehyde Molecule in a Gaussian Basis. A Self-Consistent Field Calculation

N. W. WINTER,* THOM. H. DUNNING, JR.,* AND JOHN H. LETCHER
Central Research Department, Monsanto Company, St. Louis, Missouri
(Received 19 February 1968)

Accurate LCAO–MO–SCF calculations have been carried out for the formaldehyde molecule using (73/2) and (95/3) Gaussian basis sets. The energy parameters, molecular orbitals, dipole moments, and population analyses are reported. The results are compared to a previous calculation with a minimum Slater basis and to experiment.

I. INTRODUCTION

It is now possible to obtain close approximations to the Hartree–Fock orbitals for a number of small polyatomic molecules.[1,2] These have been found by expanding the orbitals in large Gaussian basis sets. From such calculations it is possible to predict, with varying degrees of accuracy, ionization potentials, dissociation energies, many one-electron properties, etc. In order to have confidence in our results we either need to know what type and size of basis set is required to predict the properties of interest with reliable accuracy[3] or have the LCAO–MO–SCF orbitals sufficiently close to the Hartree–Fock orbitals so that no major error arises from the use of the expansion.

We report here the results of LCAO–MO calculations on formaldehyde using two uncontracted Gaussian basis sets. The smaller, a (73/2) set,[4] is estimated to be slightly better than a molecular optimized minimum Slater set and the larger, a (95/3) set,[4] is near the (sp) limit. While these wavefunctions are obviously not at the Hartree–Fock limit, they form essential units in a stepwise approach to that limit and can be expected to provide a considerable amount of chemical information.

Because of the wide range of interest in formaldehyde, a number of theoretical calculations on it have been reported. All of the calculations based on pi-electron theory[5] approximated the required atomic integrals and provided little usable information, other than possibly the spectra. More recently, accurate calculations have been made using an unoptimized minimum basis set of Slater orbitals.[6,7] Several comparisons will be made with these functions.

In the next section we give the results for the two Gaussian sets. In the following section we discuss the results. In the last section the computational details are given.

---

* Permanent address: A. A. Noyes Laboratory of Chemical Physics, California Institute of Technology, Pasadena, Calif.

[1] C_2H_4: J. M. Schulman, J. W. Moskowitz, and C. Hollister, J. Chem. Phys. 44, 2759 (1966).

[2] H_2O: D. Neumann and J. W. Moskowitz, "One Electron Properties of Near Hartree–Fock Wavefunctions. I. Water," J. Chem. Phys. (to be published).

[3] By accurate we mean, of course, in comparison to *the* Hartree–Fock result and not to experiment.

[4] We have adopted the standard notation, with (abc/ef) representing a s-orbitals, b p-orbitals, c d-orbitals, etc., on the first-row atoms and e s-orbitals, f p-orbitals, etc., on the hydrogen atoms.

[5] T. Anno and A. Sadô, J. Chem. Phys. 26, 1759 (1957); J. W. Sidman, *ibid.* 27, 429 (1957); J. A. Pople and J. W. Sidman, *ibid.* 27, 1270 (1957); R. D. Brown and M. L. Heffernan, Trans. Faraday Soc. 54, 757 (1958); J. M. Parks and R. G. Parr, J. Chem. Phys. 32, 1657 (1960); and F. L. Pilar, *ibid.* 47, 884 (1967).

[6] J. M. Foster and S. F. Boys, Rev. Mod. Phys. 32, 303 (1960).

[7] M. D. Newton and W. E. Palke, J. Chem. Phys. 45, 2329 (1966); S. Aung, R. M. Pitzer, and S. I. Chan, *ibid.* 45, 3457 (1966).

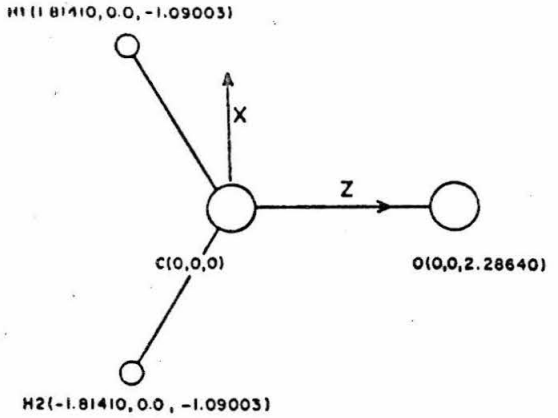

FIG. 1. The geometry of formaldehyde.

II. SCF RESULTS

For comparative purposes, the calculations were done at the geometry used by Goodfriend, Birss, and Duncan[8] which is quite close to that from the most recent structure determination[9]; see Fig. 1. The atomic energies for each of the basis sets are included in Table I. The exponents for both sets were determined from atomic SCF calculations[10] and are included in Tables III and IV.

The computed electronic energies are -144.7857 and -144.9471 a.u. for the (73/2) and (95/3) basis sets, respectively. Newton and Palke[7] give -144.5409 a.u. for a minimum Slater basis set with exponents determined from Slater's rules. As stated in the Introduction, from the energy and numerous properties for the (73/2) basis set, we estimate that this basis set is superior to a molecular optimized minimum basis set of Slater orbitals. As such, the (73/2) basis set would be a good candidate for *ab initio* studies of larger molecules, although three basis functions are recommended for the hydrogens rather than the two employed here. The (95/3) basis set should be within 0.04 a.u. of the (sp) limit for formaldehyde. It is felt that most properties are essentially at the (sp) limit and would be little affected by any additional s and p orbitals. Hollister and Sinanoğlu[11] predict the total Hartree–Fock energy of formaldehyde to be -114.0309 a.u. Thus, our wavefunction in the (95/3) Gaussian basis is approximately 0.20 a.u. from the Hartree–Fock limit. Work on other polyatomics[1,2] leads us to suspect that this is an upper limit. In any case, a significant lowering ($\sim$0.16 a.u.) would be achieved through the addition of d and f orbitals to the basis set. Most of the improvement is expected to arise from the inclusion of d orbitals.[2]

Table I compares the calculated binding energies for the three wavefunctions to the experimental value,[12] and Table II compares the orbital energies to the negatives of the experimental vertical ionization potentials.[13] From the kinetic energies given in Table II, the virial ratio $-T/E$ is found to be 0.9990 for the small Gaussian set and 0.9989 for the large set. We also see that the kinetic energy for the Slater calculation agrees with the Gaussian results much better than the molecular energy, and consequently gives a poorer virial ratio (1.0023).

The molecular-orbital coefficients for the (73/2) and (95/3) basis sets are listed in Tables III and IV, respectively. The population analyses[14] of both sets are given in Tables V–VIII.

The dipole moment is 1.018 a.u. (2.587 D) for the (73/2) set and 1.193 a.u. (3.032 D) for the (95/3) set, as compared to the experimental value 0.921 a.u. (2.34 D).[15] The minimum-Slater-basis-set calculation predicted 0.235 a.u. (0.597 D), considerably worse than either Gaussian calculation. All of the calculated dipole moments are in the direction C^+O^-. The behavior of the dipole moment is in agreement with recent observations that d orbitals are needed to describe the polarizations due to molecular formation.[2,16,17] In general, addition of d orbitals decreases the calculated dipole moment,[2,16] although such a trend may not be universal.

TABLE I. Comparison of the binding energies (B.E.) calculated from a single Slater basis and from the (73/2) and (95/3) Gaussian bases.

	Single Slater[a]	(73/2)[b]	(95/3)[b]
E_C	-37.619	-37.6551	-37.6852
E_O	-74.533	-74.7007	-74.8003
E_H	-0.500	-0.4858	-0.4970
E_{atoms}	-113.152	-113.3274	-113.4795
$E_{molecule}$	-113.4272	-113.6720	-113.8334
B.E. (a.u.)	0.275	0.3446	0.3539
(eV)	7.49	9.38	9.63
Experimental B.E.		16.24 eV	

[a] For the atomic energies, see B. J. Ransil, Rev. Mod. Phys. 32, 239 (1960); for the molecular energy, see Ref. 7a.
[b] For the atomic energies, see Ref. 10.

[8] P. L. Goodfriend, F. W. Birss, and A. B. F. Duncan, Rev. Mod. Phys. 32, 307 (1960).
[9] T. Oka, J. Phys. Soc. Japan 15, 2274 (1960); K. Takagi and T. Oka, *ibid.* 18, 1174 (1963).
[10] The exponents for the small basis set were made available to us by Dr. Murray Geller and are from calculations by D. Whitman at RIAS, Martin Company, Baltimore, Md. Those for the large set are given by S. Huzinaga, J. Chem. Phys. 42, 1293 (1964).
[11] C. Hollister and O. Sinanoğlu, J. Am. Chem. Soc. 88, 13 (1966).
[12] G. N. Lewis and M. Randall, *Thermodynamics*, revised by K. S. Pitzer and L. Brewer (McGraw-Hill Book Co., New York, 1961).
[13] C. R. Brundle and D. W. Turner, Chem. Commun. 1967, 314.
[14] R. S. Mulliken, J. Chem. Phys. 23, 1833 (1955).
[15] J. N. Shoolery and A. H. Sharbaugh, Phys. Rev. 82, 95 (1951).
[16] W. M. Huo, J. Chem. Phys. 43, 624 (1965).
[17] P. E. Cade and W. M. Huo, J. Chem. Phys. 45, 1063 (1967).

TABLE II. Orbitals energies, total energies, and kinetic energies for formaldehyde in a single Slater basis and in the (73/2) and (95/3) Gaussian bases compared to the photoelectron ionization potentials, in atomic units.[a]

Molecular orbital	Orbital energies			
	Single Slater[b]	(73/2)	(95/3)	−I.P.[c]
$1(1a_1)$	−20.6237	−20.6072	−20.5906	
$2(2a_1)$	−11.4026	−11.3576	−11.3627	
$3(3a_1)$	−1.3977	−1.4304	−1.4299	
$4(4a_1)$	−0.8314	−0.8609	−0.8666	∼−0.772
$5(1b_2)$	−0.6759	−0.6893	−0.7020	−0.621
$6(5a_1)$	−0.5932	−0.6318	−0.6437	−0.588
$7(1b_1)$	−0.4971	−0.5238	−0.5355	−0.529
$8(2b_2)$	−0.3955	−0.4269	−0.4423	−0.399
$9(2b_1)$[d]	0.2249	0.1465	0.1076	
Total energy	−113.4272	−113.6720	−113.8334	
Kinetic energy	113.6906	113.5632	113.7089	

[a] 1 a.u. of energy is 27.2098 eV.
[b] See Ref. 7a.
[c] See Ref. 13.
[d] This orbital is unoccupied in the ground state. It is the lowest π antibonding orbital.

TABLE III. Coefficient vectors and orbital energies for the (73/2) basis set.

Orbital energy			Vector 1 −20.60716	2 −11.35758	3 −1.43043	4 −0.86087	5 −0.68928	6 −0.63177	7 −0.52382	8 −0.42695
Center	Type	Exponent								
H1	S	0.2700	−0.00033	0.00255	0.01395	−0.16815	−0.17395	−0.11284	0.0	−0.36239
H1	S	1.8000	−0.00009	−0.00063	0.01364	−0.09477	−0.09599	−0.05144	0.0	−0.09414
H2	S	0.2700	−0.00033	0.00255	0.01395	−0.16815	0.17395	−0.11284	0.0	0.36239
H2	S	1.8000	−0.00009	−0.00063	0.01364	−0.09477	0.09599	−0.05144	0.0	0.09414
C	S	0.1817	0.00626	−0.01235	0.07111	−0.35181	0.0	−0.11942	0.0	0.0
C	S	0.6026	−0.00027	0.03921	0.21135	−0.34019	0.0	0.08271	0.0	0.0
C	S	3.6980	0.00049	0.44308	−0.09829	0.15255	0.0	−0.02530	0.0	0.0
C	S	11.8200	−0.00027	0.44689	−0.05696	0.08545	0.0	−0.00947	0.0	0.0
C	S	39.9100	0.00007	0.18184	−0.02080	0.03121	0.0	−0.00435	0.0	0.0
C	S	160.0000	−0.00001	0.04723	−0.00499	0.00743	0.0	−0.00090	0.0	0.0
C	S	994.7000	0.00000	0.00720	−0.00076	0.00114	0.0	−0.00015	0.0	0.0
C	X	0.2036	0.0	0.0	0.0	0.0	−0.29650	0.0	0.0	−0.02856
C	X	0.8699	0.0	0.0	0.0	0.0	−0.29774	0.0	0.0	−0.16243
C	X	4.2790	0.0	0.0	0.0	0.0	−0.06443	0.0	0.0	−0.03105
C	Y	0.2036	0.0	0.0	0.0	0.0	0.0	0.0	0.33339	0.0
C	Y	0.8699	0.0	0.0	0.0	0.0	0.0	0.0	0.24231	0.0
C	Y	4.2790	0.0	0.0	0.0	0.0	0.0	0.0	0.05756	0.0
C	Z	0.2036	0.00418	0.00106	−0.00179	0.11738	0.0	0.12914	0.0	0.0
C	Z	0.8699	0.00006	0.00097	0.13518	0.12114	0.0	0.29511	0.0	0.0
C	Z	4.2790	0.00028	0.00040	0.02979	0.02802	0.0	0.06086	0.0	0.0
O	S	0.3342	−0.01642	0.00087	0.49982	0.30572	0.0	−0.30007	0.0	0.0
O	S	1.1030	0.03963	−0.00033	0.39549	0.18151	0.0	−0.13214	0.0	0.0
O	S	6.7730	0.44059	0.00003	−0.16325	−0.07354	0.0	0.05667	0.0	0.0
O	S	21.7400	0.45708	−0.00027	−0.11392	−0.05331	0.0	0.04318	0.0	0.0
O	S	76.9300	0.18018	−0.00004	−0.03636	−0.01648	0.0	0.01293	0.0	0.0
O	S	332.2000	0.04169	−0.00002	−0.00815	−0.00375	0.0	0.00299	0.0	0.0
O	S	2200.0000	0.00569	0.00000	−0.00108	−0.00049	0.0	0.00039	0.0	0.0
O	X	0.3814	0.0	0.0	0.0	0.0	−0.27536	0.0	0.0	0.54179
O	X	1.7190	0.0	0.0	0.0	0.0	−0.24381	0.0	0.0	0.37014
O	X	8.3560	0.0	0.0	0.0	0.0	−0.06012	0.0	0.0	0.09601
O	Y	0.3814	0.0	0.0	0.0	0.0	0.0	0.0	0.45440	0.0
O	Y	1.7190	0.0	0.0	0.0	0.0	0.0	0.0	0.32506	0.0
O	Y	8.3560	0.0	0.0	0.0	0.0	0.0	0.0	0.08254	0.0
O	Z	0.3814	0.00366	0.00112	−0.11458	0.10388	0.0	−0.43448	0.0	0.0
O	Z	1.7190	−0.00142	−0.00001	−0.11122	0.09977	0.0	−0.34852	0.0	0.0
O	Z	8.3560	−0.00176	−0.00017	−0.02344	0.02563	0.0	−0.08784	0.0	0.0

TABLE IV. Coefficient vectors and orbital energies for the (95/3) basis set.

Orbital energy			Vector 1 −20.59059	2 −11.36267	3 −1.42987	4 −0.86658	5 −0.70195	6 −0.64364	7 −0.53551	8 −0.44226
Center	Type	Exponent								
H1	S	0.14830	0.00006	0.00003	−0.00357	0.05457	−0.10847	0.07776	0.0	−0.25965
H1	S	0.65770	0.00000	−0.00044	−0.01993	0.16507	−0.15062	0.08646	0.0	−0.20085
H1	S	4.23920	0.00000	−0.00009	−0.00497	0.03336	−0.03520	0.01849	0.0	−0.03155
H2	S	0.14830	0.00006	0.00003	−0.00357	0.05457	0.10847	0.07776	0.0	0.25965
H2	S	0.65770	0.00000	−0.00044	−0.01993	0.16507	0.15062	0.08646	0.0	0.20085
H2	S	4.23920	0.00000	−0.00009	−0.00497	0.03336	0.03520	0.01849	0.0	0.03155
C	S	0.15331	−0.00118	0.00001	−0.04922	0.27009	0.0	0.08407	0.0	0.0
C	S	0.49624	+0.00031	−0.00326	−0.26113	0.44897	0.0	−0.09462	0.0	0.0
C	S	1.96655	−0.00007	−0.14710	0.02694	−0.05924	0.0	0.01050	0.0	0.0
C	S	5.14773	−0.00006	−0.43684	0.08380	−0.11724	0.0	0.01412	0.0	0.0
C	S	14.18920	0.00001	−0.35845	0.04346	−0.06691	0.0	0.00826	0.0	0.0
C	S	42.49740	−0.00001	−0.15448	0.01776	−0.02541	0.0	0.00314	0.0	0.0
C	S	146.09700	0.00000	−0.04540	0.00480	−0.00715	0.0	0.00088	0.0	0.0
C	S	634.88200	0.00000	−0.00933	0.00100	−0.00144	0.0	0.00018	0.0	0.0
C	S	4232.61000	0.00000	−0.00122	0.00013	−0.00019	0.0	0.00002	0.0	0.0
C	X	0.11460	0.0	0.0	0.0	0.0	−0.06603	0.0	0.0	0.02995
C	X	0.35945	0.0	0.0	0.0	0.0	−0.32825	0.0	0.0	−0.14996
C	X	1.14293	0.0	0.0	0.0	0.0	−0.18459	0.0	0.0	−0.09817
C	X	3.98640	0.0	0.0	0.0	0.0	−0.05644	0.0	0.0	−0.02784
C	X	18.15570	0.0	0.0	0.0	0.0	−0.00949	0.0	0.0	−0.00474
C	Y	0.11460	0.0	0.0	0.0	0.0	0.0	0.0	0.12135	0.0
C	Y	0.35945	0.0	0.0	0.0	0.0	0.0	0.0	0.27727	0.0
C	Y	1.14293	0.0	0.0	0.0	0.0	0.0	0.0	0.15428	0.0
C	Y	3.98640	0.0	0.0	0.0	0.0	0.0	0.0	0.04747	0.0
C	Y	18.15570	0.0	0.0	0.0	0.0	0.0	0.0	0.00787	0.0
C	Z	0.11460	−0.00039	−0.00008	0.00883	−0.05074	0.0	0.00867	0.0	0.0
C	Z	0.35945	−0.00027	0.00039	−0.06480	−0.12354	0.0	−0.25958	0.0	0.0
C	Z	1.14293	0.00040	−0.00056	−0.10501	−0.07935	0.0	−0.19082	0.0	0.0
C	Z	3.98640	−0.00010	−0.00049	−0.02244	−0.02530	0.0	−0.04903	0.0	0.0
C	Z	18.15570	0.00002	−0.00010	−0.00487	−0.00407	0.0	−0.00924	0.0	0.0
O	S	0.28461	0.00281	−0.00019	−0.36985	−0.26524	0.0	0.29802	0.0	0.0
O	S	0.93978	−0.00091	−0.00091	−0.49433	−0.22601	0.0	0.16611	0.0	0.0
O	S	3.41364	0.14064	0.00031	0.04210	0.01325	0.0	−0.00161	0.0	0.0
O	S	9.53223	0.46100	0.00016	0.15741	0.07620	0.0	−0.06443	0.0	0.0
O	S	27.18360	0.35555	0.00016	0.08005	0.03649	0.0	−0.02836	0.0	0.0
O	S	81.16960	0.14386	0.00005	0.02941	0.01377	0.0	−0.01122	0.0	0.0
O	S	273.18800	0.04286	0.00002	0.00820	0.00375	0.0	−0.00295	0.0	0.0
O	S	1175.82000	0.00897	0.00000	0.00171	0.00079	0.0	−0.00064	0.0	0.0
O	S	7816.54000	0.00118	0.00000	0.00022	0.00010	0.0	−0.00008	0.0	0.0
O	X	0.21373	0.0	0.0	0.0	0.0	−0.12905	0.0	0.0	0.33109
O	X	0.71706	0.0	0.0	0.0	0.0	−0.25091	0.0	0.0	0.41099
O	X	2.30512	0.0	0.0	0.0	0.0	−0.15550	0.0	0.0	0.24256
O	X	7.90403	0.0	0.0	0.0	0.0	−0.04982	0.0	0.0	0.07939
O	X	35.18320	0.0	0.0	0.0	0.0	−0.00787	0.0	0.0	0.01227
O	Y	0.21373	0.0	0.0	0.0	0.0	0.0	0.0	0.26122	0.0
O	Y	0.71706	0.0	0.0	0.0	0.0	0.0	0.0	0.36369	0.0
O	Y	2.30512	0.0	0.0	0.0	0.0	0.0	0.0	0.21243	0.0
O	Y	7.90403	0.0	0.0	0.0	0.0	0.0	0.0	0.06931	0.0
O	Y	35.18320	0.0	0.0	0.0	0.0	0.0	0.0	0.01087	0.0
O	Z	0.21373	−0.00058	−0.00006	0.01237	−0.05380	0.0	0.18671	0.0	0.0
O	Z	0.71706	0.00017	0.00080	0.13094	−0.08727	0.0	0.35119	0.0	0.0
O	Z	2.30512	−0.00063	0.00036	0.06734	−0.06521	0.0	0.23027	0.0	0.0
O	Z	7.90403	−0.00165	0.00006	0.02073	−0.02038	0.0	0.07147	0.0	0.0
O	Z	35.18320	−0.00029	0.00002	0.00350	−0.00329	0.0	0.01158	0.0	0.0

TABLE V. Net atomic and gross atomic populations for the (73/2) Gaussian basis set.

MO[a]	Atom					
	H1		C		O	
	Net	Gross	Net	Gross	Net	Gross
1	0.0000	0.0000	0.0001	0.0015	1.9970	1.9985
2	0.0000	0.0004	1.9987	1.9993	0.0000	−0.0002
3	0.0012	0.0071	0.1703	0.4042	1.3488	1.5817
4	0.1098	0.2678	0.8362	1.0835	0.4535	0.3809
5	0.1159	0.2234	0.5995	0.9485	0.4538	0.6046
6	0.0436	0.0745	0.3486	0.4478	1.3378	1.3731
7	0.0000	0.0000	0.5580	0.7715	1.0150	1.2285
8	0.3558	0.3165	0.0766	0.1142	1.3902	1.2528
σ Subtotal		0.8897		5.0291		7.1914
π Subtotal		0.0000		0.7715		1.2285
Total	0.6262	0.8897	4.5880	5.8006	7.9962	8.4199

[a] The molecular orbitals are ordered according to the orbital energies. See Table II.

III. DISCUSSION

The results for formaldehyde given in the previous section illustrate the usefulness of Gaussian orbitals as expansion functions for molecular SCF calculations. Such basis functions are popular because of the ease with which the multicenter atomic integrals can be evaluated. However, this advantage is somewhat offset due to the large basis sets required to obtain accurate results. Because of this, the SCF phase of the problem can make the calculation with Gaussian orbitals as time consuming as those employing Slater orbitals. One way to overcome this disadvantage is by using contracted Gaussian sets.[1,18] Calculations on the ethylene[1] and water[2] molecules indicate that little accuracy is lost with moderate amounts of contraction. Such a procedure greatly reduces the amount of computer time required. Since our wavefunctions were calculated using uncontracted basis functions, the results can be used to optimumly determine contraction coefficients.[1] Such contracted functions may then be employed to study larger aldehydes or ketones, etc.

TABLE VI. Overlap populations for the (73/2) Gaussian basis set.

MO[a]	Overlap population			
	H1–H2	H1–C	H1–O	C–O
1	0.0000	0.0000	0.0000	0.0029
2	0.0000	0.0009	0.0000	−0.0004
3	0.0002	0.0063	0.0053	0.4552
4	0.0223	0.3068	−0.0131	−0.1190
5	−0.0238	0.2186	0.0204	0.2609
6	0.0098	0.0730	−0.0209	0.1126
7	0.0000	0.0000	0.0000	0.4270
8	−0.0957	0.0960	−0.0790	−0.1169
σ Subtotal	−0.0872	0.7016	−0.0873	0.5952
π Subtotal	0.0000	0.0000	0.0000	0.4270
Total	−0.0872	0.7016	−0.0873	1.0222

[a] The molecular orbitals are ordered according to the orbital energies. See Table II.

The dissociation energies presented in Table I are indicative of *ab inito* attempts to calculate this differential property. The problem is well documented[16,19–21] and arises because dissociation energies are small quantities obtained by subtracting two large quantities with sizable inherent errors (i.e., correlation energy). The wavefunction from the (95/3) basis set predicts 59% of the observed dissociation energy, compared to 65% for a calculation on ethylene with an identical basis set.[1] Hollister and Sinanoğlu[11] estimate the molecular extra correlation energy for formaldehyde to be 3.74 eV. Adding this to the calculated dissociation energy, we obtain a "corrected" dissociation energy of 13.37 eV, which is still in error by 2.87 eV. Presumably this error arises from basis-set truncation, particularly in the neglect of d and higher orbitals in the molecular basis set. Note that the dissociation energy for the (73/2) basis set is nearly as good as that for the (95/3) basis set and is considerably better than the single Slater result.

To the extent that Koopmans' theorem[22] holds, the negative of an orbital energy is just the vertical ionization energy needed to remove an electron from that orbital. In Table II we note surprisingly good agreement for the π orbital, $1b_1$ (calculated, 14.57 eV vs experimental, 14.40 eV), fair agreement for the so-called n orbital, $2b_2$ (calculated, 12.04 eV vs experimental, 10.86 eV), and increasingly worse agreement as the orbital becomes more tightly bound. Quite similar results are observed in ethylene.[1] The error arises from two sources: (a) a neglect of the self-con-

[18] E. Clementi and D. R. Davis, J. Comput. Phys. 1, 223 (1966); also see E. Clementi, J. Chem. Phys. 46, 3851 (1967), and succeeding papers in that series.

[19] A. C. Wahl, J. Chem. Phys. 41, 2600 (1964).

[20] P. E. Cade, K. D. Sales, and A. C. Wahl, J. Chem. Phys. 44, 1973 (1966).

[21] P. E. Cade and W. M. Huo, J. Chem. Phys. 47, 614 (1967); and P. E. Cade and W. M. Huo, *ibid.* 47, 649 (1967).

[22] T. Koopmans, Physica 1, 104 (1933).

TABLE VII. Net atomic and gross atomic populations for the (95/3) Gaussian basis set.

MO[a]	Atom H1 Net	H1 Gross	C Net	C Gross	O Net	O Gross
1	0.0000	0.0000	0.0000	−0.0002	2.0004	2.0002
2	0.0000	0.0000	1.9996	1.9998	0.0000	0.0001
3	0.0013	0.0066	0.2104	0.4752	1.2492	1.5116
4	0.1012	0.2468	0.8988	1.1235	0.4561	0.3829
5	0.1312	0.2344	0.5796	0.0237	0.4542	0.6074
6	0.0509	0.0834	0.3814	0.5022	1.2937	1.3310
7	0.0000	0.0000	0.4944	0.7101	1.0741	1.2899
8	0.3812	0.2980	0.1032	0.1375	1.4715	1.2664
σ Subtotal		0.8692		5.1619		7.0996
π Subtotal		0.0000		0.7101		1.2899
Total	0.6659	0.8692	4.6675	5.8720	7.9993	8.3895

[a] The molecular orbitals are ordered according to the orbital energies. See Table II.

sistency requirement for the ionized state, inclusion of which would decrease the calculated ionization energy, and (b) a difference in the correlation energies of the neutral and ionized molecules, inclusion of which would increase the calculated ionization energy. Thus, the correction to the ionization energy calculated using Koopmans' theorem is a balancing of two oppositely directed effects. In some cases the two errors nearly cancel, such as for the π orbital, and in others the sum may be quite large, such as for the n and more deeply buried orbitals. Of course, an additional error arises from the use of a truncated basis set, which may increase or decrease the sum of the other two errors. Calculations on water[2] lead us to believe that the orbital energies for the (95/3) basis set are within ±0.01 a.u. of the Hartree–Fock orbital energies. Our conclusions then should be unaffected by the addition of more basis functions.

The population analysis results given in Tables V–VIII can be used to classify the molecular orbitals in a qualitative, chemically interpretive, manner. In a subsequent paper, contour maps of the electronic density will be used to put this information into more pictorial form. At present we shall content ourselves with characterizing the molecular orbitals according to the various population breakdowns. The first two orbitals, $1a_1$ and $2a_1$, are the oxygen and carbon inner-shell orbitals. The following orbital, $3a_1$, is strongly CO σ bonding, with most of the charge centered on the oxygen; qualitatively, it had been assumed that this orbital was almost exclusively an oxygen $2s$ orbital; however, as we can see, molecular formation perturbs the oxygen $2s$ orbital quite strongly. The next orbital, $4a_1$, is CH σ bonding and slightly CO σ antibonding, with much of the charge associated with the carbon. The following orbital, $1b_2$, is about equally CO σ and CH σ bonding, with the charge mainly on the oxygen and carbon. The $5a_1$ orbital is only slightly CO σ and CH σ bonding, with most of the charge localized on the oxygen and carbon. The π orbital, $1b_1$, is, of course, CO π bonding, with the charge distinctly polarized in the oxygen direction. The so-called n orbital, $2b_2$, is not particularly bonding or antibonding, as one would expect if it were to be identified as a nonbonding orbital, but the charge, while mainly localized on the oxygen, does have a significance contribution from the hydrogens. These results emphasize the major conceptual difficulty associated with Hartree–Fock theory—the individual molecular orbitals do not describe regions of space which are localized between or around nuclear centers, i.e., bonds, lone pairs, etc., but rather they are delocalized over the entire molecule.

From the population analysis discussed above, we note that the n orbital has a rather large contribution

TABLE VIII. Overlap populations for the (95/3) Gaussian basis set.

MO[a]	H1–H2	H1–C	H1–O	C–O
1	0.0000	0.0000	0.0000	−0.0004
2	0.0000	0.0001	0.0000	0.0003
3	0.0001	0.0065	0.0040	0.5168
4	0.0164	0.2864	−0.0116	−0.1232
5	−0.0381	0.2176	0.0268	0.2529
6	0.0173	0.0655	−0.0179	0.1104
7	0.0000	0.0000	0.0000	0.4315
8	−0.1638	0.1184	−0.1210	−0.1682
σ Subtotal	−0.1680	0.6945	−0.1198	0.5886
π Subtotal	0.0000	0.0000	0.0000	0.4315
Total	−0.1680	0.6945	−0.1198	1.0201

[a] The molecular orbitals are ordered according to the orbital energies. See Table II.

from the hydrogen atoms. This is in distinct contradiction to the older concepts,[5,22] which assigned this orbital as a nonbonding lone pair ($2p$) orbital on the oxygen atom. As with the minimum-basis-set calculations,[24] the centroid of the n orbital (i.e., $\langle z \rangle$) indicates considerable delocalization. In fact, as the basis set was refined, the centroid shifted closer to the carbon. Our calculations also predict that the n orbital is more tightly bound than experiment indicates. In summary, an LCAO-MO-SCF wavefunction for formaldehyde near the (sp) limit has an n orbital which is not localized on the oxygen atom, as had been expected, but contains significant hydrogen contributions. From the calculations on water,[2] we expect that these results will not be appreciably changed for a wavefunction at the Hartree–Fock limit.

The CO π bond in both the (73/2) and the (95/3) basis sets is characterized by a significant amount of charge transfer from the carbon to the oxygen. This is in agreement with our intuitive chemical concepts (electronegativities, etc.). On the other hand, the minimum Slater basis set indicates a nearly homopolar bond. This evidently arose from the use of an unoptimized, limited basis set.

From the gross population analysis of the (95/3) basis set in Table VII, we see that the hydrogen atoms are σ donors (losing 0.13 electrons), the carbon is a σ acceptor (gaining 0.16 electrons) while being a π donor (losing 0.29 electrons), and the oxygen is both a σ acceptor (gaining 0.10 electrons) and a π acceptor (gaining 0.29 electrons). The σ changes are quite large, even though in a purely pi-electron approximation such charge transfer would be ignored. The problem is particularly acute for carbon, for which the two changes are in opposite directions. The net result of the above is a charge transfer from the CH_2 group to the oxygen. The residual charge on the hydrogens and the carbon is $+0.13e$, while the oxygen has a net charge of $-0.39e$.

As stated previously, in a subsequent paper we will present contour maps of the electronic density and its various partitions. We will also compare the one-electron properties of formaldehyde in the two Gaussian basis sets with the corresponding quantities from the calculation with a minimum basis set of Slater orbitals and with experiment.

IV. COMPUTATIONS

Evaluation of the integrals for both sets were performed on the CDC 6600 computer. The integral evaluation times for the (73/2) and (95/3) sets were 2.1 and 11.0 min, respectively. The SCF cycling was carried out on the CDC 6400 computer, which is a somewhat slower machine. The time for one iteration for the small set was 1.5 min and for the large set was 7.3 min. Neither calculation used symmetry-adapted basis functions. An extrapolation procedure[25] was used to increase the rate of convergence for both sets.

The vectors for the small set have converged to 10^{-6}, except for a few coefficients in the higher vectors changing in the fifth place. The large set has converged to 10^{-7}, again with the exception of a few coefficients in the higher vectors changing in the sixth place. The orbital energies for the (73/2) set were still changing in the fifth decimal place and for the (95/3) set in the sixth place. In each case the total energy had converged to more than eight decimal places.

ACKNOWLEDGMENTS

We wish to thank Dr. Lester Sachs and Dr. Murray Geller for making their Gaussian molecular SCF program MOSES available to us. Also, we are indebted to Dr. Geller and Dr. Vincent McKoy for a number of helpful discussions. The authors would like to thank Control Data Corporation (Mr. William F. Busch in particular) for their making 6000 series computers available to us for this research. Special thanks go to Mr. Robert L. Korsch, of Control Data Corporation, for his help throughout these calculations.

[22] H. H. Jaffe and M. Orchin, *Theory and Applications of Ultraviolet Spectroscopy* (John Wiley & Sons, Inc., New York, 1962); M. Kasha, Discussions Faraday Soc. 9, 14 (1950); H. McConnell, J. Chem. Phys. 20, 700 (1952).

[24] D. E. Freeman and W. Klemperer, J. Chem. Phys. 45, 52 (1966).

[25] N. W. Winter, T. H. Dunning, and V. McKoy, J. Chem. Phys. (to be published).

Reprinted from THE JOURNAL OF CHEMICAL PHYSICS, Vol. 48, No. 5, 1879-1882, 1 March 1968
Printed in U. S. A.

Numerical Solution of the S-Limit Schrödinger Equation

N. W. WINTER, DENNIS DIESTLER,* AND VINCENT MCKOY
Gates and Crellin Laboratories of Chemistry,† California Institute of Technology, Pasadena, California
(Received 8 November 1967)

Numerical solutions to the S-limit Schrödinger equation have been obtained for He and Li^+. Using these the energy and the expectation values $\langle \Sigma r_i \rangle$ and $\langle \Sigma r_i^2 \rangle$ were calculated and compared to the radial configuration interaction values. The results demonstrate that the direct numerical solution of many partial differential equations in chemical physics can be accomplished in a practical and straightforward manner.

I. INTRODUCTION

The finite difference method has been previously discussed as a means of solving the Schrödinger equation for two electrons interacting in an infinite square well.[1] Due to the nature of the potential, that calculation was not a severe test of the method's ability to solve differential equations occurring in quantum mechanics. As an example, many of the nonhomogeneous equations arising in perturbation theory could be easily attacked with a direct numerical method,[2] after they have been reduced by a partial wave expansion to a set of uncoupled two-variable partial differential equations.

Numerical methods have been used to solve the ordinary integrodifferential equations determining the Hartree–Fock orbitals for atoms. With the low cycle times and large storage capacity of modern computers we are at a point where the numerical solution of both ordinary and partial differential equations can be accomplished at a large number of points in space. This is one reason why we suggest that numerical methods of solving many differential equations in quantum mechanics be reexamined. While such methods may not be uniformly better than variational methods, they are straightforward in principle and simple to program as compared with, for example, the years already spent evaluating integrals containing interelectronic coordinates in the atomic correlation problem.

Here we describe the solution of the eigenvalue equation corresponding to a potential function which includes all radial correlation for the two-electron atom. The results are compared to accurate variational calculations. Both radial correlation and the finite difference method are adequately described elsewhere,[3,4] and therefore the first two sections give only a brief review of these topics. The third section contains the results for the finite difference method and the comparison with the variational calculations.

II. THE S-LIMIT SCHRÖDINGER EQUATION

The Hamiltonian for the two-electron atom in atomic units is

$$H = -\tfrac{1}{2}\nabla_1^2 - \tfrac{1}{2}\nabla_2^2 - Z/r_1 - Z/r_2 + 1/r_{12}. \quad (1)$$

Then by expanding the electronic interaction potential as follows,

$$1/r_{12} = \sum_l (r_<^l/r_>^{l+1}) P_l(\cos\theta_{12}), \quad (2)$$

it is evident that the spherical component of the Hamiltonian is just

$$H_0 = -\frac{1}{2}\left[\frac{1}{r_1^2}\frac{\partial}{\partial r_1}\left(r_1^2\frac{\partial}{\partial r_1}\right) + \frac{1}{r_2^2}\frac{\partial}{\partial r_2}\left(r_2^2\frac{\partial}{\partial r_2}\right)\right] - \frac{Z}{r_1} - \frac{Z}{r_2} + \frac{1}{r_>}, \quad (3)$$

where $r_> = \max(r_1, r_2)$. From the S-limit solution $\psi(r_1 r_2) = (4\pi \cdot r_1 \cdot r_2)^{-1} u(r_1 r_2)$ the differential equation for

* Present address: Department of Chemistry, University of Missouri at St. Louis, St. Louis, Missouri.
† Contribution No. 3608.
[1] D. J. Diestler and V. McKoy, J. Chem. Phys. 47, 454 (1967).
[2] V. McKoy and N. W. Winter, "Numerical Solution of Quantum-Mechanical Pair Equations," J. Chem. Phys. (to be published).
[3] E. Hololen, Phys. Rev. 104, 1301 (1956); H. Shull and P.-O. Löwden, J. Chem. Phys. 25, 1035 (1956).
[4] L. Fox, *Numerical Solution of Two-Point Boundary Problems* (Oxford University Press, London, 1957).

the function $u(r_1r_2)$ can be written

$$-\frac{1}{2}\left(\frac{\partial^2}{\partial r_1^2}+\frac{\partial^2}{\partial r_2^2}\right)u(r_1r_2)-\frac{Z}{r_1}u(r_1r_2)$$
$$-\frac{Z}{r_2}u(r_1r_2)+\frac{1}{r_>}u(r_1r_2)-Eu(r_1r_2)=0. \quad (4)$$

The function $u(r_1r_2)$ is taken to be normalized as follows

$$\int u(r_1r_2)u(r_1r_2)dr_1dr_2=1,$$

and the boundary conditions require that $u(r_1r_2)$ vanish when either variable is zero or infinity. Using the finite difference method the next section illustrates how Eq. (4) can be systematically reduced to an algebraic problem.

III. REVIEW OF THE FINITE DIFFERENCE METHOD

There are two important points to consider in treating Eq. (4) with the finite difference method. First, we want to treat the differential equation as a boundary value problem and not as an initial value one. The boundary condition at r_1 or r_2 equal to zero can be easily imposed, but the condition as r_1 or r_2 goes to infinity is more difficult and must be modified so as to describe the solution over a finite numerical grid. Fox[4] suggests two methods for handling this type of situation. The first approach, which is direct and is the one we use, is to require that $u(r_1r_2)$ vanish on the edges of a square bounded on two sides by $r_1=R$, $r_2=R$. As long as R, which in this method "represents" infinity, is sufficiently large, the solution remains a good approximation to the solution one would obtain as $R\to\infty$. The other approach, an indirect one which could be easily implemented, assumes that for large values of the variables r_1 and r_2 the differential equation has a solution $g(r_1r_2)\exp[-\alpha(r_1+r_2)]$ where, at reasonable grid sizes, $g(r_1r_2)$ varies slowly. We can allow for this by using as the boundary condition the equation $u(r_1r_2)=e^{\alpha h}u(r_1+h, r_2)$ at any convenient point r_1. The quantity h is just the spacing between grid points.

The second and more important point to consider is the level of the difference approximation to be used. The differential operators in Eq. (4) can be formally expanded in an infinite series of difference operators and the level of the approximation is determined by the truncation of this series. After some experimentation it was found that the best compromise between accuracy and ease of calculation was to employ only second differences and then extrapolate the results by the Richardson method.[5]

[5] L. Richardson and J. Gaunt, Trans. Roy. Soc. (London) A226, 299 (1927).

Fox[4] argues strongly for including higher-order difference operators by an iterative method. Although such schemes may allow one to use a coarser grid and still obtain reliable solutions, we decided to work only with second differences. This approximation best demonstrates the straightforwardness of the numerical approach.

The derivatives can be written in terms of second differences as follows,

$$h^2(\partial^2/\partial r_1^2)u(r_1r_2)$$
$$=u(r_1-h, r_2)-2u(r_1r_2)+u(r_1+h, r_2)+O(h^4), \quad (5a)$$

$$h^2(\partial^2/\partial r_2^2)u(r_1r_2)$$
$$=u(r_1, r_2-h)-2u(r_1r_2)+u(r_1, r_2+h)+O(h^4), \quad (5b)$$

where h is the grid spacing. By introducing these into the S-limit equation, there results a set of linear equations, one for each grid point, having the form

$$(1/h^2)[u(r_1-h, r_2)+u(r_1+h, r_2)+u(r_1, r_2-h)$$
$$+u(r_1, r_2+h)]+[(2Z/r_1)+(2Z/r_2)-(2/r_>)$$
$$-4+2(E)]u(r_1r_2)=0. \quad (6)$$

These can be collected into the following matrix form,

$$Du=Eu, \quad (7)$$

where D is a real symmetric banded matrix,[6] u is an eigenvector whose elements correspond to the solution values at the various grid points, and E is the corresponding eigenvalue.

At this point the solution of the S-limit equation has been reduced to the diagonalization of the difference matrix, or at least to that of finding the lowest eigenvector and eigenvalue. Since D is a banded matrix, this can be accomplished for large matrices in a fairly simple fashion. It is important to be able to solve extremely large matrix equations in order to reduce the difference truncation error to a tolerable level. The method we have used to extract the lowest eigenvector is described in the appendix. Even though matrices as large as 2600 by 2600 were diagonalized, the difference error remained important. To correct this, solutions at several grid sizes were found and the Richardson extrapolation method[5] was used to predict the results at zero grid size. The other alternative, including higher differences, was tried and found to be at best only equally as accurate as extrapolation. The inclusion of higher differences has the disadvantage that grid points outside the boundaries must be dealt with. Because of this arbitrariness, we chose to stay on firmer ground with second differences. The results for He and Li^+ are presented in the next section.

[6] See Appendix.

IV. THE FINITE DIFFERENCE RESULTS

The lowest eigenvector of the S-limit matrix was found at four different grid sizes for each atom. The radial cutoff for He was set at 5 a.u. and for Li^+ at 4 a.u. In choosing the cutoff we tried to balance the advantage of a small grid size with the disadvantage of unphysical boundary conditions.

With the eigenvectors, the energy and the expectation values $\langle\sum r_i\rangle$ and $\langle\sum r_i^2\rangle$ were found at each grid size. Simple matrix multiplication was used rather than numerical quadrature in order to be able to extrapolate the results.

Tables I–III give the initial results for each grid size as well as the extrapolated values. In the tables the second column gives the eigenvalues of the finite difference matrix. The third column gives the results of extrapolating successive values in the second column assuming that the difference between these approximate eigenvalues and the eigenvalue at zero mesh size has an h^2 dependence. The fourth column gives the result of an h^4 extrapolation, i.e., one assumes that the difference between the approximate eigenvalues and the exact eigenvalue is given by $a_0h^2+a_1h^4$. The final extrapolant is obvious. This h^2 convergence is common in many elliptic partial differential equations.[7] We will comment further on this property in the next section.

To determine the accuracy of the eigenvectors the residual vector $R=Du-Eu$ was calculated and found to have a length in the range 10^{-5} to 10^{-6} in each case. In addition, the local energy, $E(i)=(Du)_i/u(i)$ was found to be constant to more than five decimal places at each grid point. In Table IV we compare the finite difference results, including the virial ratio $V/2E$ to the radial configuration interaction (RCI) values.[8] The RCI basis orbitals were $1s$, $2s$, $3s$, $4s$, $1s'$, and $2s'$ Slater-type functions. The exponents for the helium atom were $\zeta=3.7530$ and $\zeta'=1.5427$ and for the lithium ion $\zeta=5.8249$ and $\zeta'=2.5456$. The energy compares well with the S-limit energy in both cases; however, for helium the other properties are slightly less satisfactory.

TABLE I. Total energy.

Grid size[a]	Initial result			
		Helium		
5/13	−2.512505			
		−2.851565		
5/26	−2.766800		−2.877493	
		−2.874612		−2.878682
5/39	−2.826695		−2.878608	
		−2.877609		
5/52	−2.848967			
		Lithium ion		
4/13	−6.072929			
		−7.136845		
4/26	−6.870866		−7.245837	
		−7.233727		−7.252321
4/39	−7.072455		−7.251916	
		−7.247369		
4/52	−7.148980			

[a] The grid size is defined as the radial cutoff divided by the number of strips along one side of the grid.

TABLE II. Expectation value of Σr_i.

Grid size	Initial result			
		Helium		
5/13	2.098644			
		1.870169		
5/26	1.927288		1.864165	
		1.864832		1.864173
5/39	1.892590		1.864173	
		1.864338		
5/52	1.880230			
		Lithium ion		
4/13	1.343108			
		1.152010		
4/26	1.199784		1.147341	
		1.147860		1.147435
4/39	1.170937		1.147429	
		1.147537		
4/52	1.160700			

TABLE III. Expectation value of Σr_i^2.

Grid size	Initial result			
		Helium		
5/13	2.986072			
		2.414823		
5/26	2.557635		2.399441	
		2.401150		2.399136
5/39	2.470699		2.399155	
		2.399654		
5/52	2.439617			
		Lithium ion		
4/13	1.196438			
		0.903515		
4/26	0.976746		0.896798	
		0.897544		0.896575
4/39	0.932745		0.896589	
		0.896828		
4/52	0.917031			

[7] See for example H. C. Bolton and H. I. Scoins, Proc. Cambridge Phil. Soc. 53, 150 (1956). These authors attempted a numerical solution of the S-limit equation. Their best extrapolant was −2.652 a.u. for helium.

[8] We wish to thank Dr. William A. Goddard for allowing us to use his RCI computer program for these calculations.

TABLE IV. Comparison of the finite difference values with the radial configuration interaction results.

	E	$V/2E$	$\langle\Sigma r_i\rangle$	$\langle\Sigma r_i^2\rangle$
		Helium		
FD	−2.8787	1.0007	1.8642	2.3991
RCI	−2.8790	1.0000	1.8688	2.4206
		Lithium ion		
FD	−7.2523	0.9999	1.1474	0.8966
RCI	−7.2525	1.0000	1.1475	0.8968

V. DISCUSSION

From Tables I, II, and III we see that in each case the extrapolants have converged to more than four places. This implies that further extrapolations using results at smaller grid sizes would give little or no improvement. However, for He the expectation values $\langle\sum r_i\rangle$ and $\langle\sum r_i^2\rangle$ indicate that the radial cutoff was chosen too close to the nucleus. Since it has a much smaller radial extent, the 4 a.u. cutoff for the lithium ion was a better approximation to the true boundary conditions (see Table IV). In the case of helium a cutoff of 6 a.u. would have given better agreement. A preliminary investigation of the hydride ion, which is extremely extended, gives support to this conclusion.

In spite of this difficulty, the calculations presented in this paper have shown that good accuracy can be obtained with the finite difference method in the solution of these partial differential equations. We realize that there are variational methods that give as good or better results for this particular example. However, there are other examples where the choice of the variational parameters and even the basis functions themselves can be so prejudicial that meaningful results are difficult to obtain. In the numerical method much is known about the convergence of finite difference solutions to the exact solutions. As seen, this information can be quite useful through an extrapolation process. In a variational method, even though the trial function is a linear combination of functions belonging to a complete set, little is known about the approach towards the true eigenvalue as the number of functions is increased. Even in a problem as simple as the S-limit there have been numerous estimates of the true eigenvalue.

Finally it should be reiterated that the finite difference method is definitely not limited to eigenvalue equations. As previously mentioned, the perturbation equations determining the first- and second-order wavefunctions are easily solved by this same method. The solution of these nonhomogeneous equations will be discussed in a later paper.[3] Such nonhomogeneous equations are actually simpler to solve than the eigenvalue problem. This will be an interesting application of the numerical methods discussed in this paper.

ACKNOWLEDGMENT

We are grateful to Dr. William A. Goddard for helpful discussions. One of us (D.D.) wishes to thank the National Science Foundation for a pre-doctoral fellowship.

APPENDIX: DIAGONALIZATION OF LARGE BANDED MATRICES

The banded structure of the finite difference matrices is very simple. The matrix for a one-variable equation, in the second difference approximation, is tridiagonal.[9] In such a matrix only nonzero off-diagonal matrix elements lie in the first super- and first subdiagonal. For a two-variable equation the structure is altered to include nonzero elements in the nth superdiagonal and the nth subdiagonal, where n is the number of points along one side of the grid.

Taking the matrix equation to be $Du=Eu$, the method assumes we have a guess for the eigenvector. Let the trial vector be u_0 and define a correction vector as follows,

$$c_0=u-u_0.$$

Then substituting into the matrix, we obtain the following equation for c_0,

$$(D-E)c_0=-(D-E)u_0. \tag{8}$$

The right side is known and the solution of the nonhomogeneous matrix equation yields the correction to u_0. From this we can construct a new trial vector $u_1=u_0+c_0$ and repeat the process to find a new correction vector c_1. The one difficulty is that Eq. (8) requires the previous knowledge of the eigenvalue E. In order to circumvent this, we approximate E by the Rayleigh mean of D with respect to u_0, that is,

$$E_{\rm rm}{}^0=u_0Du_0/u_0u_0. \tag{9}$$

Then Eq. (8) becomes

$$(D-E_{\rm rm}{}^0)c_0=-(D-E_{\rm rm}{}^0)u_0, \tag{10}$$

where the right side is just the residual vector R_0. Upon succeeding iterations the correction vector c_i becomes smaller, as does the residual vector R_i, and the trial vector u_i approaches the exact solution. The ultimate accuracy depends on the machine error, but depending on the initial guess three to four passes are sufficient to reduce the residual vector to a length less than 10^{-6} and have the Rayleigh mean agree with the local energy to five decimal places at each point.

The important key to the method is the accurate solution of Eq. (10). This was possible due to the efficient program for the solution of simultaneous linear equations developed by McCormick.[10]

[9] For a discussion of matrix techniques see L. Fox, *An Introduction to Numerical Linear Algebra* (Clarendon Press, Oxford, England, 1964).

[10] C. W. McCormick and K. J. Hebert, "Solution of Linear Equations with Digital Computers," California Institute of Technology Report, 1965 (unpublished).

Reprinted from THE JOURNAL OF CHEMICAL PHYSICS, Vol. 48, No. 12, 5514–5523, 15 June 1968
Printed in U. S. A.

Numerical Solution of Quantum-Mechanical Pair Equations*

VINCENT MCKOY AND N. W. WINTER
Gates and Crellin Laboratories of Chemistry,† California Institute of Technology, Pasadena, California
(Received 26 January 1968)

We discuss and illustrate the numerical solution of the differential equation satisfied by the first-order pair functions of Sinanoğlu. An expansion of the pair function in spherical harmonics and the use of finite difference methods convert the differential equation into a set of simultaneous equations. Large systems of such equations can be solved economically. The method is simple and straightforward, and we have applied it to the first-order pair function for helium with $1/r_{12}$ as the perturbation. The results are accurate and encouraging, and since the method is numerical they are indicative of its potential for obtaining atomic-pair functions in general.

INTRODUCTION

In the Hartree–Fock approximation each electron moves in a potential averaged over the motions of all others. This is an excellent starting point, and a great deal of chemical knowledge can be obtained this way. Many properties require more accurate wavefunctions for their prediction and understanding. The difference between the Hartree–Fock and exact wavefunction is referred to as the correlation wavefunction. It is important to have methods of finding the correlation wavefunction and its effect on physical observables.

Sinanoğlu[1] has developed a many-electron theory of atoms and molecules. This theory can provide the wavefunction and energy of an atom or molecule to chemical accuracy, and it does so in such a way that it does not become rapidly difficult or uneconomcial as the number of electrons increases. In one of his early papers[1] the first-order correction to the single-particle wavefunction was expressed in terms of pair functions which describe the correlation between pairs of electrons.[2] These first-order pair functions are solutions of nonhomogeneous partial differential equations. The equations are just like those for an actual two-electron system, except that each electron moves in the Hartree–Fock (HF) field of the entire medium. This has not been fully appreciated, especially from a computational standpoint. Each pair energy has a variational principle, and attempts to solve the pair equations have been mainly

* Supported in part by a grant from the NSF (GP 6965).
† Contribution No. 3642.
[1] Some early references are O. Sinanoğlu in J. Chem. Phys. 33, 1212 (1960); Phys. Rev. 122, 493 (1961); Proc. Roy. Soc. (London) A260, 379 (1961); Proc. Natl. Acad. Sci. U.S. 47, 1217 (1961). For a review of the theory and an extensive list of references see O. Sinanoğlu, Advan. Chem. Phys. 6, 315 (1964).

[2] In later papers the pair theory was made accurate to all orders, i.e., beyond first order. We refer the reader to the review article in Ref. 1. The complete form of the many-electron theory is not a perturbation theory.

by this method. The variational method reduces the calculation to the evaluation of a large number of integrals. The presence of a nonlocal potential in the HF operator does lead to some difficult integrals, which can become more difficult if higher powers of the interelectronic coordinate are included. A large effort has gone into evaluating such atomic integrals.

In this paper we discuss and illustrate the numerical solution of the differential equation satisfied by a pair function. An expansion of the pair function in spherical harmonics and the use of finite-difference methods convert the differential equation into a set of simultaneous equations. Large systems of such equations can be solved quite economically, e.g., about 2000 equations in two minutes. The method has many attractive features, and we have applied it to the equation of the first-order pair function for the helium atom. The results are accurate and encouraging, and since the method is numerical, these results are truly indicative of its potential in solving for atomic pair functions in general.

THEORY

A. Sinanoğlu's Pair Equations

The total Hamiltonian, H, and the zeroth-order Hamiltonian, H_0, for an N-electron atom are

$$H=\sum_{i=1}^{N}\left(-\tfrac{1}{2}\nabla_i^2-\frac{Z}{r_i}\right)+\sum_{i<j}^{N}\frac{1}{r_{ij}} \tag{1}$$

and

$$H_0=\sum_{i=1}^{N}(h_i^0+V_i), \tag{2a}$$

respectively. In Eq. (2a) V_i is the Hartree–Fock potential, which is the same for all electrons. For closed-shell atoms V_i is uniquely defined.[3] Also in Eq. (2a),

$$h_i^0=-\tfrac{1}{2}\nabla_i^2-(Z/r_i). \tag{2b}$$

The zeroth-order function $\psi^{(0)}$ satisfies

$$H_0\psi^{(0)}=E_0\psi^{(0)}, \tag{3}$$

where

$$E_0=\sum_i \epsilon_i$$

and each HF orbital satisfies the equation

$$(h_i^0+V_i)\phi_i=\epsilon_i\phi_i. \tag{4}$$

The zeroth-order wavefunction $\psi^{(0)}$ is just the antisymmetrized product of HF orbitals,

$$\psi^{(0)}=A(\phi_1(1)\phi_2(2)\cdots\phi_n(N)) \tag{5}$$

The first-order correction to $\psi^{(0)}$, $\psi^{(1)}$, satisfies the equation

$$(H_0-E_0)\psi^{(1)}=(E_1-H_1)\psi^{(0)}, \tag{6}$$

where the perturbation H_1 is

$$H_1=\sum_{i<j}^{N}\frac{1}{r_{ij}}-\sum_{i=1}^{N}V_i. \tag{7}$$

Equation (6) is an inhomogeneous partial differential equation in $3N$ spatial variables. It has solutions if the corresponding homogeneous equation are orthogonal to the inhomogeneity, $(E_1-H_1)\psi^{(0)}$. The general solution of Eq. (6) is

$$\psi^{(1)}=\psi_p^{(1)}+c\psi^{(0)}, \tag{8}$$

i.e., a sum of a particular solution, $\psi_p^{(1)}$, plus a contribution from the homogeneous solution. The constant, c, is chosen so that $\langle\psi^{(0)},\psi^{(1)}\rangle=0$.

From Sinanoğlu's analysis[1] the first-order wavefunction can be written as

$$\psi^{(1)}=\sum_{i<j}^{N}\frac{A}{\sqrt{2}}(\phi_1(1)\phi_2(2)\cdots\phi_{i-1}\mathfrak{a}_{ij}^{(1)}\phi_{j+1}\cdots\phi_N), \tag{9}$$

where $\mathfrak{a}_{ij}^{(1)}(\mathbf{x}_i,\mathbf{x}_j)$, a first-order pair function, satisfies the nonhomogeneous differential equation

$$(e_i+e_j)\mathfrak{a}_{ij}^{(1)}=-Q(1/r_{12})B(\phi_i(1)\phi_j(2)). \tag{10}$$

The operator, Q, makes a two-electron function orthogonal to all occupied H–F orbitals; i.e.,

$$Q=1-\sum_{i=1}^{N}(|\phi_i(1)\rangle\langle\phi_i(1)|+|\phi_i(2)\rangle\langle\phi_i(2)|)+\sum_{i<j}^{N}|B(\phi_i(1)\phi_j(2))\rangle\langle B(\phi_i(1)\phi_j(2))|, \tag{11}$$

and e_i is just the HF operator minus an orbital energy, ϵ_i,

$$e_i=-\tfrac{1}{2}\nabla_i^2-\frac{Z}{r_i}+\sum_{j=1}^{N}S_j(\mathbf{x}_i)-\sum_{j=1}^{N}R_j(\mathbf{x}_i)-\epsilon_i, \tag{12}$$

with

$$B(\phi_i(1)\phi_j(2))=(1/\sqrt{2})(\phi_i(1)\phi_j(2)-\phi_i(2)\phi_j(2)), \tag{13a}$$

$$S_j(\mathbf{x}_i)\phi_k(\mathbf{x}_i)=\left(\int\phi_j(\mathbf{x}_j)r_{ij}^{-1}\phi_j(\mathbf{x}_j)\,d\mathbf{x}_j\right)\phi_k(\mathbf{x}_i), \tag{13b}$$

and

$$R_j(\mathbf{x}_i)\phi_k(\mathbf{x}_i)=\left(\int\phi_j(\mathbf{x}_j)r_{ij}^{-1}\phi_k(\mathbf{x}_j)\,d\mathbf{x}_j\right)\phi_j(\mathbf{x}_i). \tag{13c}$$

We also define

$$V_e(\mathbf{x}_i)=\sum_{j=1}^{N}S_j(\mathbf{x}_i) \tag{14a}$$

[3] For a discussion of the many-electron theory for open-shell systems see H. J. Silverstone and O. Sinanoğlu, J. Chem. Phys. 44, 1899, 3608 (1966).

and

$$V_s(\mathbf{x}_i) = \sum_{j=1}^{N} R_j(\mathbf{x}_i). \tag{14b}$$

The pair functions are also rigorously orthogonal to all occupied HF orbitals, i.e.,

$$\int \hat{u}_{ij}^{(1)}(\mathbf{x}_1, \mathbf{x}_2)\phi_k(\mathbf{x}_1)\,d\mathbf{x}_1 = 0.$$

The second-order energy, E_2, is

$$E_2 = \sum_{i<j}^{N} \langle B(\phi_i(1)\phi_j(2)), r_{12}^{-1}\hat{u}_{ij}^{(1)}(\mathbf{x}_1, \mathbf{x}_2)\rangle. \tag{15}$$

The pair function, $\hat{u}_{ij}^{(1)}$, is the solution of the first-order part of the Schrödinger equation for two electrons in the HF "sea." The effect of the medium enters through the HF potentials in the operators e_i and Q.

One can write the solution of Eq. (10) as follows:

$$\hat{u}_{ij}^{(1)} = Qu_{ij}, \tag{16}$$

where Q is defined in Eq. (11) and u_{ij} satisfies the equation

$$(e_i+e_j)u_{ij} = [J_{ij} - K_{ij} - (1/r_{12})]B(\phi_i(1)\phi_j(2)), \tag{17}$$

with J_{ij} and K_{ij} the Coulomb and exchange integrals for orbitals ϕ_i and ϕ_j. This approach has some advantages if one needs to expand u_{ij} in a series of spherical harmonics. The general solution to Eq. (17) is obtained by orthogonalizing a particular solution to $B(\phi_i\,\phi_j)$. If $B(\phi_i(1)\phi_j(2))$ belongs to a two-electron irreducible representation, then Eq. (17) has a unique solution, e.g., $1s^2$ pair of electrons. However, when $B(\phi_i(1)\phi_j(2))$ is not a pure two-electron symmetry state, then Eq. (16) does not have a solution,[1] and one must write

$$B(\phi_i\phi_j) = \sum_{s=1}^{m} a_s\phi_{ij}^s, \tag{18}$$

where ϕ_{ij}^s are unperturbed pure symmetry states. Then,

$$u_{ij} = \sum_{s=1}^{m} a_s u_{ij}^s \tag{19}$$

$$(e_i+e_j)u_{ij}^s = [\langle\phi_{ij}^s(1/r_{12})\phi_{ij}^s\rangle - (1/r_{12})]\phi_{ij}^s. \tag{20}$$

The solution of Eq. (10) does not require any vector coupling schemes such as Eqs. (18) and (20), but the obvious symmetry properties of u_{ij}^s are convenient if u_{ij} is expanded in spherical harmonics. We have given Eqs. (17) and (20) because the use of symmetry pairs leads to simplifications in the numerical treatment of these equations. Equation (17) is also very similar to the equation one obtains starting from a bare nuclei Hamiltonian, i.e., a hydrogenic $\psi^{(0)}$. In that case, the first-order wavefunction is again written like Eq. (9) but with $\hat{u}_{ij}^{(1)}$ replaced by u_{ij}, which satisfies an equation very similar to Eq. (17), i.e.,

$$[-\tfrac{1}{2}\nabla_1^2 - \nabla_2^2 - (Z/r_1) - (Z/r_2) - e_i - e_j]u_{ij} = -[J_{ij} - K_{ij} - (1/r_{12})]B(\phi_i(1)\phi_j(2)). \tag{21}$$

The comparison between Eqs. (17) and (21) is obvious.

In the perturbation study of helium, starting from an unscreened hydrogenic $\psi^{(0)}$, one usually writes

$$H_0 = -\tfrac{1}{2}\nabla_1^2 - \tfrac{1}{2}\nabla_2^2 - (Z/r_1) - (Z/r_2), \tag{22}$$

$$H_1 = 1/r_{12}, \tag{23}$$

and $\psi^{(1)}$ satisfies Eq. (6). Comparison of Eqs. (6), (21), (22), and (23) shows that $\psi^{(1)}$ is just an example of a pair function. This is the example we use to illustrate our method of solution of pair equations. Numerical details of the method demonstrate that these results are indicative of its usefulness for obtaining atomic pair functions in general.

B. Reduction of Pair Equations

For quantitative results one must solve Eqs. (10), (17), or (21). Most attempts so far have used a variational approach. Equation (15) can be written

$$E^{(2)} = \sum_{i<j} \epsilon_{ij}^{(2)}, \tag{24}$$

and one has a minimum principle[1] for each $\epsilon_{ij}^{(2)}$, i.e.,

$$\epsilon_{ij}^{(2)} \approx \epsilon_{ij}'^{(2)} = 2\langle B(\phi_i\phi_j), m_{ij}\hat{u}_{ij}'^{(1)}\rangle + \langle\hat{u}_{ij}'^{(1)}, (e_i+e_j)\hat{u}_{ij}'^{(1)}\rangle, \tag{25}$$

with

$$m_{ij}(1,2) = (1/r_{12}) - \bar{S}i(1) - \bar{S}_i(2) - \bar{S}_j(2) - \bar{S}_j(1) + J_{ij} - K_{ij}, \tag{26a}$$

$$\bar{S}_i(1) = S_i(1) - R_i(1), \tag{26b}$$

and $\hat{u}_{ij}'^{(1)}$ is varied to minimize $\epsilon_{ij}'^{(2)}$. With a variational form for $\hat{u}_{ij}'^{(1)}$, one evaluates all the integrals in Eq. (25) and determines $\hat{u}_{ij}^{(1)}$. For different types of pairs one has a choice of $\hat{u}_{ij}^{(1)}$, e.g., a configuration-interaction (CI), open-shell, and a r_{12}-type $\hat{u}_{ij}^{(1)}$. We will comment later on their relative merits in comparison with the numerical method. We now show that these pair functions can be obtained accurately by solving the partial differential equation by numerical methods. The method is direct, with simple programming requirements.

The pair function, $\hat{u}_{ij}^{(1)}$, is expanded in a series of surface harmonics, the coefficients in the expansion being functions of the radii of the two electrons,[4]

$$\hat{u}_{ij}^{(1)} = \sum_{lm:l'm'} (r_1r_2)^{-1}\hat{u}_{lm:l'm'}(r_1, r_2) \times S_{lm}(\theta_1, \phi_1)S_{l'm'}(\theta_2, \phi_2). \tag{27}$$

For a spherically symmetric pair function the spatial part of $\hat{u}_{ij}^{(1)}$ depends only on r_1, r_2, and θ_{12}. However, for states of arbitrary symmetry one has to expand in

[4] For a suggestion along these lines see J. Musher in *Modern Quantum Chemistry–Istanbul Lectures, Part II, Interaction*, O. Sinanoğlu, Ed. (Academic Press Inc., New York, 1965).

terms of angular symmetries with respect to the two electrons separately. The $1/r_{12}$ term on the right-hand side of Eq. (10) can be written

$$r_{12}^{-1}=\sum_{l=0} U_l(r_1, r_2) \sum_{m=-l}^{l} S_{lm}(\theta_1, \phi_1) S_{l-m}(\theta_2, \phi_2), \quad (28)$$

where $U_l(r_1, r_2)$ stands for

$$\left(\frac{r_<^l}{r_>^{l+1}}\right)$$

and S_{lm} is a surface harmonic. Substitution of the expansion Eq. (27) into Eq. (17) or Eq. (10) gives

$$(\epsilon_i+\epsilon_j)a_{ij}^{(1)}(r_1, r_2)$$

$$=\sum_{lm,l'm'}\left[-\frac{1}{2r_1^2}\frac{\partial}{\partial r_1}\left(r_1^2\frac{\partial}{\partial r_1}\right)-\frac{1}{2r_2^2}\frac{\partial}{\partial r_2}\left(r_2^2\frac{\partial}{\partial r_2}\right)+\frac{l(l+1)}{2r_1^2}+\frac{l'(l'+1)}{2r_2^2}+V(r_1)+V(r_2)-\epsilon_i-\epsilon_j\right]$$

$$\times(r_1r_2)^{-1}a_{lm:l'm'}(r_1, r_2)S_{lm}(\theta_1, \phi_1)S_{l'm'}(\theta_2, \phi_2). \quad (29)$$

For closed-shell systems the Hartree–Fock potential, $V(r_1)$, is spherically symmetric. For open-shell systems one still requires the potential to be spherically symmetric and the orbitals, symmetry orbitals.[3] With the expansion, Eq. (28), the right-hand side of Eq. (10) or Eq. (17) becomes a sum of terms,

$$\sum_{ll'mm'} G_{lml'm'}(r_1, r_2)S_{lm}(1)S_{l'm'}(2).$$

The $G_{lm:l'm'}$ are combinations of terms $U_l(r_1, r_2)$ and the radial factors of the H–F orbitals. One now obtains a set of uncoupled equations, one for each term in Eq. (27),

$$\left(-\frac{1}{2}\frac{\partial^2}{\partial r_1^2}-\frac{1}{2}\frac{\partial^2}{\partial r_2^2}+\frac{l(l+1)}{2r_1^2}+\frac{l'(l'+1)}{2r_2^2}+V(r_1)+V(r_2)-\epsilon_i-\epsilon_j\right)a_{lm:l'm'}^{(1)}=r_1r_2G_{lm:l'm'}(r_1, r_2). \quad (30)$$

In deriving Eq. (30) we have used relationships such as

$$S_{ij}(\theta, \phi)S_{kl}(\theta, \phi)=\sum_{\alpha\beta} a_{ijkl}^{\alpha\beta}S_{\alpha\beta}(\theta, \phi), \quad (31)$$

where $a_{ijkl}^{\alpha\beta}$ are numerical coefficients. Equation (30) is our basic equation. It is a second-order elliptic partial differential equation in two variables, and no closed-form solution exists.

C. Analysis

Of the numerical methods for solving partial differential equations, those employing finite differences are most frequently used. Finite-difference methods are approximate in the sense that derivates at a point are approximated by difference quotients over a small interval; i.e., $\partial\phi/\partial x$ is replaced by $\delta\phi/\delta x$ where δx is small, but the solutions are not approximate in the sense of being crude estimates. In these methods the area of integration is divided into a set of square meshes, and an approximate solution to the differential equation is found at these mesh points. This solution is obtained by approximating the partial differential equation by n algebraic equations. The values at the mesh points form a vector which is the solution of the set of simultaneous linear equations. A numerical solution contains no arbitrary constants, so that we always obtain particular integrals rather than complete primitives of the differential equation.

In operator notation Taylor's series can be written[6]

$$y(x+h)=y(x)+h(dy/dx)+\tfrac{1}{2}h^2(d^2y/dx^2)+\cdots$$

$$=\exp(hD)y(x). \quad (32a)$$

Define a central difference operator δ,

$$\delta y(x+\tfrac{1}{2}h)=y(x+h)-y(x), \quad (32b)$$

and one has the operator equation

$$\delta=\exp(\tfrac{1}{2}hD)-\exp(-\tfrac{1}{2}hD)$$

$$=2\sinh(\tfrac{1}{2}hD), \quad (32c)$$

and hence

$$h^2D^2=(2\sinh^{-1}\tfrac{1}{2}\delta)^2$$

$$=\delta^2-\tfrac{1}{12}\delta^4+\tfrac{1}{90}\delta^6-\cdots. \quad (33)$$

The second derivative of a function at the ith point is

$$h^2(d^2y/dx^2)_i=\delta^2y_i-\tfrac{1}{12}\delta^4y_i+\tfrac{1}{90}\delta^6y_i. \quad (34)$$

The operators δ^2 and δ^4, etc., are defined by the equations

$$\delta^2y(x)=y(x+h)+y(x-h)-2y(x), \quad (35)$$

$$\delta^4y(x)=y(x+2h)-4y(x+h)+6y(x)$$

$$-4y(x-h)+y(x-2h). \quad (36)$$

[6] See, for example, L. Fox, *The Numerical Solution of Two-Point Boundary Problems in Ordinary Differential Equations* (Oxford University Press, New York, 1957).

Here, h is the spacing between neighboring mesh points, and the partial derivatives of Eq. (30) become

$$h^2[(\partial^2/\partial x^2)+(\partial^2/\partial y^2)]u(x,y)$$
$$=(\delta_x^2+\delta_y^2)u(x,y)-\tfrac{1}{12}(\delta_x^4+\delta_y^4)u(x,y)+O(\delta^6). \quad (37)$$

At a point $u(x,y)$ one has

$$[(\partial^2/\partial x^2)+(\partial^2/\partial y^2)]u(x,y)$$
$$=(1/h^2)[u(x+h,y)+u(x-h,y)+u(x,y+h)$$
$$+u(x,y-h)-4u(x,y)]+Cu(x,y), \quad (38)$$

with

$$C=-(1/12h^2)(\delta_x^4+\delta_y^4)+(1/90h^2)(\delta_x^6+\delta_y^6)-\cdots. \quad (39)$$

As a first approximation we neglect Cu in Eq. (38) and therefore replace the differential operator by the first term on the right-hand side. This leads to a truncation error in the expansion of the differential operator. The form of this truncation error is important, as it allows us to predict the convergence of the numerical solution as one approaches the exact solution (see Appendix A). From Eqs. (33)–(39) it is obvious that the local truncation error in the second-difference approximation is $O(h^2)$. The term Cu in Eq. (39) contains higher difference operators, which can be included by an iterative technique (see Appendix B).

One must now specify the boundary conditions for Eq. (30). We treat the problem as a boundary-value one, specifying the value of the solution on a boundary enclosing the area of integration (Dirichlet boundary conditions). The functions $\hat{u}_{lm;l'm'}{}^{(1)}$ vanish along the boundaries $r_1=0$, $r_2=0$. These functions also vanish as r_1 or $r_2\to\infty$. This boundary condition must be modified so as to handle the equation on a finite numerical grid. There are two alternatives, and both are based on the condition that the solutions approach zero exponentially and essentially do so at some finite value of the independent variable. One can choose a value of $r_1=R_1$ and make the solution vanish on this boundary, i.e., $u(R_1,r_2)=u(r_1,R_1)=0$. One then moves this boundary out to $r_1=R_2$, R_3, etc., until at least two adjacent values at the boundary are zero to the required number of significant figures. The boundary condition is then accurately satisfied. The other alternative is based on the asymptotic form of the solution of Eq. (30). We can use this as a boundary condition. For large values of r_1 and r_2 the solution behaves like $g(r_1,r_2)\exp[-\alpha(r_1+r_2)]$, where $g(r_1,r_2)$ varies slowly. This behavior becomes a boundary condition,

$$u(r_1,r_2)=e^{\alpha h}u(r_1+h,r_2). \quad (40)$$

The boundary condition is satisfied when Eq. (40) holds between neighboring points. Both alternatives work well and bring all atoms of interest within reach of the method.

With Eq. (38) the differential equation is obviously replaced by a set of algebraic equations. In matrix form these equations are

$$\mathbf{A}u=\mathbf{b}, \quad (41)$$

where u is a column vector, the components of which are approximate solutions to the differential equation at a set of internal points. Were it not for the nonlocal exchange potentials of Eq. (30) [see Eqs. (13b) and (14b)], the matrix $\mathbf{A}$, Eq. (41), would have a very simple structure; e.g., for M divisions along each dimension the only nonzero elements lie on the diagonal, the super-, and sub-diagonal, and on lines parallel to the diagonal but M strips above and below the diagonal. This is a banded matrix of half-bandwidth equal to M. We now show that (a) large systems of such equations can be solved rapidly and accurately, and (b) once such solutions have been obtained, the nonlocal operators can be taken into account with a small increase in computing time. We put more emphasis on (a), but (b) is shown quite convincingly.

For B internal points in each dimension we have N equations with $N=B^2$. The matrix A then has dimensions $B^2\times B^2$; e.g., with B about 40 one has a 1600×1600 matrix. We use the method of triangular resolution to solve the matrix equation, Eq. (41). The method has been efficiently programmed,[6] and very large systems of equations can be solved economically. We give a very brief outline of the method. If the leading minors of the matrix A are nonzero, there is a unique lower triangular matrix $\mathbf{L}$ and a unique upper triangular matrix $\mathbf{U}$ so that $\mathbf{A}=\mathbf{LU}$. An upper triangular matrix is one which has zeros above the diagonal. The solution proceeds by eliminating the lower triangular elements, taking pivots successively along the principal diagonal, and the only recorded quantities are the multipliers needed for the triangular resolution ($\mathbf{L}$) and the triangularized array ($\mathbf{U}$). The band structure is preserved in the $\mathbf{L}$ and $\mathbf{U}$ factors.[7] Solution of the linear equations is straightforward; i.e., for $\mathbf{Ax}=\mathbf{b}$ one solves $\mathbf{Ly}=\mathbf{b}$ and $\mathbf{Ux}=\mathbf{y}$ by forward and backward substitution. The $\mathbf{L}$ and $\mathbf{U}$ matrices can be used to operate on any number of right-hand vectors,[8] i.e., $\mathbf{b}$ of Eq. (42).

[6] It can be shown that there is no limit on the number of rows of equations that can be handled and that the upper limit on the bandwidth is set by the requirement of having $\frac{1}{2}M^2$ terms in memory at any one time. For an IBM 7094 an upper limit to the M is about 200. This corresponds to a large number of equations. For details of the program see C. W. McCormick and K. J. Hebet, "Solution of Linear Equations with Digital Computers," Tech. Rept., Engineering Division, California Institute of Technology, 1965 (unpublished).

[7] L. Fox, *Numerical Solution of Ordinary and Partial Differential Equations* (Pergamon Press, Inc., London, 1962).

[8] Most of the computing time is required to obtain the L and U factors and the time to forward- and back-substitute is much less. This feature enables us to include, by an iterative scheme, both nonlocal potentials and higher-order differences. See Appendix B for details.

For a method to be practical the computing-time requirements must be realistic. The real advantage of triangular resolution for band matrices is that the running time for inversion of an $N\times N$ matrix is proportional to N^3 rather than M^2N for triangular resolution. M is the half-bandwidth. For this differential equation $N\approx M^2$, and the ratio of running times for matrix inversion to triangular resolution is M^2. Matrix inversion does not preserve band structure, and the time to determine a new set of roots, i.e., solve Eq. (40) with a new vector b, is proportional to N^2. The time savings involved here are significant, e.g., a factor of 1600 for $M\approx 40$. In the next section we give an example which shows that the method is numerically and economically feasible.

RESULTS

When the differential equation is converted into a set of simultaneous linear equations the term $V_c(r_1)$ [see Eq. (14a)] is just an algebraic operator evaluated at every mesh point on the grid. For H–F orbitals one would evaluate integrals such as $S_i(r_2)$, Eq. (13a), analytically and tabulate them at the necessary points. For a numerical method it makes no difference to the analysis whether the potential term, $V_c(r_1)$, in Eq. (30) is given by HF orbitals or is just the electron–nucleus attraction, i.e., hydrogenic zeroth-order Hamiltonian. They both give rise to numerical arrays, which are evaluated even before the numerical analysis really begins. Hence, to demonstrate our method we pick the simplest pair equation, that for the helium atom starting from a hydrogenic H_0. The important issue here is the practicality of solving the number of simultaneous equations which must be solved so as to obtain an accurate value of a pair energy. Also, for helium we have a series of previous results on the energy contribution of each partial wave to the second-order energy.

Consider Eqs. (21) and (27). For a u_{ij} of S symmetry only those $u_{lm:l'm'}$ with $l=l'$ are nonzero, and $u_{lm:l'-m}$ is independent of m. This gives the partial wave expansion,

$$u(1s^2)=\sum_{l=0}^{\infty}\frac{u_l(r_1,r_2)}{r_1r_2}P_l(\cos\theta_{12}). \tag{42}$$

Recall that $u(1s^2)$ must be made so that $\langle u(1s^2), B(1s\alpha 1s\beta)\rangle=0$. The differential equations are

$$\left(-\frac{1}{2}\frac{\partial^2}{\partial r_1^2}-\frac{1}{2}\frac{\partial^2}{\partial r_2^2}-\frac{Z}{r_1}-\frac{Z}{r_2}-2\epsilon_{1s}\right)u_0(r_1,r_2)=P_{1s}(r_1)P_{1s}(r_2)(J_{1s1s}-r_>^{-1}), \tag{43}$$

$$\left(-\frac{1}{2}\frac{\partial^2}{\partial r_1^2}-\frac{1}{2}\frac{\partial^2}{\partial r_2^2}+\frac{l(l+1)}{2r_1^2}+\frac{l'(l'+1)}{2r_2^2}-\frac{Z}{r_1}-\frac{Z}{r_2}-2\epsilon_{1s}\right)u_l(r_1,r_2)=-\frac{r_<^l}{r_>^{l+1}}P_{1s}(r_1)P_{1s}(r_2) \tag{44}$$

for $l=0$ and $l\geq 1$, respectively, and

$$P_{1s}(r)=rR_{1s}(r). \tag{45}$$

In Eqs. (43) and (44) we have $\epsilon_{1s}=-2.0$, $E_1=1.25$, and $R_{1s}=4\sqrt{2}e^{-2r}$. Tables I and II give the results for the first three partial waves. Here the second-order energy decouples into a sum over the partial wave contributions, $E_2(l)$. All integrations are done by the trapezoidal rule, and

$$E_2(l=0)=\langle u_0(r_1,r_2),\,(1/r_{12})B(1s(1)1s(2))\rangle - E_1\langle u_0,\,B(1s(1)1s(2))\rangle, \tag{46a}$$

$$E_2(l\geq 1)=\langle u_l(r_1,r_2),\,(1/r_{12})B(1s(1)1s(2))\rangle. \tag{46b}$$

TABLE I. Results for the $l=0$ partial wave of the helium pair function.[a]

Mesh size[b]	Number of equations[c]	$E_2(l=0)$	Execution time (seconds on IBM 7094)
$\frac{1}{4}$	361	−0.12605	3[d]
$\frac{1}{5}$	576	−0.12678	16[e]
$\frac{1}{6}$	841	−0.12664	27
$\frac{1}{7}$	1156	−0.12640	52
$\frac{1}{8}$	1521	−0.12619	82
$\frac{1}{9}$	1936	−0.12603	115
$\frac{1}{10}$	2401	−0.12591	169

[a] See Eq. (43). The perturbation is $1/r_{12}$.
[b] Spacing between grid points.
[c] Number of points at which an approximate solution to the differential equation is obtained.
[d] This size problem fits completely in random access memory.
[e] This size problem requires auxiliary disk storage.

In Tables I and II we have given the computing times necessary to solve the equations at each mesh size. We feel it is important to communicate the computing needs of a given method. Computing times for this method are quite low. For $l=0$ we require $u(r_1,r_2)$ to vanish at $R=5$ and obtained the solutions at seven different mesh sizes: $h=\frac{1}{4},\frac{1}{5},\frac{1}{6},\frac{1}{7},\frac{1}{8},\frac{1}{9},\frac{1}{10}$. To test the boundary condition we allowed $u(r_1,r_2)$ to vanish at $R=6$ and, at a mesh size of $\frac{1}{4}$, found $E_2(l=0)=-0.12607$, compared to -0.12605 for the same condition at $R=5$. With the exponential behavior of the function as a boundary condition at $R=5$ we obtained $E_2(l=0)=-0.12607$, while at $R=4$ one finds $E_2(l=0)=-0.1261$. The boundary condition poses no difficulty. For $h=\frac{1}{4}$ there are 361 equations, and the entire problem can be loaded into the random access memory of an IBM 7094 and

TABLE II. Results for the $l=1$ and 2 partial waves of the helium pair function.

Mesh size	$E_2(l=1)$	$E_2(l=2)$	Execution time[b]
$\frac{1}{4}$	−0.033051[a]	−0.0056616	2[c]
$\frac{1}{5}$	−0.030387	−0.0049862	3[c]
$\frac{1}{6}$	−0.029073	−0.0046351	12[d]
$\frac{1}{7}$	−0.028333	−0.0044302	23
$\frac{1}{8}$	−0.027874	−0.0043007	37
$\frac{1}{9}$	−0.027569	−0.0042137	50
$\frac{1}{10}$	−0.027356	−0.0041525	82

[a] All integrals evaluated by the trapezoidal rule.
[b] Execution time in seconds on an IBM 7094.
[c] This size problem fits entirely in core.
[d] This size problem requires auxiliary storage.

solved within 3 sec. At $h=\frac{1}{8}$ one requires disk storage to handle the 576 equations, and the execution time is 16 sec. Table II gives the results for $l=1$ and $l=2$ partial waves. The execution times are lower than those for the $l=0$ case, since the exponential boundary condition could be imposed at $R=4$ for these higher partial waves. One can expect this behavior for the higher l components of pair functions. Requiring the function to vanish at $R=6$ affected the seventh significant figure in the energy.

Tables III–V give the results of extrapolating the values at varying mesh sizes (Tables I and II). In Appendix A we derive the convergence of the solution of the corresponding finite difference equations, $u(h)$, towards the solution of the differential equation itself, u. We show that

$$u-u(h)=a_2h^2+a_4h^4+\cdots, \tag{47}$$

TABLE III. Extrapolants from finest meshes.[a]

l	Mesh size	Results from direct quadrature	h^2 extrapolants[c]	h^4 extrapolants[d]
	$\frac{1}{8}$	−0.126194[b]		
			−0.12541	
$l=0$	$\frac{1}{9}$	−0.126030		−0.12531
			−0.12537	
	$\frac{1}{10}$	−0.125905		
	$\frac{1}{8}$	−0.027874		
			−0.026422	
$l=1$	$\frac{1}{9}$	−0.027569		−0.026498
			−0.026449	
	$\frac{1}{10}$	−0.027356		
	$\frac{1}{8}$	−0.0043007		
			−0.0038862	
$l=2$	$\frac{1}{9}$	−0.0042137		−0.003902
			−0.0038919	
	$\frac{1}{10}$	−0.0041525		

[a] See Eq. (48) of text.
[b] Results from direct quadrature on numerical solutions (Tables I and II).
[c] Extrapolants from pairs of successive values in the preceding column assuming an h^2 convergence.
[d] Extrapolants from the three values in the first column assuming an h^2 and h^4 convergence.

TABLE IV. Extrapolants from intermediate meshes.[a]

l	Mesh size	Results from direct quadrature	h^2 extrapolants[c]	h^4 extrapolants[d]
	$\frac{1}{8}$	−0.126642[b]		
			−0.12562	
$l=0$	$\frac{1}{9}$	−0.126194		−0.12526
			−0.12539	
	$\frac{1}{10}$	−0.125905		
	$\frac{1}{8}$	−0.029073		
			−0.026332	
$l=1$	$\frac{1}{9}$	−0.027874		−0.026495
			−0.026436	
	$\frac{1}{10}$	−0.027356		
	$\frac{1}{8}$	−0.0046351		
			−0.0038707	
$l=2$	$\frac{1}{9}$	−0.0043007		−0.0038996
			−0.0038892	
	$\frac{1}{10}$	−0.0041525		

[a] See Eq. (48) of text.
[b] Results from direct quadrature on numerical solutions (Tables I and II).
[c] Extrapolants from pairs of successive values in the preceding column assuming an h^2 convergence.
[d] Extrapolants from the three values in the first column assuming an h^2 and h^4 convergence.

where u, $u(h)$, a_2, and a_4 are functions of the independent variables and h is the mesh size. We therefore know exactly how an approximate solution approaches the exact one. This convergence property forms the basis of an extrapolation technique which allows us to obtain a high degree of accuracy for the pair energies. We checked the use of Eq. (47) by comparing an actual solution with an extrapolated one. The agreement is excellent.

The integrals for E_2 are evaluated by the trapezoidal rule. The error term for quadrature by the trapezoidal rule can be expressed as a power series in the interval size, h. In Appendix A we show that the second-order energy, evaluated by the trapezoidal rule and with the finite difference solution, converges to the exact value

TABLE V. Extrapolants from values at various meshes.

l	Values used in extrapolation	Extrapolants
	$(\frac{1}{6}, \frac{1}{7})$[a]	−0.12574
$l=0$	$(\frac{1}{8}, \frac{1}{9}, \frac{1}{10})$	−0.12512
	$(\frac{1}{7}, \frac{1}{8}, \frac{1}{9})$	−0.12521
	$(\frac{1}{4}, \frac{1}{5})$	−0.02564
	$(\frac{1}{5}, \frac{1}{6})$	−0.02609
$=1$	$(\frac{1}{4}, \frac{1}{5}, \frac{1}{6})$	−0.02645
	$(\frac{1}{5}, \frac{1}{6}, \frac{1}{7})$	−0.02649
	$(\frac{1}{4}, \frac{1}{5})$	−0.003786
	$(\frac{1}{5}, \frac{1}{6})$	−0.003837
$l=2$	$(\frac{1}{4}, \frac{1}{5}, \frac{1}{6})$	−0.003878
	$(\frac{1}{4}, \frac{1}{5}, \frac{1}{6}, \frac{1}{7})$	−0.003896
	$(\frac{1}{4}, \frac{1}{5}, \cdots \frac{1}{9}, \frac{1}{10})$	−0.003905

[a] The values at these mesh sizes were used in the extrapolation.

as follows:

$$E_2 = E_2(h) + b_2h^2 + b_4h^4 + \cdots, \quad (48)$$

where $E_2(h)$ is the energy obtained at each mesh size. With Eq. (48) we can derive very accurate extrapolants. To obtain the best results one obviously extrapolates the results from the finer meshes. If one simply wants a good estimate of a pair energy, extrapolation from coarser meshes may be sufficient. Tables III and IV give the extrapolants based on results from the finest meshes, i.e., $h=\frac{1}{8}, \frac{1}{9}, \frac{1}{10}$ and those derived from the results at $h=\frac{1}{6}, \frac{1}{8}, \frac{1}{10}$, respectively. The various columns of Tables III and IV correspond to an extrapolation from a successively higher-order polynomial, i.e., an h^2 and h^4 extrapolation. The successive columns of both Tables indicate that the extrapolation is stable and yields excellent results. Table V lists extrapolants derived from the results at various mesh sizes. We do this primarily to show the kind of extrapolants one can obtain from results at cruder meshes. These compare well with the best results of Table III. This approach can yield useful estimates of pair correlation energies. For the $l=1$ partial wave extrapolation from mesh sizes $\frac{1}{4}, \frac{1}{5}, \frac{1}{6}$ give -0.02645. These solutions were obtained with a total computing time of 17 sec. Table V also lists some extrapolants based on very high-order polynomials; e.g., use of the results at all seven mesh sizes implies an h^{10} extrapolation and for $l=2$ gives $E_2(l=2)=-0.003905$. Other extrapolants indicate a similar stability.

For comparison we use the most recent results on the helium-atom pair function. Byron and Joachain[9] solved the pair equation variationally and also gave the contributions of the various partial waves to E_2. They used two different types of trial functions. For $u_l(r_1, r_2)$ of Eq. (42) they chose (a) a "configuration-interaction" type expansion,

$$u_l(r_1, r_2) = \sum_{m,n} c_{lmn}(r_1^m r_2^n + r_1^n r_2^m) \times r_1 r_2 \exp[-2(r_1+r_2)], \quad (49a)$$

and (b) a function of the form

$$u_l(r_1, r_2) \sum_{m,n} c_{lmn} r_1 r_2 r_>^m r_<^n \exp[-2(r_1+r_2)]. \quad (49b)$$

TABLE VI. Comparison of numerical results with variational calculations.

$E_2(l)$	Variational Case I[a]	Variational Case II[b]	Variational Case III[c]	Numerical[d]
$l=0$	−0.12533	−0.12532	−0.12501	−0.12531
$l=1$	−0.026495	−0.026475	−0.025903	−0.026498
$l=2$	−0.003906	−0.003893	−0.003531	−0.003902

[a] See Eq. (49b) (30 variational parameters).
[b] See Eq. (49b). Only positive powers of r with 36 variational parameters.
[c] Equation (49a) with 20 parameters.
[d] Numerical integration of the partial differential equations.

[9] F. W. Byron and C. J. Joachain, Phys. Rev. 157, 1 (1967).

TABLE VII. Upper bounds derived from numerical solution.[a]

Mesh size	M[b]	$E_2(l=0)$	M	$E_2(l=1)$	M	$E_2(l=2)$
$\frac{1}{4}$	7	−0.1239	8	−0.02554	7	−0.003222
$\frac{1}{5}$	7	−0.1246	7	−0.02605	8	−0.003630
$\frac{1}{6}$	7	−0.1251	8	−0.02625	9	−0.003753
$\frac{1}{7}$	7	−0.1252	7	−0.02634	9	−0.003802
$\frac{1}{8}$	9	−0.1252	8	−0.02641	9	−0.003839

[a] See Eq. (50b).
[b] $M-1$ is the order of a polynomial covering a triangular region.

Functions of type (a) are standard, and those of type (b) are correlated in their radial part, and they avoid some difficult integrals due to nonlocal potentials that appear when interelectronic coordinates are used. Such functions may seem inadmissible as trial functions, since they have a finite discontinuity in the first derivative at $r_1=r_2$. The variational principle nevertheless is still valid giving an upper bound. Table VI gives their values[9] listed as Cases I–III and our best extrapolants. For Case I a function of type (b) is used but each partial wave contains 30 terms with $-1\leq m+n\leq 4$. In Case II functions of type (b) are again used, but with 36 terms and $m+n\leq 7$ (no negative powers of r_1 r_2). For Case III they[9] used a function of type (a) with 20 variational parameters. The results of Table VI clearly show that the numerical method of finite differences, coupled with extrapolation based on the convergence properties of the finite difference solution, can give results as accurate as the variational method.

It is easy to derive a convenient analytical fit to the numerical solution by simply projecting various functional forms on to it. To demonstrate this we use functions of the type in Eq. (49b). These analytical fits can obviously provide upper bounds to E_2. Since the solutions of Eqs. (43) and (44) are symmetric about the line $r_1=r_2$, consider the region $r_1>r_2$ and let $x=r_1$ and $y=r_2$ there. The numerical solution should have the form[10]

$$u(x, y) = \exp[-\alpha(x+y)]\pi(x, y), \quad (50a)$$

where $\pi(x, y)$ is a polynomial in the triangular area $r_1>r_2$,

$$\pi(x, y) = \sum_{m=1}^{M}\sum_{n=1}^{m} c_{mn} x^{m-n} y^{n-1}. \quad (50b)$$

In principle α can be varied, but here it is clearly equal to two. One just takes the solution vector, multiplies it by $\exp[\alpha(x+y)]$, and puts a polynomial, $\pi(x, y)$, through a selected number of points of the resulting vector. Equation (25) then gives an upper bound. The equation determining the c_{mn}'s can be solved in a matter of seconds. Table VII gives some of these results. At crude meshes one can obtain estimates that compare

[10] See comments below Eq. (49b) on the use of such functions in the variational expression. One must handle the integrals containing the kinetic energy operator properly.

well with the configuration-interaction results of Table VI; e.g., at a mesh size of $\frac{1}{8}$ for the $l=1$ and 2 partial waves $E_2(l)=-0.02605$ and -0.00363, respectively, versus -0.025903 and -0.003531 of Table VI. An interesting observation is that the numerical result always lies below the best available estimate of the energy of each partial wave, so that the true value is apparently bracketed by the numerical and variational results; e.g., at a mesh size of $\frac{1}{16}$ $E_2(l)$ for $l=0$, 1, and 2 is -0.1259, -0.02736, and -0.00415, respectively, by numerical integration and -0.1252, -0.02641, and -0.003839 variationally. These bracket the accurate results of -0.12533, -0.026495, and -0.003906. This bracketing occurs at all mesh sizes, and the limits become smaller as the mesh is refined.

NONLOCAL POTENTIALS

Our results demonstrate that the pair equations can be solved by the finite-difference method if the exchange potentials in Eq. (30) were absent. In that case the differential equation is replaced by a matrix equation in which the matrix is banded. Such a system of equations can be solved quite efficiently by triangular decomposition; i.e., A[Eq. (41)] is decomposed into its L and U factors. With the matrix A in triangular form the system $\mathbf{Ax}=\mathbf{b}$ is solved by a forward and backward substitution. The lower and upper triangular matrices, L and U, are stored and are always available. This allows one to include nonlocal potentials and higher difference corrections (Appendix B) by an iterative technique, with a small increase in computing time.

There are two starting points. One can drop the exchange operator $V_e(r)$ completely [see Eqs. (13b) and (14b)] and solve the resulting equations

$$\mathbf{Au}_0=\mathbf{b}. \tag{51}$$

The term $-[V_e(r_1)+V_e(r_2)]u(r_1, r_2)$ has been neglected for the first iteration. Write $u\approx u_0+\Delta u_0$, and the correction Δu_0 is approximately given by the equation

$$\mathbf{A}(\Delta\mathbf{u}_0)=[V_e(r_1)+V_e(r_2)]\mathbf{u}_0, \tag{52}$$

which can be solved by a forward and backward substitution since the L and U factors are available. One would really like to replace the nonlocal operator by a local operator. Various effective local potentials can approximate the exchange potential quite well, e.g., those of Slater[11] and Kohn and Sham.[12] Slater suggests that the exchange potential be represented by

$$V_e^s(r)=(3/2\pi)[3\pi^2 n(r)]^{1/3}, \tag{53}$$

where

$$n(r)=\sum_{i=1}^{N}\psi_i^*(r)\psi_i(r),$$

and $\psi_i(r)$ satisfies an equation like the HF equations, but with V_e of Eq. (53). The advantage is that this $V_e^s(r)$ is an algebraic operator, and one now has an equation like Eq. (51) with a different band matrix, A_e:

$$A_e u_0=b. \tag{54}$$

The operator $(V_e^s-V_e)$ is neglected for the first iteration. As in Eq. (52), one solves for the correction Δu^0.

Since the facility of including exchange potentials is important, we give some estimates of the additional computing requirements. If the problem fits in random access memory, a solution of the matrix equation requires about $\frac{1}{2}M^4+2M^3$ operations. But with the L and U matrices available only $2M^3$ operations are required to solve for a new root. Thus, the additional time per iteration to include the nonlocal potentials will be about $4/(4+M)$ of the initial time, which for $M=20$ is about 16%. With auxiliary storage and bandwidths that are not too large, one can prove that this percentage will be less than 25% and will decrease the larger the number of equations becomes.

CONCLUSIONS

We have shown that the first-order pair equations proposed by Sinanoğlu can be solved both economically and conveniently by numerical integration. One of the advantages of the method is its simplicity, and its success depends on the ability to solve a large number of simultaneous linear equations efficiently. One can obtain an approximate solution at around 2000 mesh points in just under 2 min on an IBM 7094. Such solutions would be sufficient for many purposes. With this number of equations one must use auxiliary disk storage, and a fair bit of time is spent transmitting information between computing units. On a machine with a larger random access storage but, hypothetically, with the same basic cycle time, such a calculation would take about 40 sec. The programming is simple, and the few integrations necessary are done by the trapezoidal rule. Nonlocal potentials can be treated with a small increase by the same iterative technique.

We also prove how the finite difference solution must converge toward the exact solution as the mesh size goes to zero. This convergence forms the basis of a stable extrapolation procedure which gives an accurate value for the pair energy. On the other hand, very little is known about the convergence properties of variational methods. The expansion in spherical harmonics has some conceptual advantage, and the solutions for the radial functions converge nicely for all l values. The boundary condition poses no difficulty.

We chose the first-order pair function as the example in this paper, but there are other pairs that are more accurate than these first-order pairs.[2] In many cases one expects $a_{ij}^{(0)}$ to suffice, but if one wants to go to more accurate pairs, numerical methods are also applicable.

[11] J. C. Slater, Phys. Rev. 81, 385 (1951).

[12] W. Kohn and L. J. Sham, Phys. Rev. 140, A1133 (1965). For comments on this choice of exchange potential see J. C. Slater, Massachusetts Institute of Technology, Solid State and Molecular Theory, Quarterly Progress Report No. 58, 1965 (unpublished).

For example, consider the pair equation which satisfies the equation[9]

$$(e_i+e_j+Qm_{ij})\hat{\psi}_{ij}=0. \tag{55}$$

Q is defined in Eq. (11), and

$$\hat{\psi}_{ij}=B(\phi_i(1)\phi_j(2))+\hat{u}_{ij}. \tag{56}$$

The corresponding pair energy provides a lower bound to the exact pair energy.[13] One can write

$$(e_i+e_j)\hat{u}_{ij}=-Q(1/r_{12})B(\phi_i(1)\phi_j(2))-Qm_{ij}\hat{u}_{ij}. \tag{57}$$

Neglecting the second term on the right-hand side, Eq. (57) becomes identical with Eq. (10) for $\hat{u}_{ij}^{(1)}$. An obvious approach to the solution of Eq. (57) would be iterative; i.e., take $\hat{u}_{ij}^{(1)}$ and use the L and U matrices to solve for Δu_{ij} due to the term $Qm_{ij}\hat{u}_{ij}$ [see discussion below Eq. (52)]. The algebra on the spherical harmonics may be more involved, but comparison between $\hat{u}_{ij}^{(1)}$ and $\hat{u}_{ij}$, Eq. (57), will be informative.

APPENDIX A

An advantage of the numerical method is that one can derive the convergence of the numerical solution, $u(x, y, h)$, towards the exact solution, $u(x, y)$. One expands $u(x, y)$,

$$u(x, y)=u(x, y, h)+Ah+Bh^2+Ch^3+\cdots, \tag{A1}$$

where $A, B, C, \cdots$, are functions of x and y. The differential equation, Eq. (30), has the form

$$f(D)u=g(x, y), \tag{A2}$$

where

$$f(D)=-\tfrac{1}{2}(\partial^2/\partial x^2)-\tfrac{1}{2}(\partial^2/\partial y^2)+p(x, y), \tag{A3}$$

and the numerical solution, $u(h)$, satisfies

$$Lu(h)=g(x, y). \tag{A4}$$

The difference between Eq. (A2) and Eq. (A4) is the local truncation error, Eq. (39). This error contains only even powers of h, with zero constant term, so

$$Lu(h)=[f(D)+(ch^2+dh^4+\cdots)]u(h). \tag{A5}$$

Substituting for $u(h)$ and equating powers of h,

$$f(D)u=g(x, y), \tag{A6}$$

$$f(D)A=0, \tag{A7}$$

$$f(D)B-cu=0, \tag{A8}$$

$$f(D)C+cA=0. \tag{A9}$$

Note that Eq. (A5) has its form due to the use of central differences. From Eqs. (A7) and (A9) A and C are zero. Thus, Eq. (A1) becomes

$$u-u(h)=Bh^2+Dh^4+\cdots, \tag{A10}$$

The basic integrals are of the type

$$I=\int_0^a dx\int_0^z f(x, y)\,dy. \tag{A11}$$

Here $f(x, y)$ contains the numerical solution, and this is known approximately at fixed intervals. In evaluating I there are two sources of error: (i) that of Eq. (A10), and (ii) the quadrature by the trapezoidal rule. With a known function $f(x, y)$, the form of I would be

$$I=T(h)+ah^4+O(h^6), \tag{A12}$$

where $T(h)$ is the value of the integral evaluated by the trapezoidal rule. Use of the numerical solution, instead of the exact solution, to evaluate $T(h)$ introduces terms proportional to h^2, h^4, etc., into Eq. (A12). The final form is

$$I=T_0(h)+a_2h^2+a_4h^4+\cdots. \tag{A13}$$

APPENDIX B

In Eq. (38) we neglected the term Cu and retained just the second difference operator. Instead of going to very fine meshes one may include fourth differences, e.g., Eq. (36), and this may give an accurate solution at coarser meshes.[7] Consider the first term of Eq. (39),

$$C=-(1/12h^2)(\delta_x^4+\delta_y^4), \tag{B1}$$

and write the new matrix equation

$$(A+C)y=b. \tag{B2}$$

The matrix A dominates, and for a first approximation, $y^{(1)}$, one has

$$Ay^{(1)}=b. \tag{B3}$$

The first correction z to $y^{(1)}$ is approximately

$$Az=-Cy^{(1)}. \tag{B4}$$

With the L and U matrices available, Eq. (B4) is easily solved. At points next to the boundary the term $Cy^{(1)}$ requires values of the function beyond the boundaries [see Eq. (36)]. One often extrapolates across the boundary, but there is an apparent indeterminacy at the boundary [see Eq. (43)]. One can derive a relation between the point next to the boundary and the first external one through a cusplike condition. In the region $r_1>r_2$ let $x=r_1$, $y=r_2$, and $y\to 0$; we have

$$-\frac{1}{2}\left(\frac{\partial^2 u}{\partial x^2}\right)_{x_i}-\frac{1}{2}\left(\frac{\partial^2 u}{\partial y^2}\right)_{y\to 0}+\left[\left(\frac{l(l+1)}{2y^2}-\frac{Z}{y}\right)u\right]_{y\to 0}=0. \tag{B5}$$

Substitution from Eq. (35) into Eq. (B5), and with

$$(\partial u/\partial y)_{y_i}=\{[u(x, y_2+h)-u(x, y_2-h)]/2h\}+O(h^2), \tag{B6}$$

one obtains the necessary relationship. The limits $(u/y)_{y\to 0}$ and $(u/y^2)_{y\to 0}$ are evaluated using L'Hopital's rule for indeterminate forms.

[9] O. Sinanoğlu (private communication).

Reprinted from THE JOURNAL OF CHEMICAL PHYSICS, Vol. 49, No. 10, 4728-4730, 15 November 1968
Printed in U. S. A.

Numerical One-Center Calculation of the ns-σ Rydberg Series of H_2^+

N. W. WINTER AND VINCENT MCKOY

A. A. Noyes Laboratory of Chemical Physics, California Institute of Technology, Pasadena, California 91109*

(Received 6 May 1968)

We have calculated the energies and quantum defects for the lowest eight s-σ states of H_2^+ using the first-order perturbation theory. In zero-order, we retain only the spherical component of the core potential. The zero-order equation has previously been solved by Chen[1] for the lowest six s-σ states and his results for the ground state have been corrected by Cohen and Coulson,[2] and by Hauk and Parr.[3] The perturbation is simply the nonspherical part of the core potential, and its effects on the Rydberg orbital are included by solving the first-order perturbation equation. It is well known that such a procedure is not sufficient for the ground state[4]; however it is expected to be a better approximation for the highly excited Rydberg levels.[5] For these orbitals, the spherical component of the core potential plays a more dominant role in determining the eigenvalue.

The partial wave expansion of the core potential for H_2^+ is

$$-r_a^{-1}-r_b^{-1}=-2\sum_l (r_<^{2l}/r_>^{2l+1})\,P_{2l}(\cos\theta), \quad (1)$$

where $r_<=\min(R,r)$, $r_>=\max(R,r)$, and $2R(=2$ a.u.) is the internuclear separation. The zero-order equation for the ns-σ states is

$$[-\tfrac{1}{2}(d^2/dr^2)-(2/r_>)]\psi_n^0(r)=E_n^0\psi_n^0. \quad (2)$$

If we expand the first-order wavefunction in the same form as the perturbation, the first-order equation decouples to give a separate equation for each partial wave of the form

$$\left(-\frac{1}{2}\frac{d^2}{dr^2}+\frac{2l(2l+1)}{2r^2}-\frac{2}{r_>}-E_n^0\right)\psi_n^1(2l;r) = (2r_<^{2l}/r_>^{2l+1})\psi_n^0(r). \quad (3)$$

Both Eqs. (2) and (3) were solved by the matrix finite-difference method which we have discussed elsewhere.[6,7] The first-order wavefunction for the ground-state included partial waves up to $2l=16$ and the remaining states up to $2l=12$. The results for each level are given in Table I along with the exact values of the energy for the lowest three states.[8] In addition, the quantum defects δ_n were found from the formula

$$E_n=-Z_c^2/2(n+\delta_n)^2, \quad (4)$$

TABLE I. Perturbation energies for the ns-σ Rydberg series of H_2^+ at an internuclear separation of 2 a.u.

n	$-E_0$	$-E_2$	$-E_3$	$-E_4$	δ_n
1	1.018507	0.061408	0.016398	1.096313(1.10263)	0.3507
2	0.350367	0.007912	0.002218	0.360497(0.36087)	0.3554
3	0.174455	0.002396	0.000735	0.177586(0.17768)	0.3559
4	.0104041	0.001043	0.000339	0.105423	0.3556
5	0.068995	0.000538	0.000177	0.069710	0.3563
6	0.049069	0.000323	0.000110	0.049502	0.3563
7	0.036687	0.000203	0.000068	0.036958	0.3563
8	0.028456	0.000138	0.000047	0.028641	0.3564

TABLE II. Contribution of each partial wave to $-E_2$.

n \ $2l$	2	4	6	8	10	12
2	0.007034	0.000640	0.000150	0.000052	0.000023	0.000012
3	0.002125	0.000197	0.000047	0.000016	0.000007	0.000003
4	0.000922	0.000087	0.000020	0.000007	0.000003	0.000002
5	0.000477	0.000045	0.000011	0.000004	0.000002	0.000001
6	0.000285	0.000027	0.000006	0.000002	0.000001	0.000000_4
7	0.000180	0.000017	0.000004	0.000001	0.000000_4	0.0
8	0.000122	0.000012	0.000003	0.000001	0.0	0.0

where Z_c is the charge on the core, and are listed in the last column. The contributions of the partial waves to the second-order energy are given in Table II for each excited state.

The results of Table I clearly show the rapid convergence of the perturbation energies for the higher Rydberg levels. Even for the third state, the energy agrees with the exact result better than 0.1%. On the other hand, from Table II we can see that the convergence of the partial wave expansion is about the same for each state. Within the accuracy of the numerical results (about five decimal places) the quantum defect has converged nicely to a limiting value of 0.356.

Because the method we have used is numerical, it should not be difficult to apply to a more general diatomic molecule. The charge distribution due to the core electrons can be determined from an appropriate two-center calculation and then expanded in a partial wave series in the same manner as the nuclear potential. The resulting zero- and first-order equations are very much like those we have solved here for H_2^+. A method which accounts for exchange effects and yet yields a local potential has been developed by Goddard[9] and thus would be particularly suited for numerical work. Another alternative is the use of a pseudopotential theory such as proposed by Hazi and Rice.[10] In any case, once a few of the higher levels have been determined, the energies can be fitted to a Rydberg formula and the remaining members of the series calculated.

* Contribution No. 3764.

[1] T. C. Chen, J. Chem. Phys. 29, 347 (1958).
[2] M. Cohen and C. A. Coulson, Proc. Cambridge Phil. Soc. 57, 96 (1961).
[3] P. Hauk and R. G. Parr, J. Chem. Phys. 43, 548 (1965).
[4] For a complete bibliography of one-center calculations, see E. F. Hayes and R. G. Parr, Progr. Theoret. Phys. (Kyoto) Suppl. 40, 78 (1967).
[5] R. S. Mulliken, J. Am. Chem. Soc. 86, 3183 (1964).
[6] N. W. Winter, D. Diestler, and V. McKoy, J. Chem. Phys. 48, 1879 (1968).
[7] V. McKoy and N. W. Winter, J. Chem. Phys. 48, 5514 (1968).
[8] D. R. Bates, K. Ledsham, and A. L. Steward, Trans. Roy. Soc. (London) A246, 215 (1953).
[9] W. A. Goddard III, "A New Foundation for the Use of Pseudopotentials in Metals," Phys. Rev. (to be published).
[10] A. Hazi and S. Rice, J. Chem. Phys. 45, 3004 (1966).